Sandia National Laboratories

date: 15 November 2019

to: Paul E. Shoemaker, 8880
Todd Zeitler, 8862
Ross Kirkes, 8883

from: Rob P. Rechard, 8842

subject: Improbability of Nuclear Criticality in Transuranic Waste after Compaction by Salt Creep in Bedded Salt Repository

ABSTRACT

Based on the rationale presented here, nuclear criticality is improbable after salt creep compacts various forms of transuranic (TRU) waste disposed at the Waste Isolation Pilot Plant (WIPP), an operating repository in southeastern New Mexico for the geologic disposal of TRU waste from atomic energy defense activities. In the past, concern about criticality in TRU waste has been low because either remote-handled TRU waste canisters are neutronically isolated by salt or the low initial concentration of fissile material in contact-handled TRU waste drums cannot be compacted sufficiently by salt creep. These situations are still valid for the majority of TRU waste that is disposed at WIPP. However, renewed evaluation of the criticality potential was undertaken for the disposal of TRU waste where every drum in a shipment can have the maximum 0.2-kg fissile content (i.e., pipe overpack container—POC—constructed of an inner stainless steel pipe and fiberboard dunnage) and disposal plans for TRU waste with a produced waste form with high initial concentrations of fissile material (i.e., criticality control containers/overpack—CCO—also constructed of an inner stainless steel pipe). The criticality potential of POCs during three representative phases of repository conditions were evaluated: (1) salt creep closure of a room of POCs without brine seepage and subsequent gas generation to permit maximum compaction in the first 1000 years, (2) some brine seepage and consumption of some POC fiberboard (cellulose) dunnage in the second 1000 years, and (3) full brine inundation of POC and consumption of all fiberboard dunnage, thereafter. High-fidelity modeling of salt creep closure of a room filled with 12-inch and 6-inch POCs calculated a distribution of final spacings after 1000 years (when room closure has asymptotically approached completion). Analysis of 0.2-kg ^{239}Pu optimally moderated spheres at the calculated distributed spacing showed that neither 12-inch nor 6-inch POCs are critical as the sea of reflector material changes to represent the three phases of repository conditions. As regards CCOs, the mixing of borated carbide with the produced TRU waste form prevents criticality. Hence, criticality caused by salt creep compacting containers has not been included in the performance assessment for the 2019 Compliance Recertification of WIPP.

I. INTRODUCTION

To certify the compliance of a geologic repository for radioactive waste, the US Environmental Protection Agency (EPA) requires estimates of the range of future behavior through models that capture essential feature, events, and processes (FEPs) of the disposal system. At the Waste Isolation Pilot Plant (WIPP), an operating repository in southeastern New Mexico owned by the US Department of Energy (DOE) for disposal of wastes containing transuranic (TRU) radioisotopes from atomic energy defense activities (Fig. 1), one potential FEP is the possibility of sufficient fissile mass and concentration causing a self-sustained neutron chain reaction (hereafter, succinctly referred to as criticality). In the past, concern about criticality in TRU waste has been low because of the low initial concentration and limit on mass of fissile material (mostly plutonium) in contact-handled containers in the transportation cask, the neutronic isolation of remote-handled containers, and the natural tendency of fissile solute to disperse after release from degraded containers, as discussed in 2001 and summarized in 2015.[1-3] However, waste destined for WIPP has expanded to include TRU waste with high initial concentration (although still low fissile mass in individual containers),[4] and/or containers that have larger combined mass limits in a transportation cask. Hence, a renewed evaluation of the likelihood of assembling a critical mass and concentration in or near a repository after closure has been undertaken.

The update for the criticality potential of the new waste streams is divided into three parts: evaluation of (1) neutronic criteria necessary for criticality in geologic media,[5; 6] (2) hydrologic and geochemical processes present in the disposal system, and their inability to assemble fissile material into critical concentrations,[7] and (3) physical compaction of the containers in the disposal rooms through salt creep. This memorandum focuses on the third part, the potential for compaction to cause criticality sometime in the future after repository closure. The analysis supports the 2019 Compliance Re-certification Application (CRA-2019), which is the latest periodic compliance demonstration with EPA performance criteria since WIPP opened in 1999. This report greatly expands upon previously published calculations for physical compaction conducted for the initial 1996 Compliance Certification Application (CCA-1996).[1; 3]

Study of the criticality scenario class in a geologic setting is interesting and instructive because behavior of fissile material differs from common expectations. However, a practical reason also exists to devote effort to evaluating criticality in a geologic setting. The usual adage, verified by numerous performance assessments, is that if spent nuclear fuel (SNF), high-level radioactive (HLW), or TRU waste can be transported, it can be disposed in a geologic repository under EPA regulations without additional treatment, provided social-political limitations on the type and amount of waste are met. Yet, the possibility of a criticality occurring in a repository sometimes seemingly challenges this adage in that steps taken to ensure the impossibility of critical event during transport, such as required spacing between canisters, do not necessarily remain applicable after repository closure as the salt creep compacts containers tightly together over the first 1000 years. Administrative controls can be placed on radioactive waste placement in the repository. Also, engineering controls can require mixing long-lived neutron poisons in the waste form. For example, disposal of non-pit surplus Pu as plutonium dioxide (PuO_2) mixed with concrete-like components could have a high 185 kg/m^3 Pu concentration when shipped in a criticality control container (CCC). Adding 50 g borated carbide (B_4C) in each CCC to the Pu mixture makes criticality highly unlikely, as discussed in a supporting report.[8] However, these administrative and engineering controls can have real consequences by adding costs, delay in implementing disposal,

and adding additional worker exposure to radiation if existing containers must be reopened in comparison to small hypothetical consequences of criticality.[3]

Using this report in combination with companion reports on neutronic criteria for criticality and hydrologic and geochemical constraints on concentrating fissile in various geologic settings demonstrates that the possibility of criticality is remote in a geologic setting without imposing additional procedures or waste treatment for standard contact-handled TRU waste, remote-handled TRU waste, and TRU waste arriving in pipe overpack containers. Hence, criticality has not been included in the performance assessment (PA) for CRA-2019.
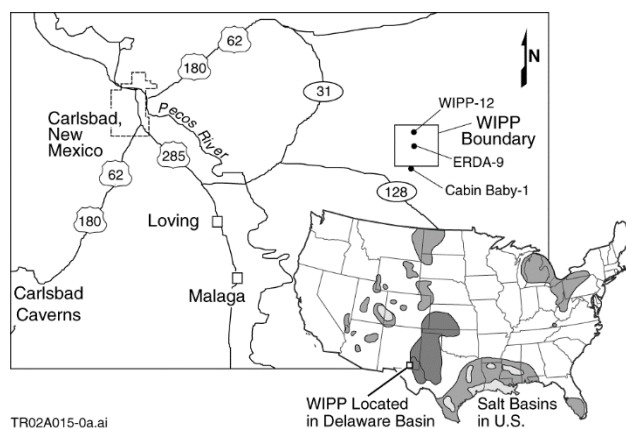

Fig. 1. WIPP repository in southeastern New Mexico.[1, Fig. 1]

II. OVERVIEW ON SCREENING POST-CLOSURE CRITICALITY
II.A. Low Probability Criteria for Screening Criticality Scenario Class

In Appendix C of 40 CFR 191[9; 10] and in 40 CFR 194.32,[11; 12] EPA provides three criteria for excluding FEPs or scenario classes such as criticality from the performance assessment: (1) regulatory fiat; (2) low probability of occurring; and (3) low consequence. Exclusion of low probability FEPs and scenario classes is via a (a) qualitative argument that the FEPs and scenario classes are not credible based on site, waste, or repository characteristics or (b) quantitative demonstration that the probability is $<10^{-4}$ over 10^4 years. [9,Appendix B; 10, Appendix C] Although quantitative calculations are conducted, the approach here develops a qualitative low-probability rationale to exclude criticality in the underground facility based on arguments that physical compaction cannot sufficiently concentrate fissile ^{239}Pu (similar to CCA-1996).[2]

II.B. Time Frame

Evaluating post-closure criticality potential occurs within the probabilistic regulatory framework for disposal,[9; 10] because EPA does not designate post-closure criticality for special consideration.[a] Hence, the time frame for considering post-closure criticality is the 10^4-year regulatory period.[b]

---

[a]For the draft and final 10^6-year site-specific standard for the Yucca Mountain repository, (40 CFR 197) [13; 14] EPA did not set apart criticality when evaluating the post-closure behavior even though EPA had the opportunity to do so when EPA used criticality as a FEP screening example in the preamble.

[b]In the draft 40 CFR 197, EPA stated "…we do not require that DOE consider in-package criticality beyond 10,000 years if it has not been considered for the first 10,000 years… We see such an exercise as being of no value. Rather, we believe it would be detrimental to the licensing process, as well as contrary to our 'reasonable expectation' concept and the idea that performance assessment should represent credible projections of disposal system safety…We believe that any potential FEPs to be included [beyond 10,000 years] are likely to be overwhelmed by increasing uncertainties or larger-scale FEPs such as climate change. For this reason, we do not believe the inclusion of such FEPs will add materially to the understanding of the disposal system's performance or will lead to a safer disposal system.[13, p. 49054]

15 November 2019

II.B. Probability of Criticality Scenario Classes

The probability of WIPP criticality $\wp\{\mathcal{A}_C\}$ can be expanded to include probabilities from various situations here called computational scenarios ($\mathcal{A}_k^{CS}$). No sharp distinction between the coarse criticality scenario class and the underlying computational scenarios; rather a continuum exists. Here, the terms distinguish between the broad overall category of criticality and fine groupings of futures for organizing the rationale. Because EPA guidance implies the mean (over epistemic uncertainty— $\overline{\wp}^{E}$) provides an adequate estimate for screening,[c] the probability of criticality is

$$\overline{\wp}^{E}\{\mathcal{A}_C\} = \sum_{k=1}^{n_{CS}} \overline{\wp}^{E}\{\mathcal{A}_k^{CS}\} \tag{1}$$

II.C. Conditions Considered for Criticality Probability

In 40 CFR 191 and 40 CFR 194,[9; 10; 16] EPA requires DOE to demonstrate that WIPP will comply with the performance criteria after humans unknowingly intrude into the repository with an exploratory drill hole using present technology. Thus, two environmental conditions (*e*) were considered for defining the criticality computational scenarios: (1) the undisturbed condition (*e~U*) and (2) the condition after inadvertent human intrusion (e~*H*).

In addition, the potential for criticality was evaluated at two feature locations of the disposal system (*f*): (1) the underground repository (*f~R*), and (2) the Culebra in the natural geologic barrier (*f~GB*). Location is not usually a convenient means of defining a PA scenario class since location is not associated with scenarios and aleatoric uncertainty; rather, the likelihood of radionuclides such as fissile material residing in a specific location is modeled as part of epistemic uncertainty. However, here it useful to subdivide the criticality scenario class by location even though it is not possible to assign a distinct probability by location. The probability of fissile material in both locations (i.e., $\wp\{\mathcal{A}_R^{CS}\}$ and $\wp\{\mathcal{A}_{GB}^{CS}\}$) is eventually approximately one, but the probabilities do differ in the first 10^4 yr.

A third criticality computational scenario class considered is the contribution to probability from various phenomena/processes (*p*) such as physical compaction, precipitation, adsorption, and colloidal filtering.

A fourth criticality computational scenario class considered was based on the container type (*c*) to account for the different packaging (drum containers—Drum; remote handled containers—RH; pipe overpack containers—POCs; and criticality control containers/overpacks—CCOs, as introduced in §III.A). As noted later (§III.D), the transportation constraints on the containers are the primary technical constraints on waste management at WIPP.

In summary:

$$\overline{\wp}^{E}\{\mathcal{A}_C\} = \sum_{k=1}^{n_{CS}} \overline{\wp}^{E}\{\mathcal{A}_k^{CS}\}$$

$$= \sum_{c}^{Drum,RH,POC,CCO} \overline{\wp}^{E}\{\mathcal{A}_{U,R,compact,c}^{CS}\} + \sum_{e}^{U,H}\sum_{f}^{R,GB}\sum_{p}^{precip,adsorp,filter} \overline{\wp}^{E}\{\mathcal{A}_{e,f,p}^{CS}\} \tag{2}$$

This memorandum focuses on the first summation of container compaction by salt creep in the repository (particularly, compaction of the pipe over containers—POCs) but evaluates the isolation provided by salt for remote-

---

[c] The use of the mean probability for screening FEPs is emphasized by NRC in the Yucca Mountain Review Plan (YMRP) [15, 2.2-14] "…the mean of the distribution range is to be used to screen an event from the performance assessment…" Consequently, the WIPP Project does not present a distribution for the probability of criticality.

handled canisters, summarizes past compaction evaluations of standard TRU drums and boxes, and cites the current evaluation of CCOs. That is, we notionally discuss the low probability rationale as the sum of the probability of salt creep sufficiently compacting four categories of containers. As noted in Eq. (2), compaction is considered primarily prior to human intrusion (i.e., undisturbed computational scenario). Although the brine chemistry is slightly different with and without inadvertent human intrusion, using Castile brine chemistry after human intrusion, which has less chloride and boron, and, thus, less ability to curtail criticality, simplifies the rationale.

II.E. Approximation of Mean Probability

The mean with respect to the epistemic uncertainty (i.e., $\overline{\wp}^{\,\varepsilon}\{\mathcal{A}^{CS}_{U,RP,compact,c}\}$ in Eq. (2) or $\overline{\wp}^{\,\varepsilon}\{\mathcal{A}^{CS}_{k}(\mathbf{e})\}$ in Eq. (1)) is not formally evaluated for screening scenario classes but rather approximated. Herein, we use compaction calculations of POCs that represent typical behavior. We then use maximum 0.2-kg fissile container loading from transportation constraints in a conservative spherical configuration to assert that the probability of criticality is qualitatively very small because criticality cannot occur for the representative compaction calculations with bounding fissile loading and configuration.

The use of mean or representative values for evaluating the probability of criticality after disposal and closure of the repository when humans are absent differs substantially to screening criticality during WIPP operations when humans are present. The rationale for eliminating the need to consider criticality during operations is rule-based (ANSI/ANS-8.1)[17] whereby several worse-case scenarios of assembling fissile material are developed and then calculations made to demonstrate the impossibility of criticality in order to ensure human safety.[18; 19]

III WIPP DISPOSAL SYSTEM
III.C Transuranic Waste
III.C.1.General Categories of TRU Waste.

The two types of TRU waste destined for WIPP, as defined in the *WIPP Land Withdrawal Act*, are[20] (1) contact-handled transuranic (CH-TRU) waste with an external dose rate <0.56 µSv/s (200 mrem/h), and (2) remotely handled transuranic (RH-TRU) waste with > 0.56 µSv/s but < 2.8 mSv/s (1000 rem/h).

The projected activity of TRU waste in WIPP for CCA-1996 was 275 PBq (7.44 MCi) with a heat power of 136 kW when initially placed. Of the projected 136 kW, 97.8% was from radioactive decay of CH-TRU actinides, of which 65% was from ^{238}Pu (generated at Savannah River Plant (SRP) for power generators in space and elsewhere), 18% from ^{239}Pu , 5% from ^{240}Pu, and 11% from ^{241}Am. The remaining 2.2% was primarily from decay of fission products in RH-TRU. The fission products are from contaminated material that results when dealing with reprocessing fuel elements for producing ^{239}Pu. Because much of the RH-TRU activity is from fission products, the activity drops off an order of magnitude after 100 years, but not as dramatically as SNF and HLW (Fig. 2).
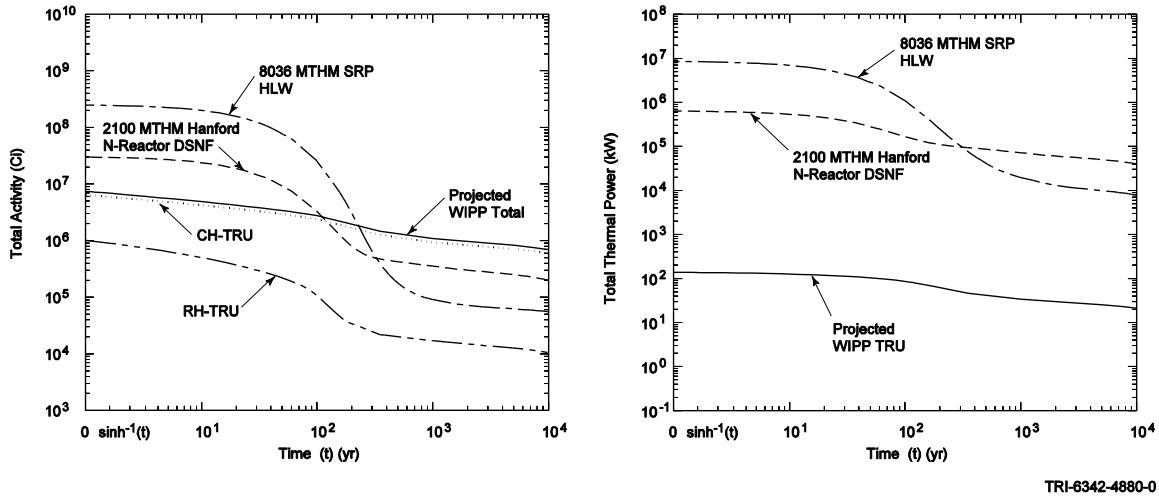
Fig. 2. Projected activity and thermal power of TRU waste in CCA-1996. Activity and thermal power of 2100 MTHM (metric tons of heavy metal) of N-Reactor defense spent nuclear fuel (DSNF) at Hanford reservation and 8036 equivalent MTHM of HLW at Savannah River Plant (SRP) shown for comparison.

The standard waste form of CH-TRU has consisted of a variety of debris contaminated with TRU radionuclides, including organics (e.g., cellulose, such as paper, cardboard, laboratory tissues, wood, cloth, rubber, plastics), inorganics (e.g., iron and aluminum alloys, equipment, concrete, glass, firebrick, ceramics), and solidified materials (e.g., waste water treatment sludge, cemented liquid waste, inorganic particles and soils) (Table I). The amounts of organics and inorganics can influence the criticality calculations. Here, however, we only consider the cellulose, plastic, and Fe metal/alloys in the POC (Tables II and III).

Table I. Average Volume Percentage of Various Components in Standard TRU Waste destined for WIPP in CCA-1996.[21; 22]

Material	Volume (%)
Organics	
Cellulose	30.5
Plastics & Rubber	15.0
Inorganics	
Metal	21.8
Solidified Material	
Sorbents	7.1
Sludges	25.6

15 November 2019

Table II. Average Volume Percentage of Various Components in Pipe Overpack Containers destined for WIPP. [22]

Material	Volume (%)
Organics	
Cellulose	73.27
Plastics	1.57
Solidified Organic Matrix	0.08
Rubber	0.02
Inorganics	
Other Inorganic Material	13.70
Fe-Based Metal/Alloys	6.66
Other Metal/Alloys	2.04
Al-Based Metal/Alloys	0.02
Solidified Material	
Solidified Inorganic Matrix	2.64
Soils	0.00
Total	100.00

Table III. Projected Fe-based metal and cellulose in 2033 for certifications of WIPP

Material	CCA-1996[a] CH (tonne)	CCA-1996[a] RH (tonne)	CRA-2004[b] CH (tonne)	CRA-2004[b] RH (tonne)	CRA-2009[c] CH (tonne)	CRA-2009[c] RH (tonne)	CRA-2014[d] CH (tonne)	CRA-2014[d] RH (tonne)	CRA-2019[e] CH (tonne)	CRA-2019[e] RH (tonne)
Fe-based Metal										
Waste	28 640		18 500		13 700		10 900	1 350	14 100	1 330
Packaging	23 600		28 600		31 400		30 000	6 860	31 200	16 500
Total	52 240		47 100		45 100		40 900	8 210	45 300	17 830
Lead										
Packaging							0	8.28	0	13 800
Cellulose										
Waste	9 100		10 100		6 670		3 550	118	4 100	170
Packaging					867		723	0	1 470	0
Emplace Operations					226		260		224	
Total	9 100		10 100		7 537		4 533	118	5 794	170

[a]Ref[23, Appendix BIR Revision 3]
[b]Ref[24]
[c]Ref[25]
[d]Ref[26]
[e]Ref[27]

For the CCA-1996, the masses of the two most important fissile materials, ^{235}U and ^{239}Pu, were 8.1 and 12.8 metric tons (MT), respectively (Table IV). The projected average ^{235}U enrichment at emplacement for the CCA-1996 was 4.9% for CH-TRU and 6.5% for RH-TRU. The anticipated uranium enrichment of CH-TRU has remained less than 4.9%. The RH-TRU uranium enrichment has fluctuated more and is currently at 8.4%. (Table IV).

As noted previously, the ^{239}Pu content dropped after CCA-1996 but is now slightly above with the addition of 6.6 MT non-pit plutonium waste. However, the fissile mass equivalent (FME) is still less. In general, the ^{239}Pu fissile mass equivalent for RH-TRU derives mostly from ^{235}U while ^{239}Pu and ^{240}Pu only contributes a small amount to FME (Table IV). The ^{239}Pu enrichment was 90% for the CCA-1996 and has remained near that value, except for the CRA-2014.

Table IV. Projected fissile material in 2033 for certifications of WIPP

Radioisotope	CCA-1996[a] CH (kg)	RH (kg)	CRA-2004[b] CH (kg)	RH (kg)	CRA-2009[c] CH (kg)	RH (kg)	CRA-2014[d] CH (kg)	RH (kg)	CRA-2019[e] CH (kg)	RH (kg)
Uranium										
^{233}U	860	16	130	3.5	16	5.3	10	0.42	11	1.8
^{234}U	75	6.9	45	6.0	49	0.83	34	0.52	77	1.6
^{235}U	5900	2 100	610	440	2 000	33	4 000	31 000	2 100	860
^{238}U	120 000	31 000	73 00	390 000	81 000	880	104 000	88 000	117 000	9 300
Enrichment ^{233}U+^{235}U	4.9%	6.5%	1.0%	0.11%	2.5%	4.1%	3.7%	26%	1.8%	8.4%
Plutonium										
^{238}Pu	15	0.09	73	0.16	86	0.30	35	0.34	55	1.3
^{239}Pu	13 000	170	11 000	87	8 200	47	9 100	120	14 000	68
^{240}Pu	920	22	470	7.5	630	4.4	740	35	1 400	14
^{241}Pu	2.2	0.13	5.0	0.23	4.9	0.04	6.3	0.14	18	0.44
^{242}Pu	310	0.04	6.8	0.12	19	0.32	420	1 600	38	4.0
^{239}Pu fissile kg equivalent[f]	16 700	1 560[g]	11 200	370[g]	9 590	73.0	11 800	20 300[g]	15 500[g]	624[g]
Enrichment ^{239}Pu	90%	88%	95%	92%	92%	90%	88%	6.5%	90%	78%

[a]Ref[23, Appendix BIR Revision 3]

[b]Ref[24]; masses were updated and differ somewhat for the EPA-requested CRA-2004 PABC analysis[24]

[c]Ref[25]

[d]Ref[26]

[e] See Appendix B; also Ref[27]

[f]Pu fissile mass equivalence (FME) is the mass of ^{239}Pu plus various factors of the masses of $0.113 \cdot ^{238}$Pu, $0.0225 \cdot ^{240}$Pu, $2.25 \cdot ^{241}$Pu, $0.0075 \cdot ^{242}$Pu, $0.9 \cdot ^{233}$U, $0.643 \cdot ^{235}$U, $0.015 \cdot ^{237}$Np, $0.0187 \cdot ^{241}$Am, $34.6 \cdot ^{242m}$Am, $0.0129 \cdot ^{243}$Am, $15 \cdot ^{245}$Cm, $0.5 \cdot ^{247}$Cm, $45 \cdot ^{245}$Cf, and $90 \cdot ^{251}$Cf.

[g]Pu FME for RH-TRU primarily derives from 0.643 ^{235}U

III.C.2. Regulatory and Legislative Disposal Constraints on TRU Waste

In its disposal regulation 40 CFR 191, EPA defined TRU waste requiring deep geologic disposal as material contaminated with α-emitting TRU isotopes with an activity > 3.7 MBq/kg (>100 nCi/g) and half-life of >20 years. In addition, the *Waste Isolation Pilot Plant Land Withdrawal Act* codifies several limits on TRU waste disposal at WIPP,[20, §9] based on prior social-political agreements (primarily, the 1981 Consultation and Cooperation Agreement, and its 1984 modification between the State of New Mexico and DOE). WIPP is limited to 175 564 m^3 (6.2×10^6 ft^3) of which 7079 m^3 may be RH-TRU, leaving 168 485 m^3 for CH-TRU. Furthermore, TRU waste must have been produced from atomic energy defense activities for disposal at WIPP. The total activity of RH-TRU is limited to 5.1×10^6 Ci. Also, the activity concentration for RH-TRU waste received at WIPP is limited to 2.3×10^4 Ci/m^3 (averaged over the volume of the canister). Finally, no more than 5% of RH-TRU can exceed 100 rem/h.

III.C.3. Excess Non-Pit Plutonium

As part of the 1991 Strategic Arms Reduction Treaty (START I) with Russia to dismantle ~80% of strategic nuclear weapons, the US Department of Energy (DOE) identified ~50 MT of surplus Pu in various stages of manufacturing at several sites that needed to be addressed in the 1996 Programmatic Environmental Impact Statement (EIS) (51.7 MT are specifically identified below). Although DOE preferred to directly dispose this excess Pu, the US relented and agreed in the 1997 record of decision (ROD) for the Programmatic EIS to fabricate ~33 MT into mixed oxide (MOX) fuel (eventually identified as ~34 MT in 2003) to be consistent with plans in Russia. The other ~17 MT were to be immobilized (identified as 17.7 MT below) in a new facility at either Hanford in Washington or the Savannah River Site (SRS) in South Carolina. The immobilized Pu was then to be disposed in a geologic repository. In the 1999 Surplus Plutonium Disposition (SPD) EIS, DOE examined options to implement the dual Pu disposition pathway and decided in the January 2000 Record of Decision (ROD) to build a MOX Fuel Fabrication Facility (MFFF)

and a Pu immobilization facility at SRS. In 2002, DOE cancelled building a new Pu immobilization facility. In the 2007 Notice of Intent (NOI) to produce a SPD Supplemental EIS, ~4 MT of unirradiated fuel of the 17.7 MT was set aside for non-defense research.[28] The remaining 13.7 MT of Pu, included 7.1 MT of Pu from weapon pits (which would require extra processing to convert to MOX), 6.0 MT non-pit Pu unsuitable for producing MOX fuel, and ~0.6 MT of miscellaneous Pu. DOE's preferred option in 2007 was disposal of 13.1 MT of Pu at the proposed Yucca Mountain (YM) repository as lanthanide borosilicate glass in small canisters that were to be inserted inside standard HLW canisters using existing facilities at SRS.[28] Disposition of 13.1 MT of Pu in lanthanide borosilicate glass and 34 MT of Pu as MOX (and subsequent disposal of the resulting spent nuclear fuel) was included in the license application for the proposed YM repository.[29] After the YM repository was halted in 2010, DOE decided in 2011 to process the ~0.6 MT of miscellaneous Pu at SRS and send it to WIPP. DOE proposed in the 2012 amended NOI for the SPD Supplemental EIS to process the 7.1 MT of weapon pit Pu into MOX fuel and dispose of the 6.0 MT of non-pit Pu at WIPP.[30]

The SPD Supplemental EIS was completed April 2015 without any preferred action for the 13.1 MT of Pu. But in April 2016, DOE selected one of the analyzed options: disposal of the 6.0 MT of non-pit Pu at WIPP and subsequently added it to the WIPP inventory along with the 0.6 MT added previously (Table IV);[4] however, it has not yet been shipped. Because bounding estimates were used in CCA-1996, and because estimates for CRA-2004 and thereafter greatly decreased the ^{239}Pu inventory, the disposal of 6.6 MT Pu only represents a small increase in ^{239}Pu mass and the Pu FME is still less than originally planned in 1996 (Table IV).

III.D. TRU Container Constraints

Because of the robust capability of geologic disposal in general, and the WIPP salt repository, in particular, few technical constraints exist on waste management and emplacement beyond the technical constraints for transportation (i.e., if the waste can be shipped it can be disposed provided social-political agreements in the *WIPP Land Withdrawal Act* are met). The primary disposal function of the waste packaging is to allow for retrievability of the waste during operations. None of the containers used at WIPP act as an engineered barrier to release after closure of the repository. Although the structural strength of some of the stainless-steel inner containers of the POCs and CCCs could remain for a prolonged period, they are not strong enough to prevent salt creep from buckling the inner containers.

Hence, the transportation limits on waste packages sets the boundary conditions for the potential for criticality inside the package. Transportation packaging is the primary barrier between the radioactive material being transported and radiation exposure to the public and workers. The type of transportation packaging used is determined by the total radioactive hazard presented by the material within the packaging. Four basic types of packaging are used: Excepted, Industrial, Type A, and Type B (49 CFR 173.400). Excepted and Industrial packaging can be used to transport radioactive materials at very low concentration when of limited hazard to the public and the environment.

Type A packaging is designed to protect and retain its contents under normal conditions of transport (NCT) and maintain sufficient shielding to limit radiation exposure to handling personnel (10 CFR 71.71, Subpart F). Four types of Type A packaging (here after referred to as the payload container) are considered in this memorandum (i.e., c~Drum, POC, RH, CCO)

III.D.5. Type B Transportation Casks

Radioactive materials shipped in Type A payload containers are subject to specific radioactivity limits in tables of 10 CFR 71 and 49 CFR 173.435. If the limits are exceeded, the material or the Type A payload container must be shipped in a Type B cask. In addition to the normal conditions of transport described for Type A containers, a Type B cask must (1) provide shielding from radiation, (2) dissipate the heat generated by the waste, and (3) withstand a hypothetical accident condition (HAC) without releasing radioactive material (e.g., 9-m drop onto unyielding surface, 1-m drop onto 15 cm steel bar, and 800 °C fully engulfing fire for 30 minutes). Currently five Type B truck casks, approved by the US Nuclear Regulatory Commission (NRC), exist for shipping TRU waste: TRUPACT-II (Transuranic Package Transporter Model 2), HalfPACT, TRUPACT-III (only for large standard waste boxes), RH-TRU 72-B, and 10-160B. Up to 3 TRUPACTs or 3 HalfPACTs are transported on a truck to WIPP (Fig. 3). One RH-TRU 72-B cask is transported on a truck at a time (Fig. 4). The RH-TRU 72-B cask can transport a payload (including the payload canister) weighing 3628 kg. [31] The cask fissile limits depend upon the Type A container shipped.
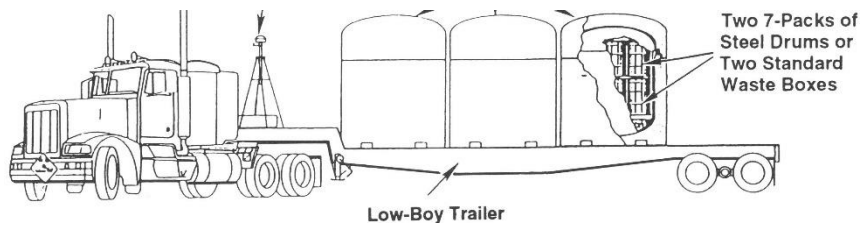

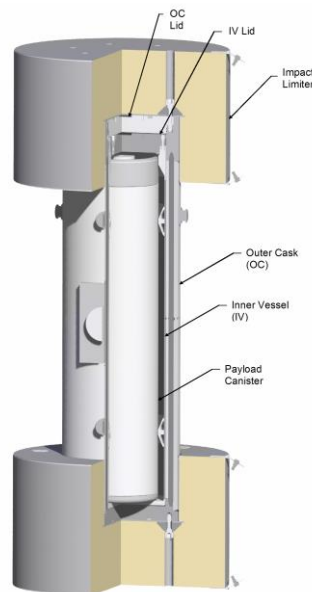Fig. 3. TRUPACT-II truck casks for contact-handled TRU waste.

Fig. 4. RH-TRU 72-B cask (outer container and inner vessel) with payload canister for remote-handled TRU waste.[32, Figure 1.1.1]

III.D.1. CH-TRU Waste Drums Type A Containers

About 54% of CH-TRU waste containers are standard 55-gal drums. Standard drums are bound together in hexagon-shaped packs of seven for transportation and disposal (one container surrounded by 6 containers). The truck transportation cask, TRUPACT-II, holds 2 seven packs (14 drums). The HalfPACT holds one seven pack.

About 20% of CH-TRU containers are 100-gallon drums that often contain machine super-compacted (~60 MPa compression >> 15 MPa lithostatic pressure at WIPP) mixed waste from the advanced mixed waste treatment project (AMWTP), placed inside 100-gallon drums, which are bound together as 3 packs for shipment in the HalfPACT.[22] Also, 85-gallon short and 85-gallon tall drums are available (Table V). Another 7% of CH-TRU containers are standard waste boxes (0.94 m high, 1.3 m wide, 1.8 m long) (Fig. 5). Two standard waste boxes are shipped in TRUPACT-II and one in HalfPACT.

The ten-drum overpack (TDOP) is ~ 4% of the CH-TRU containers at WIPP. One TDOP is placed in TRUPACT-II cask, with the usual 0.325 kg Pu FME. However, any one drum in the overpack may be at the 0.325 kg Pu FME limit. [d]
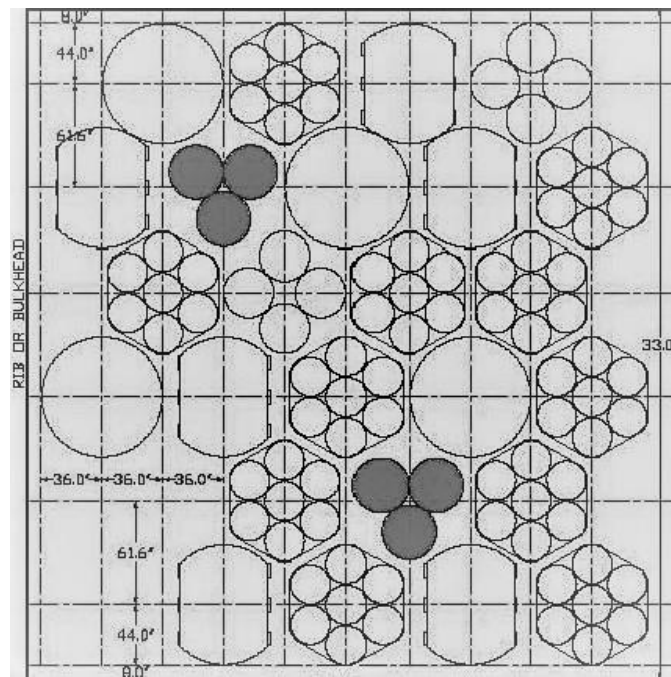

Fig. 5. Hypothetical arrangement of TRU waste containers in disposal room at WIPP; top row consists of 10-drum overpack 7-pack of 55 gallon drums or 7-pack of POCs; standard waste box; 85-gallon tall or 85-gallon short 4-pack; second row consists of standard waste box; 100-gallon 3-pack or shielded container 3-pack; 10-drum overpack; standard waste box; and 7-pack of 55 gallon drums or 7-pack of POCs.[22, Figure 3]

As licensed by the NRC, TRUPACTs and HalfPACTs have a maximum transportation limit of 0.325 kg Pu fissile mass equivalence (FME) when drums or boxes are shipped, if the waste is not machine compacted, contains ≤ 1% weight of beryllium (Be/BeO), and has no reported ^{240}Pu (Table V).[19; 33, Table 1] No credit is given for the ability of drums and boxes to maintain fissile separation after an accident. Thus, the critical limit is based on the maximum mass that can remain subcritical as a sphere optimally moderated with 74%vol water (a worse-case situation if the drum is

---

[d] In the future, the individual drum restriction for drums may be raised to 0.325 kg/m³, similar to the situation for ten-drum overpacks, because an array of drums or boxes is far from critical.

submerged in an accident), 1%vol Be (expressed as 1%vol rather than 1%wt for computational convenience since the change has limited influence), 25%vol polyethylene bagging inside the drum (about double the percentage of polyethylene sheeting that can be stuffed into a 55-gallon drum). Polyethylene decreases the minimum critical mass from that of pure water. The optimally moderated spherical mass is surrounded by a thick water reflector approximating a reflector of infinite extent. An infinite array of TRUPACT-IIs with 0.325 kg Pu FME is subcritical (i.e., the transport index, defined by NRC, is zero for the TRUPACT-II).[34]

The fissile limit of any one drum is further limited to 0.2 kg Pu FME. The limit is not based on transportation accident analysis but rather is an administrative limit imposed by generator sites to ensure that an array of drums or boxes (uncompacted) is subcritical without requiring explicit criticality analysis and controls during storage at sites. Thus, if a drum is at the administrative maximum of 0.2 kg Pu FME, the TRUPACT-II and HalfPACT cask can carry only a little more than one drum (i.e., 0.2 kg + 0.125 kg =0.325 kg FME maximum for TRUPACT-II); the other drums in the transportation cask must be dunnage.

Table V. Transportation and administrative limits for CH-TRU containers shipped in casks to WIPP.[35]

| Conditions | Type A Payload Containers | | Type B Cask | |
| | | | TRUPACT-II | HalfPACT |
		Pu Administrative FME+2σ (kg)	Pu Transport FME+2σ (kg)	Pu Transport FME+2σ (kg)
Not machine Compacted ≤ 1%wt Be/BeO	No ^{240}Pu Drums (55-gal: two 7-pacts or one 7-pact;	0.200	0.325	0.325
	85-gal short: two 4-pacts in TRUPACT;	0.200	0.325	
	85-gal tall: one 4-pact in HalfPACT	0.200		0.325
	100-gal: one 3-pact in HalfPACT)	0.200		0.325
	5 g ^{240}Pu (similar FME package limits for 55-gal, 85-gal short 85-gal tall, and 100-gal as for "No ^{240}Pu"	0.200	0.340	0.340
	15 g ^{240}Pu (similar drum packaging configurations)	0.200	0.360	0.360
	25 g ^{240}Pu (similar drum packaging configurations)	0.200	0.380	0.380
	No ^{240}Pu Standard Waste Box (SWB) & SWB large[a]	0.325	0.325	0.325
	5 g ^{240}Pu	0.325	0.340	0.340
	15 g ^{240}Pu	0.325	0.360	0.360
	25 g ^{240}Pu	0.325	0.380	0.380
	Ten-Drum Overpack (TDOP): one in TRUPACT	0.325	0.325	
	Pipe Overpack Container (POC)	0.200	2.800	1.400
	(Std 12-in; Std 6-in; S100, S200, S300):			
	two 7-pacts or one 7-pact			
	Shielded Container: one 3-pact in HalfPACT	0.200		0.325
	Criticality Control Container (CCC):	0.380	5.320	2.660
	two 7-pacts or one 7-pact			
Not machine Compacted > 1%wt Be/BeO	Drum (55-gal, 85-gal short, 85-gal tall, 100-gal)	0.100	0.100	0.100
	SWB	0.100	0.100	0.100
	TDOP: one in TRUPACT	0.100	0.100	
	POC: two 7-pacts or one 7-pact	0.200	2.800	1.400
	Shielded Container	Unauthorized	Unauthorized	Unauthorized
	CCC	Unauthorized	Unauthorized	Unauthorized
Machine Compacted ≤ 1%wt Be/BeO	Drum (55-gal, 85-gal short, 85-gal tall, 100-gal)	0.200	0.250	0.250
	SWB	0.250	0.250	0.250
	TDOP: one in TRUPAC	0.250	0.250	NA
	POC	Unauthorized	Unauthorized	Unauthorized
	Shielded Container: one 3-pact in HalfPACT	0.200		0.245
	CCC	Unauthorized	Unauthorized	Unauthorized

[a] Large SWB uses TRUPACT-III with same limits as TRUPACT-II except it cannot transport machine compacted waste or waste with > 1% Be

III.D.2. Pipe Overpack Container

Pipe overpack containers (POC), a 55-gallon drum with an interior stainless-steel pipe (Fig. 6), are used to transport standard CH-TRU waste, where more than one standard drum might approach the 0.2 kg Pu FME limit of a drum and 0.325 kg Pu FME limit of TRUPACT-II (Table V). During a transportation accident, a POC has the ability to maintain fissile separation; hence, each POC in a shipment can be at the maximum 0.2 kg FME and TRUPACT-II and HalfPACT casks can transport a maximum 2.8 kg FME and 1.4 kg Pu FME, respectively (Table V).

The space between the inner pipe and 55-gallon outer drum is filled with fiberboard (Fig. 6), which protects the waste from high-speed impact transportation accidents and handling accidents but provides little structural support at slow strain rates from salt creep. Without structural support, the 12-inch inner stainless-steel pipes are susceptible to shell buckling (like the bellows of an accordion) since the diameter -to-thickness ratio is 54.8 and length-to-diameter ratio is 2.1.
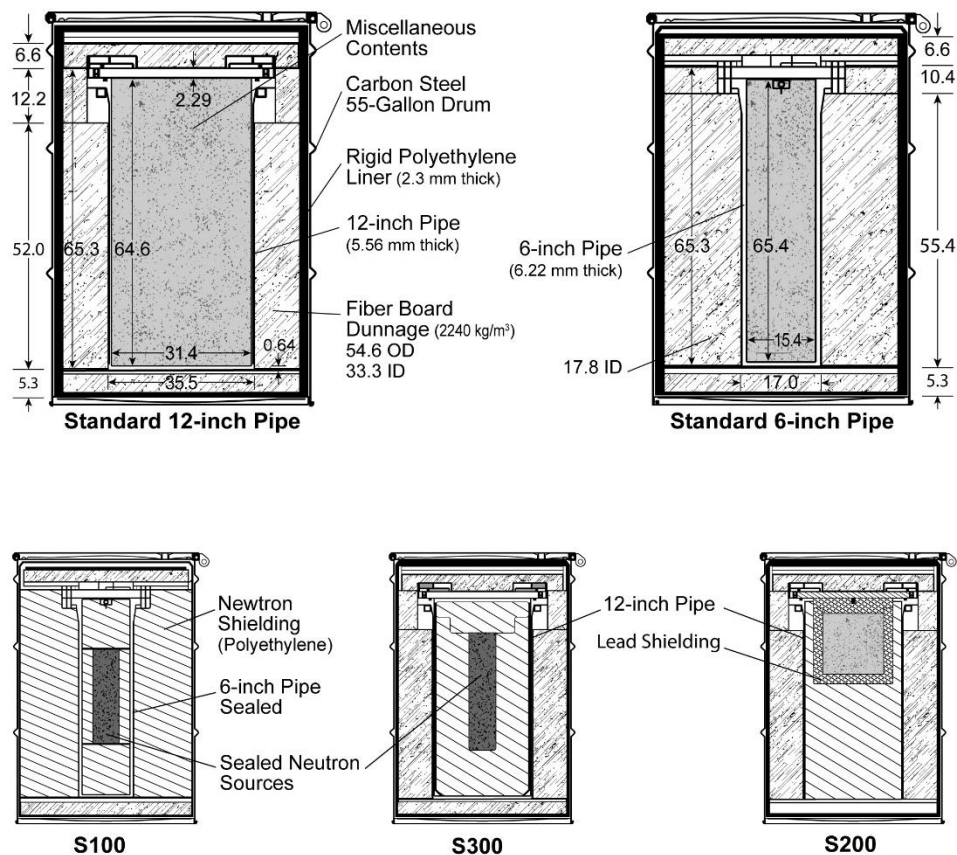

Fig. 6. Pipe overpack containers (POC): the standard 12-inch POC is most common; the standard 6-inch POC and S200 are approved but have not been used at WIPP.

CH-TRU waste from cleaning up the Rocky Flats plant in Colorado was sent to WIPP and placed in Panels 1 and 2 in ~17 000 pipe overpacks (POCs) (Fig. 7 and Fig. 8).[22] Since that time ~10 000 more POCs from various sources have been sent to WIPP (Fig. 9). A total of 176 178 CH containers have been shipped; hence, ~15% of the containers are POCs. However, the POCs represent a small portion of the total volume of TRU waste received to WIPP. As the volume is currently measured using the outer most container, 75 800 m^3 has been received at WIPP, of which 1270 m^3 is POC, or 1.7%.

Currently, standard 6-inch POC (Fig. 6) have not been used at WIPP (Table VI), but their use has been evaluated should they be needed in the future. Furthermore, the 6-inch POCs behave like CCOs (described next in §III.D.4), which will likely be used in the future for the 6.6 MT of excess Pu.

Table VI. Volume and counts for TRU containers emplaced at WIPP as of April 2019

Container	Unit Volume (m³)	Admin Fissile Limit[a] (kg)	Unit Fissile Concen (kg/m³)	Ship Config	Waste Volume (m³)	Approx Dispose Area (m²)	Count	Count (%)	Volume[b] (m³)	Volume (%)	Total (%)
CH											
55-Gallon Drum	0.216	0.2	0.93	7-Pack	1.50	3.52	94 924	53.9	20 503.58	27.3	27.0
				2, 7-Pack	3.00						
85-Gallon Drum Tall	0.324	0.2	0.62	4-Pack	1.33	3.23	5	0.0	1.62	0.0	0.0
85-Gallon Drum Short	0.315	0.2	0.64	2, 4-Pack	2.52	3.48	0	0	0	0	0
100-Gallon drum	0.385	0.2	0.52	3-Pack	1.15	3.21	34 290	19.5	13 201.65	17.6	17.4
Standard Waste Box	1.880	0.325	0.17	One	1.35	2.33	13 155	7.5	24 731.40	32.9	32.6
Large Waste Box 2	7.380	0.325	0.044	One	7.39		232	0.1	1 712.26	2.3	2.3
Ten-Drum Overpack	2.16[c]	0.325	0.15	One	2.05	3.43	6 685	3.8	13 704.26	18.2	18.1
12-inch Pipe Overpack	0.0488	0.2	4.10	7-Pack	0.34	3.52	25 985	14.8	1 268.07	1.7	1.7
				2, 7-Pack	0.68						
6-inch Pipe Overpack	0.0120	0.2	16.67	7-Pack	0.09	3.52	0	0	0	0	0
				2, 7-Pack	0.18						
S100 Pipe Overpack	0.00163	0.2	122.70[d]	7-Pack	0.011	3.52	846	0.5	1.38	0.0	0.0
				2, 7-Pack	0.022						
S300 Pipe Overpack	0.00269	0.2	74.35[d]	7-Pack	0.019	3.52	56	0.0	0.15	0.0	0.0
				2, 7-Pack	0.038						
Criticality Control Container	0.00206[e]	0.38	184.47	7-Pack	0.014	3.52	0	0	0	0	0
				2, 7-Pack	0.029						
CH Total							176 178	100.1	75 124.47	100.0	
RH											
Canister (removal lid)	0.939	0.245	0.26	One	0.94		719	96.4	672.98	99.5	1.0
Shielded Drum	0.117[f]	0.2	1.26	3-Pack	0.35	3.31	27	3.6	3.16	0.6	0.0
RH Total							746	100.0	676.14	100.0	
Total									75 800.40		100.0

[a] see Tables V and VII; minimum Pu FME reported
[b] Volume based on inner volume of outer most container
[c] Volume when overpacking ten 55-gallon drums; directly loaded volume is 4.37 m³
[d] Neutron source disposal
[e] Volume used for transporting non-pit surplus Pu; total available volume is 0.0128 m³
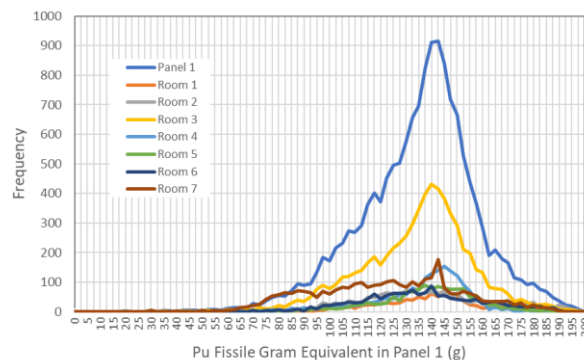[f] Volume is for authorized 30-gallon inner drum

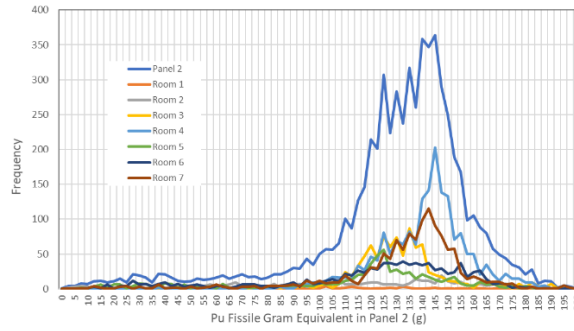Fig. 7. Distribution of Pu fissile gram equivalent in pipe overpack containers in Rooms 1 through 7 of Panel 1.[36]

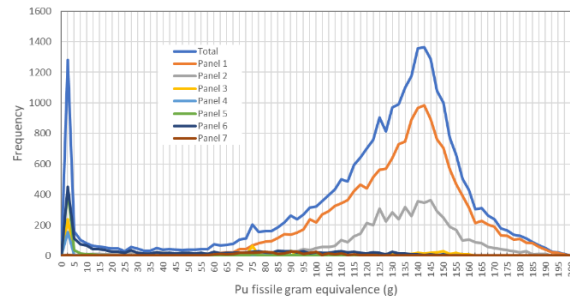Fig. 8 Distribution of Pu fissile gram equivalent in pipe overpack containers in Panel 2 at WIPP.[36]

Fig. 9. Distribution of Pu fissile gram equivalent in pipe overpack containers in Panels 1 through 7 at WIPP.[36]

III.D.4. Criticality Control Container

Non-pit, 6.6-MT Pu waste is likely to be shipped in a criticality control container (CCC) of 304 stainless steel. The CCC has a flange on the top *and* bottom, which differs with the 6-inch POC. Like the POC, the CCC is overpacked in a standard 55-gal carbon steel drum (i.e., criticality control overpack or CCO). The CCC is held in place inside the CCO by plywood on the top and bottom of the drum, but more plywood is used than in the POC (Fig. 10). Nothing is placed in the space between the pipe and 55-gallon drum, unlike the 6-inch POC.

The 6-inch inner stainless-steel pipes are susceptible to column buckling since the diameter-to-thickness ratio is 24.0 and length-to-diameter ratio is 4.0. The 6-inch POC is also susceptible to column buckling because the easily compressed fiberboard dunnage does not provide lateral structural support.

The maximum fissile content for a CCO is 0.38 kg Pu FME (Table V); thus, ~17 370 drums would be required to ship 6.6 MT of non-pit Pu. During a transportation accident, a CCO has the ability to maintain fissile separation; hence, each POC in a shipment can be at the maximum 0.38 kg Pu FME and TRUPACT-II and HalfPACT casks can transport a maximum 5.32 kg Pu FME and 2.66 kg Pu FME, respectively (Table V).[37] Based on a surplus Pu volume of 2.06×10^{-3} m^3, the concentration of Pu in the concrete waste form is high at 184 kg/m^3 (0.380 kg in 2.06×10^{-3}·m^3). If other components are added to the waste form the volume and total density change somewhat.[8]

Disposal of 6.6 MT of non-pit Pu metal differs from other TRU waste at WIPP, and POCs in particular, in that a uniform waste form is planned. Creating a uniform waste form, creates the opportunity to more readily define the conditions for criticality analysis and add engineering controls to help prevent criticality, if desired.
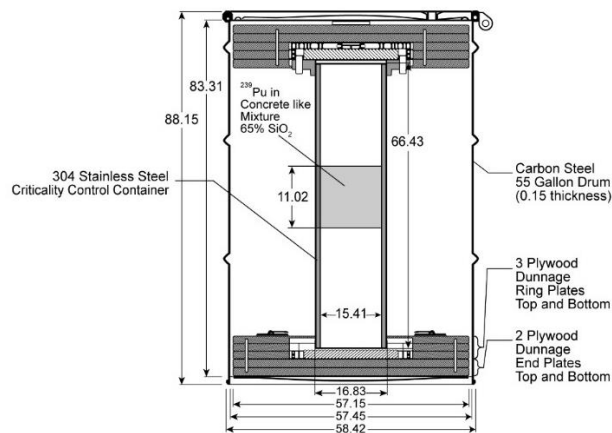
15 November 2019

Fig. 10. Criticality control container (CCC), and criticality control overpack (CCO).[38]

III.D.6. RH-TRU Type A Containers

RH-TRU waste is shipped in either (a) 3-pack of carbon steel containers with 2.54-cm lead shielding and dimensions of 58.4 cm outer diameter 90.8 cm outer height, 0.794 cm thickness in the HalfPACT; or (b) one carbon steel (or 304 stainless steel) payload canister with 66 cm outer diameter, 306 cm outer height including 21 cm lid, and 0.635 cm thickness in the RH-TRU 72-B cask (Fig. 4). The shielded container internal volume is 0.159 m^3; the payload canister volume is 0.936 m^3.[32] The RH payload canister has a 0.37 kg FME limit provided $\geq$ 25 g of ^{240}Pu is present and $\leq$ 1% Be/BeO is present (Table VII).[33, Table 3]

Similar to drums, shielded containers have a 0.2 kg FME limit (Table V). Shielded containers can maintain fissile separation during an accident, but the effort to certify this capability has not been made. Hence, the Pu FME limit for the HalfPACT is set at the default value of 0.325 kg (Table V).

As of April 2019, 2005 containers in 719 RH-TRU payload canisters (i.e., often with 3 containers per canister) have been placed in room walls and 27 shielded drums from Argonne National Laboratory (ANL) have been emplaced in the rooms. For the 27 drums, the average Pu FME is 5.33×10^{-4} kg and derives mostly from ^{235}U (average of 5.55×10^{-4} kg ^{235}U). Although handled and emplaced like CH-TRU drums, the contents are counted against the RH-TRU waste statutory limit (§III.C.2).

II.D.7 Critical Limit and Bias

A system is "critical" when a nuclear chain reaction is sustained, which is mathematically expressed by a neutron multiplication factor (k) of unity, where k is defined as the number of neutrons in one generation divided by the number of neutrons in the preceding generation for the entire fissile system or assembly (i.e., integrated over the entire system). Traditionally, k^{eff} denotes a multiplication factor for a system of finite extent, finite mass, and specified configuration, and k^{∞} denotes the multiplication factor for homogenous infinite media with fissile material.[39, pp. 75-84]

The limit for when a fissile configuration is considered critical is derived from the bias and uncertainties associated with the criticality code (e.g., MCNP), the underlying nuclear data, and the modeling fidelity. In an engineered system on the surface with humans present, great care is taken to conservatively define an appropriate limit to prevent criticality (i.e., critical limit = 1– (calculational bias + uncertainty + administrative factor)). For the transportation analysis of Type B containers, the critical limit is 0.938.

Table VII. Transportation limits for RH-TRU 72-B cask shipping RH-TRU waste to WIPP.[40]

Conditions		RH-TRU 72-B Cask Pu FME+2σ (kg)
Not machine compacted ≤ 1%wt Be/BeO	No ^{240}Pu	0.315
	5 g ^{240}Pu	0.325
	15 g ^{240}Pu	0.350
	25 g ^{240}Pu	0.370
Not machine compacted > 1%wt Be/BeO are chemically bound to Pu		0.305
Not machine compacted > 1%wt Be/BeO not chemically bound to Pu		0.100
Machine compacted ≤ 1%wt Be/BeO		0.245
Machine compacted > 1%wt Be/BeO		Unauthorized

III.A. Geologic Characteristics of WIPP Disposal Horizon

The 600-m-thick Salado Formation hosts the WIPP repository 654 m below the surface. Near the repository, the Salado consists of nearly horizontal (<1° regional dip) halite (NaCl), argillaceous halite, and interbeds of clay and anhydrites ($CaSO_4$) near the repository horizon(Fig. 11).[1, Fig. 4] The clay interbeds near the repository are included in the salt creep modeling reported here because slippage in the clay influences the rate and extent of vertical and horizonal salt movement as the salt creeps closes the mined disposal rooms.

Fractured anhydrites and the disturbed halite around the disposal rooms allow intergranular Salado brine to enter the rooms as the salt slowly creeps and encapsulates the TRU waste. The high chloride and boron concentration in the Salado brine decrease the potential for criticality within the rooms.

Within the land-withdrawal boundary of WIPP (Fig. 1), one exploratory borehole (WIPP-12) intersected a pressurized brine reservoir in a fractured anhydrite layer of the Castile Formation, which underlays the Salado Formation.[23, Appendix DEL, Section 7.5] WIPP PAs assume (1) a pressurized brine reservoir beneath a portion of the repository, and (2) Castile brine could enter the repository through a new exploratory borehole in the next 10 000 years. Castile brine has substantially less magnesium, potassium, boron, and chloride compared to Salado brine (Table VIII).
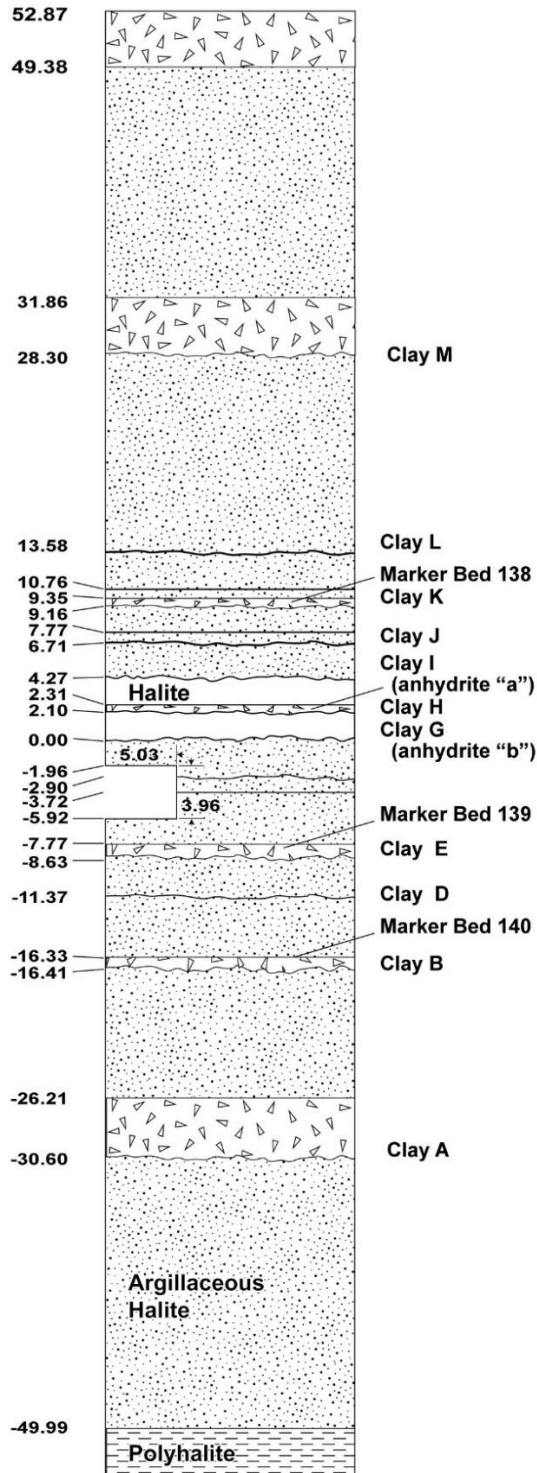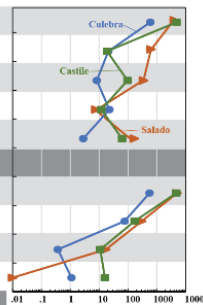
Fig. 11. Idealized stratigraphy around the WIPP disposal room horizon with elevations referenced to clay seam G, which is 648 m below the surface.[41]

Table VIII. Composition of Castile, Salado, and Culebra brines near WIPP.[42]

Brine Concentration (mM or mole/m³)			
Constituent	Culebra (Air Intake Shaft)	Salado (G - Seep)	Castile (ERDA - 6)
Sodium (Na^{+1})	600	4110	4870
Magnesium (Mg^{+2})	21	630	19
Potassium	8.3	350	97
Calcium (Ca^{+2})	23	7.68	12
Boron (B^{+3})	2.8	144	63
Chloride (Cl^{-1})	567	5100	4800
Sulfate (SO$_4^{-2}$)	77	303	170
Bromine (Br^{-1})	0.37	17.1	11
Bicarbonate (HCO$_3^{-1}$)	1.1	0.01	16
Ionic strength	800	6700	5300
Total dissolved solids (kg/m³)			
Calculated	43.2	337	305
Measured	42.6	355	330
Specific Gravity	1.040	1.230	1.216
pH	7.70	6.10	6.17

III.B. Design of the Repository

The WIPP 1.5×10^5-m^2 underground facility is constructed in the Salado Formation between a depth of 648 and 654 m (Fig. 11). The excavated disposal region is 4.38×10^5 m^3. In the original design, excavated disposal region was divided into eight panels (of which 6 panels were filled as of the beginning of 2014) plus two equivalent panels composed of the 4 central connecting drifts. A full panel is ~4.6×10^4 m^3. Because of the accidental release of primarily ^{241}Am in 2014 that contaminated some of the underground, DOE plans to abandon the southern equivalent panel to keep worker exposure low. For the same reason, closures between Panels 3, 4, 5, and 6 in the southern portion of the repository are to be abandoned. Only closures for panels in the northern portion are planned (i.e., closures for Panels 1, 2, 7, 8, 9, and 10—Fig. 12).

A full panel is divided into 7 rooms. All the openings are rectangular in cross section (10.01 m wide, and 3.96 m high. CH-TRU is disposed in the excavated rooms. Seven-pack of drums are stacked 3 high and 6 across the width of rooms and connecting drifts. Not including the connecting drifts, a room is 91.4 m long with a volume of 3642 m^3. Ideally, 57 seven-drum packs can be arranged along the 91.4-m length. Thus, a total of 7182 standard 55-gallon drums can ideally fit in a room; however, much analysis for creep closure and gas generation assumes 6804 drums per room.[22] Including the connecting drifts, ideally 76 356 standard 55-gallon drums can fit in a panel. Standard waste boxes, 85-gallon tall drums, 100-gallon drums and ten-drum overpacks are also used (Table VI), that change the maximum packing (Fig. 5).

About 5% of the remaining volume is filled with usually 1905 kg polypropylene bags of magnesium oxide placed on every other row of 7-pack of drums. The average initial porosity (including the porosity in the waste) is about 85%. Magnesium oxide (MgO) acts as a buffer to control pH of any brine seeping into the rooms prior to encapsulation. The MgO also combines with any CO_2 formed during degradation of organic matter, such that highly soluble Pu carbonate species are not formed.
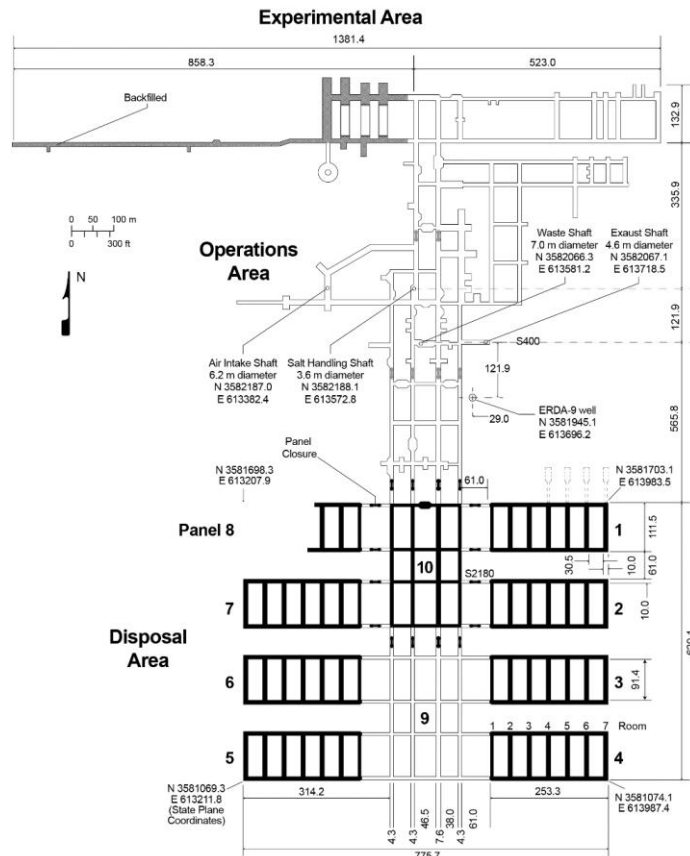
Fig. 12. The transuranic waste disposal area for the WIPP repository in bedded salt currently consists of 7 complete panels, one partial panel, and one equivalent panel in the north central region.

Originally, all RH-TRU was to arrive in RH-TRU 72-B payload canisters and be disposed in boreholes in the repository walls (ribs) (Fig. 13). While RH-TRU waste may still be disposed in repository walls, future RH-TRU waste may come in lead shielded containers (Table V) and be disposed in the excavated rooms.
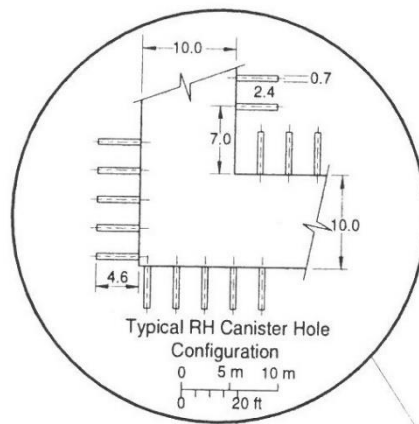

Fig. 13. Placement of RH-TRU in wall of disposal rooms.

15 November 2019

IV. Compaction Modeling
IV.A. Conceptual Model

For criticality analysis, three phases of repository conditions are envisioned: (1) salt creep compaction of containers to the maximum extent up to 1000 years with not much brine available (regardless whether from brine inflow or initial saturation) such that not much corrosion of metals and microbial degradation of cellulose and plastic occurs; (2) influx of sufficient brine for more metal corrosion and cellulose degradation and to partially saturate pores; and then (3) influx of more brine to saturate containers (possibly from inadvertent human intrusion borehole into underlying Castile brine pocket) but eventually partial drying from brine consumption necessary to complete metal corrosion and cellulose degradation.

IV.A.1. Undisturbed Conditions with Little Brine Inflow up to 1000 Years

Initially, the disposal rooms, mined in the Salado Formation (Fig. 11), are filled with a mixture of mostly CH-TRU drums, standard 12-inch POCs, and some TRU waste boxes (Fig. 5), stacked 3 high. (Fig. 6 and Fig. 10). Here we assume for simplicity that the disposal room contains only one type of waste container (e.g., standard CH-TRU drums or standard 12-inch POCs (Fig. 6))

In 1996, MgO was placed on every 7-pack of drums in Panels 1 and 2. However, now usually 1905 kg of MgO in polypropolyene sacks is placed on every other row of 7-pack of drums. (Fig. 14a).

During the first 20 years after closure of a room, salt rock fall and creep mostly fills/closes the unfilled void space in the room (Fig. 14b). Large block of salts that detach at the clay seam can form but the air gap between the waste drums and ceiling is a maximum of 1.3 m (prior to salt creep diminishing the distance) such that the block cannot accelerate much before is strikes and settles on top of the containers. Furthermore, ~5% of the air gap is filled with the MgO polypropylene bags that easily burst, spilling the contents between the containers, and cushioning the shock. Hence, the waste containers do not scatter and cluster in one area of the disposal room because of rock fall.

Thereafter, salt creep begins to compact/buckle the drums. By 250 years, a substantial number of drums have been compacted/buckled. While drums are still basically stacked 3 high at the edge of the disposal room, the drums have been compacted and shifted so that the drums are mostly stacked 2 high in the center of the room. Any brine in the salt mostly flows into the disturbed rock zone. Although some brine may seep into small voids within the rooms and waste, the first phase assumes little brine available to promote metal corrosion of the containers and microbial degradation of cellulose and plastics. Even if brine is available and the fastest degradation rates occurs, 90% of the cellulose is still present in the repository at 250 years (Fig. 14c).

With little brine influx, little gas is generated and the salt continues to creep into the room excavation but at slower rates until it asymptotically approaches a maximum at 1000 years. At the fastest degradation rates, 60% of the fiberboard dunnage remains in the container. Hence, individual POCs remained fairly neutronically isolated by the fiberboard dunnage and iron in the containers. The vertical creep closure is much greater than the horizontal closure, which creates a single stack of crumpled drums in the center of the room (Fig. 14d).
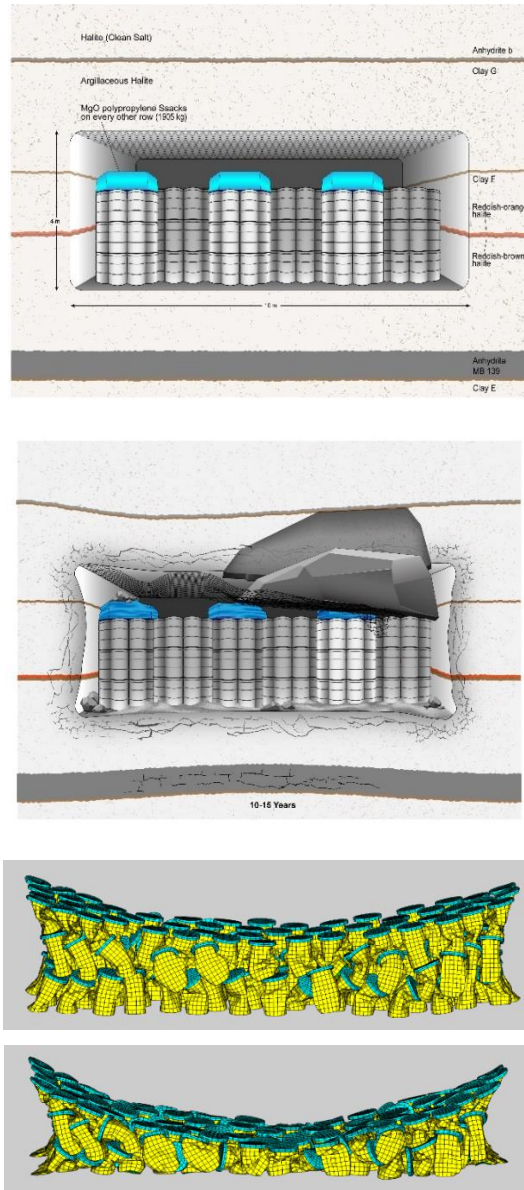
Fig. 14. Hypothetical future for creep closure in the lower horizon when little brine flows and gas generation in the first 1000 years (a) initial conditions after disposal, (b) early rock fall fills some of void space in the first 10 year and salt creep has closed vertical gap by 30 years, (c) substantial number of drums have been compacted/buckled by 250 years with vertical compaction 75% of maximum and horizontal compaction 80% of maximum, (d) vertical and horizontal compaction completed by 1000 years.

IV.A.2. Undisturbed Conditions with Brine Influx up to 2000 Years

The next phase envisioned assumes the influx of sufficient brine in the disposal rooms to promote more degradation of cellulose and corrosion of the steel containers and metal waste. The situation described here assume the brine is from the Salado Formation; not Castile brine that inundates the repository after an intrusion. Because metal corrosion initially consumes O_2, the O_2 is quickly depleted. Thereafter, anoxic corrosion occurs which produces rust and H_2 gas. Slow microbial degradation of organic materials (plywood and fiberboard dunnage as part of the drum packaging and organics in the waste) produces gases such as methane (CH_4), hydrogen sulfide (H_2S), and carbon dioxide (CO_2). Gases generated in the room fill interstitial voids. The gases also migrate into anhydrite layers where

the brine has been depleted, but the general low permeability of the Salado Formation causes pressures to increase and eventually arrest salt creep. At modest gas generation rates, the room inflates somewhat; at high gas generations rates, the void space created is almost equivalent to initial emplacement conditions. Because salt creep is arrested by the gases, the ability of salt to completely fill interstitial spaces and fully encapsulate the waste can be limited until gas pressures are relieved by an inadvertent drilling intrusion or very slow gas leakage through anhydrite layers.

Brine seepage hydrates the MgO and combines with available CO_2. To elaborate, the MgO engineered barrier is added to combine with the CO_2 to form hydromagnesite ($Mg_5(CO_3)_4(OH)_2 \bullet 4H_2O$) to prevent acidic conditions that would enhance dissolution of radionuclides when CO_2 dissolves into available brine and forms carbonic acid ($H_2CO_3^*$), The hydromagnesite, which may eventually convert to thermodynamically stable magnesite ($MgCO_3$), also buffers the brine chemistry between pH 8.8 and 9.

Because some forms of microbial degradation of cellulose consumes water and other forms release water, microbial degradation is assumed to have no influence on the water balance. However, the consumption of water in the corrosion of steel and hydration of MgO leaves additional Cl^{-1} and B^{+3} behind (beyond that present in the brine) to arrest neutronic coupling of the fissile material in POCs and CCOs as the fiberboard dunnage is consumed.

IV.A.3. Undistributed Conditions with Brine Inundation after 2000 Years

In CCA-1996 and CRA-2004, DOE set the probability of microbial degradation at 0.5, regardless of the quantity of brine in a disposal room. In 2005, EPA stated its position that microbial degradation of cellulose would occur, albeit sometimes at low or near zero rates, therefore for a revised CRA-2004 and beyond, "the revised performance assessment must implement a change so that the modeled probability of microbial degradation is 1."[43] Between 2000 and 10,000 years much of the cellulose, including the fiberboard dunnage in the POC, would often have been degraded and no longer able to isolate Pu in individual containers. In addition, the metal would be mostly corroded but the Fe would still be present. The disposal region could be saturated with brine or fairly dry from consumption of all the brine in metal corrosion. However, brine or precipitated Cl^{-1} and B^{+3} ions would be readily present throughout the waste and between containers (e.g., brine would have mixed with any absorbed water originally present in solidified waste).

IV.A.4. Disturbed Conditions

For the compaction criticality analysis, the focus is on the initial compaction for the undisturbed scenario; the disruptive human intrusion event in the disturbed scenario can occur at any time after the first 100 years. The initial intrusion relieves gas pressure and thus induces more salt creep to more thoroughly encapsulate the waste. If the intrusion intersects a brine pocket below the repository, it injects more brine into the disposal region than is already present in the undisturbed scenario, which increases the likelihood that remaining cellulose and metals are completely degraded. For intrusion into a brine pocket, the fluid is dominated by Castile brine, which has substantially less magnesium, potassium, boron, and chloride, compared to Salado brine (Table VIII). Except for this chemical change, the intrusion conditions do not produce additional conditions conducive to criticality from compaction that are not already captured by an undisturbed scenario with brine influx sufficient to alter all the Fe-based metal and cellulose.[e]

---

[e]Brine influx and subsequent movement and deposition of fissile material elsewhere in the WIPP disposal system is discussed in a companion memorandum.[7]
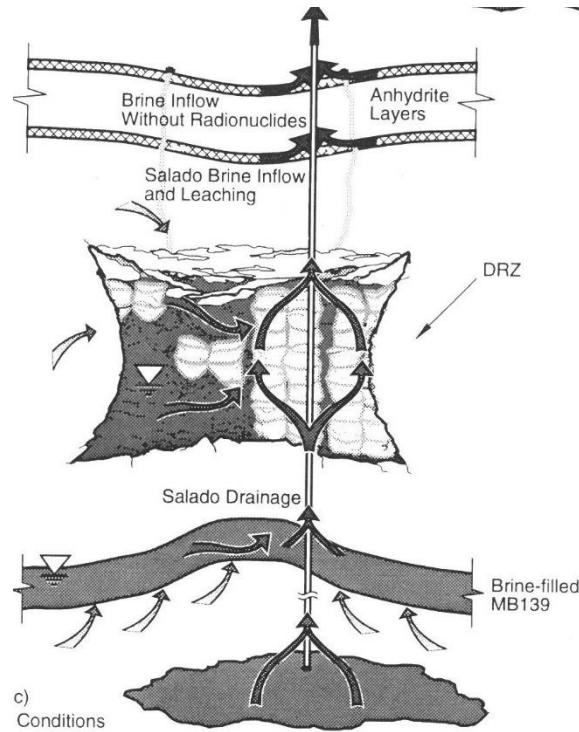
Fig. 15. Hypothetical WIPP future after inadvertent human intrusion into repository allowing much brine to flow into the repository from hypothetical underlying brine pocket.

IV.B Salt Creep Modeling for PA

IV.B.1 Creep Closure Porosity in PA

In the PA repository exposure model, the effects of salt creep are represented by the change of the overall porosity of the disposal room as a function of gas generated. The change of porosity is abstracted from numerous simulations of the two-dimensional, finite-element, large-deformation, quasi-static structural mechanics code, SANTOS.[44]

In the analysis, salt creep was modeled using the Munson-Dawson model with several parameters adjusted to match room-sized experimental results at WIPP.[41] The drums were represented by a single, isotropic volumetric plasticity model. In the calculations, the compressive properties (e.g., Young's modulus) of the isotropic volumetric plastic material was assigned the properties of an individual standard drum, which is reasonable given the weak crushing strength of a standard drum.

The analysis for CCA-1996[1] found the room porosity drops monotonically for the first 100 to 500 years, depending on the value of fraction (f) of baseline gas generation rate. For moderate gas generation ($f \cong 0.5$, vertical compression ceases after 250 years and the porosity holds steady. At values of $f>0.5$, the porosity increases after reaching a minimum. For high gas generation ($f=2.0$), maximum vertical compression occurs after 100 years and begins to inflate room and ultimately creates void space equivalent to initial room porosity of 0.848. For f<0.5, the porosity continues to decrease.
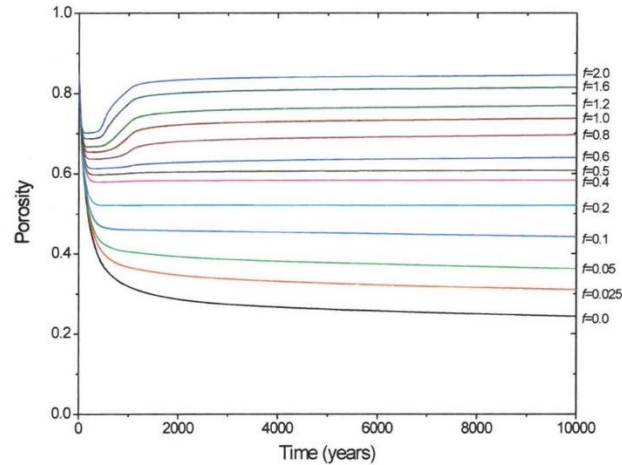
Fig. 16. Porosity history for WIPP disposal room containing standard waste drums at various values of gas generation parameter (*f*) for CCA-1996.[22, Figure 34; 45, Figure 8]

The simulation of compaction of a homogeneous, isotropic TRU waste standard drum with no gas generation shows the salt ceiling contacting the waste at 25 years and slowly compressing it over the next 10,000 years (Fig. 17). The room wall contacts the waste at ~150 years. Based on Fig. 17, a rough estimate of vertical closure is ~38% (final height of ~1.5 m). The horizontal closure is ~55% (final width of 5.5 m). Thus, most of the creep closure occurs from vertical deformation.[45] On average, the volume of a filled disposal room was reduced and the density increased by a factor of 5[f] when no gas generation occurs (i.e., in Fig. 16, waste is compacted from an initial porosity (ϕ_i) of 0.848 to an average porosity of 0.243 for *f*=0 such that $\rho_i/\rho_f = (1 - \phi_f) / (1 - \phi_i) = 5$).[22, Figure 34; 45, Figure 8]

Most of the porosity reduction is from removing the empty space in the disposal room. Because the entire empty space is removed, the final porosity of the room (0.243) is about the same as the final porosity of the individual drums. The initial porosity of an individual drum containing the average components of waste destined for WIPP (Table II) was 0.681.[21; 22, p. 19; 46] Hence, the density increase for the drum contents is a factor of 2.4 rather than 5 (i.e., $\rho_i/\rho_f = 2.4 = (1 - \phi_f) / (1 - \phi_i) = (1-0.243)/(1-0.681)$). By comparison, 60-MPa super compaction of 55-gallon drums containing debris waste stored at Idaho National Laboratory has a final volume between 15 and 35 gallons, or between 27% and 64% with average of 45% of the original volume.[22, p. 23] This range reasonably brackets the estimated 36% reduction in porosity volume (0.243/0.681) from 15 MPa lithostatic pressure at WIPP.

---

[f] The criticality screening rationale for CCA-1996 used an average final porosity of 0.08 to be more conservative, which results in a factor of 6 increase in density.[1]
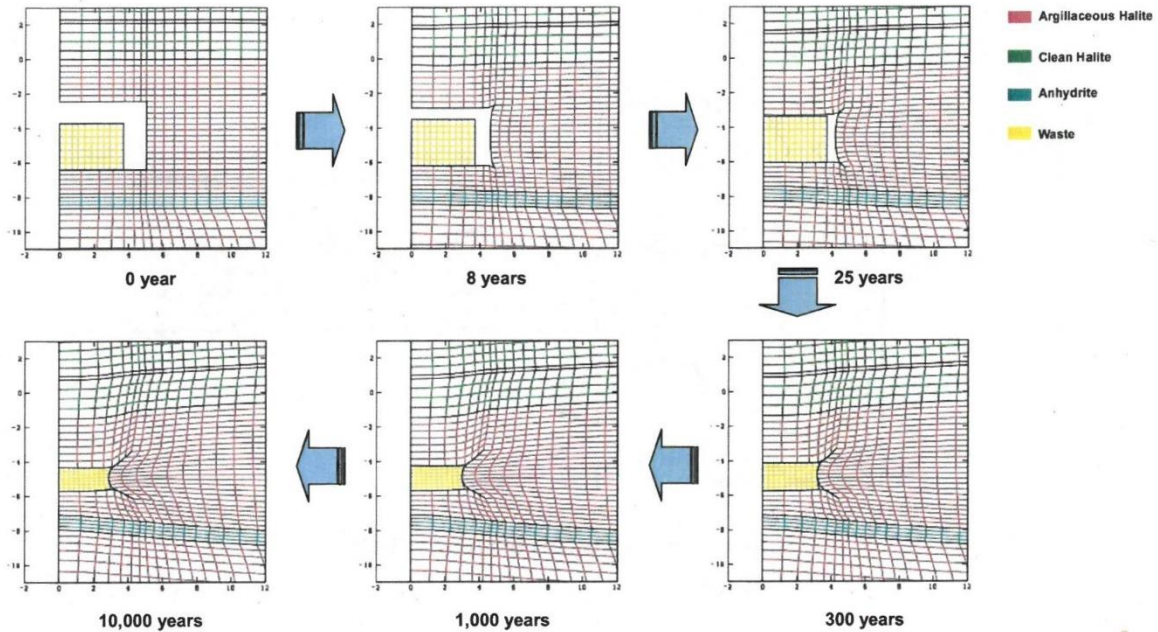
Fig. 17. Simulated compaction of homogeneous, isotropic material representing a standard TRU waste drums filled with the volume average waste destined for WIPP when no gas generation occurs for CCA-1996 [22, Figure 22; 45]

IV.B.2. Compaction of Pipe Overpacks

For CRA-2009, supplemental analysis was conducted on the compaction of POCs.[22] The stainless steel inner pipe and fiberboard dunnage do not increase or decrease, respectively, the density or porosity substantially from standard waste and so initial drum porosity and, therefore, the initial room porosity is almost the same as with standard waste drums (initial porosity of 0.843 for room filled with POCs versus initial porosity of 0.848 for room filled with standard drums).[22]

The engineering properties for the compressibility of an individual POC were determined experimentally.[21; 46] Based on analysis with SANTOS, the final room porosity for a room filled the POC with no gas generation was 0.612 (versus 0.243 for standard waste drums).[22, Figure 36] Based on the 0.843 initial room porosity, the density increase is 2.5 (i.e, one half of that for standard waste drum); however, the density increase inside the POC is only 1.2 if one assumes most of the porosity decrease is from removing the initial room void volume (i.e., $\rho_i/\rho_f = 1.2 = (1-\phi_f)/(1-\phi_i) = (1-0.612)/(1-0.681)$).

In the 2009 analysis, the compaction properties of an ensemble of POC drums was again assigned the properties of an individual POC drum, which is not necessarily conservative for the stiff POC because individual drums are not structurally connected in the 7-pack ensemble. Hence, the POC ensemble in 2009 was modeled much stiffer than likely, but an alternative approach awaited more advanced computational capabilities now available.[47]

IV.C. Large-Block Salt Fall on POCs to Support Conceptual Model

During the first 20 years of room closure, some rock fall may occur along with rapid salt creep closure. A discrete rock fall model was constructed to evaluate the potential of rock fall scattering and clustering POCs and, thereby, potentially producing a reactive POC configuration prior to fully compaction from salt creep. Although only 12-inch POCs have been disposed at WIPP (Table VI), 6-inch POC are authorized for disposal and so included in the analysis.

Sophisticated models of rock fall require weeks to run and so making hundreds of simulations is not possible. Hence, several conservative assumptions were made to construct a reasonably bounding case to support the reasonableness of the conceptual model for 12-inch and 6-inch POCs. The assumptions of the rock fall model are as follows:[47]

1. A right-triangular-shaped block, thick on one side and thin on the other, is modeled. This situation emulates the largest rock fall observed at WIPP, which occurred in Room 4 of Panel 7 (Fig. 18). The large rock block detached at the clay seam and so a thicker block is unlikely. Having a block thick on one side creates a situation with the potential to push and cluster the containers to one side of the room.

2. The right-triangular-shaped block is not allowed to fracture and break up.

3. Each stacked layer of the containers is offset 2.54 cm (1 inch) in the same direction from the center of the containers below to facilitate shifting and toppling the containers toward the thinnest and lightest part of the salt block

4. The rock fall occurs immediately such that salt creep has not reduced the gap between the ceiling and the containers.

5. The polypropolyene sacks containing MgO are omitted from the model to conservatively avoid dissipating any shock and increase the free rock fall distance.

6. The constitutive equation for the salt block omits any plastic deformation or fracturing of the salt, such that all the energy of the impact is absorbed by the assembly of containers.

7. The constitutive equation of the materials in the POCs and CCOs (carbon steel 55-gallon drum, fiberboard dunnage, and stainless-steel inner pipes) used parameters based on slow strain rates. These materials are all stronger and stiffer at the high strain rates from the rock block shock at impact.

8. The constitutive equation of the stainless steel and carbon steel use the minimum annealed yield strength

9. The plywood strength was reduced 80% to promote greater inner pipe movement,

Fig. 18. Roof fall of large salt block in Room 4 of Panel 7 at WIPP in November 2016.

In the roof-fall simulations, the salt block bounces slightly then settles on top of the drum ensemble, causing less than 5% drum deformation, without scattering the POCs (Fig. 19). Consequently, large salt block falls shortly after disposal are not likely to cause collapse and major clustering of drums prior to later salt creep.

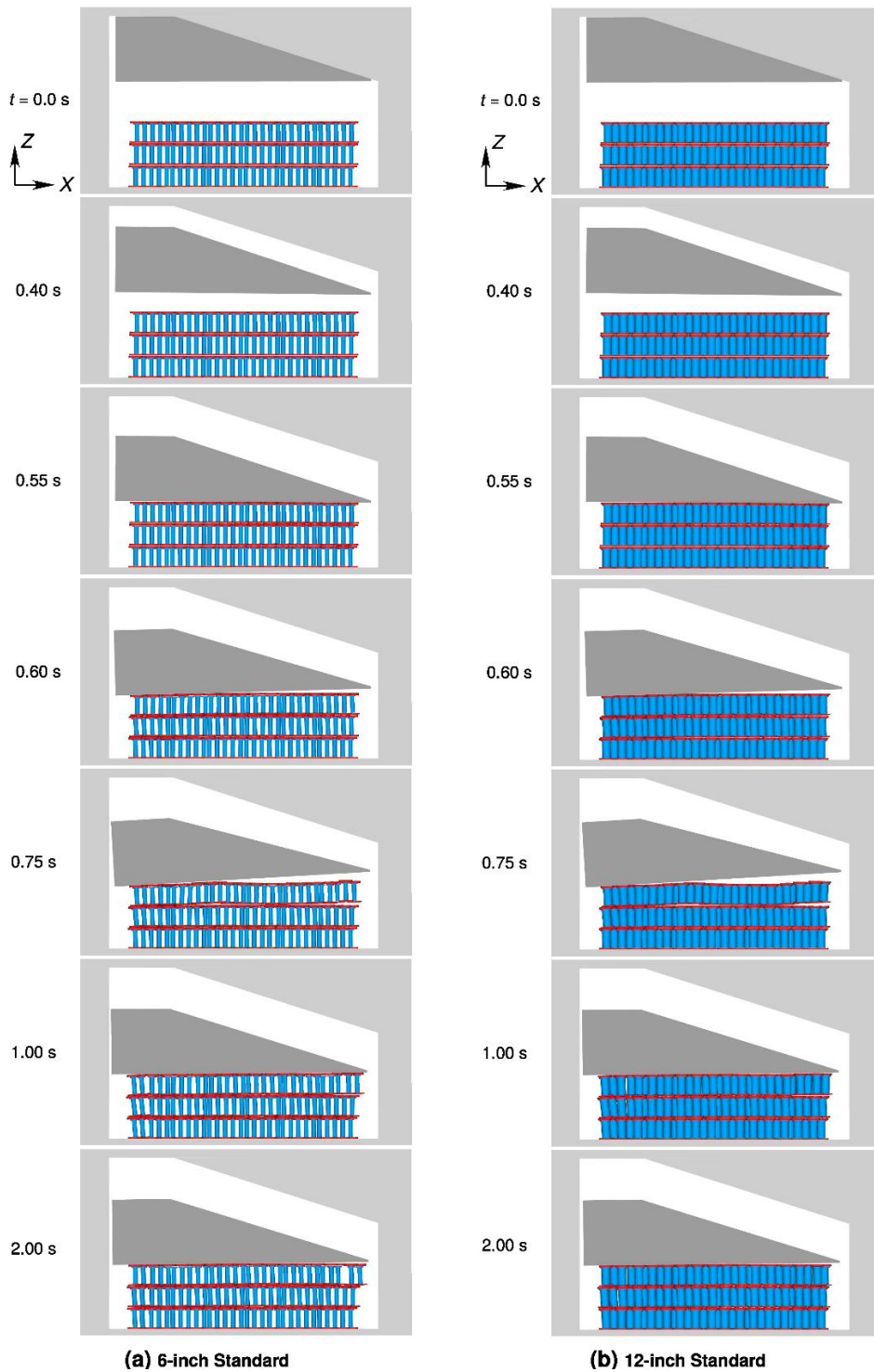**(a)** 6-inch Standard   **(b)** 12-inch Standard

Fig. 19. Negligible deformation and disruption of containers after large block fall onto room filled with (a) 6-inch POCs, and (b) 12-inch POCs; where blue is flanged inner pipe, and red is top and bottom fiberboard and plywood; fiberboard on sides and 55-gallon drums removed in visualization.[47, Figure 3-1]

IV.C. Salt Creep Closure of Rooms Filled with Discrete Pipe Overpack Containers to Support Conceptual Model.

IV.C.1. Modeling

In the conceptual model, salt creep is envisioned to rapidly close the gap between the room ceiling and the waste containers, after which the waste containers begin to buckle and consolidate. High-fidelity salt creep simulations were conducted of 153 discrete POCs occupying the full 10-m width (x-direction) and 4-m height (z-direction) and a slice of a room length (y-direction) to more accurately predict the final configuration than possible when the POCs are modeled as a structurally connected isotropic mass. With 153 discrete POCs, the calculation progressed in a feasible amount of time (2.5 weeks) yet produced a wide variety of deformed spacing between POCs. The analysis used the Sierra/Solid Mechanics finite-element code system at Sandia National Laboratories.[48] The simulations used explicit dynamic numerical solution where the salt visco-plastic strain rate was scaled (sped up). The scale factor was small initially and then gradually increased to several orders of magnitude over the course of the simulation. [47]

In the analysis of the 12-inch and 6-inch, the four POC components (internal stainless-steel pipe, its plywood stabilizer on the top and bottom, the fiberboard dunnage, and outer 55-gallon carbon steel drum shell—Fig. 6) are discretely modeled with individual elastic-plastic-failure material models.[47; 49] Salt creep is modeled with an updated Munson-Dawson model that matched vertical closure rates measured at WIPP reasonably well using laboratory measured salt properties without adjusting model parameters.[50; 51]

IV.C.2. Room Closure

Shortly after the room ceiling contacts the POC drums (~40 years after closure for drums in the room center and ~70 years for drums near the room walls) the POC drums begin to buckle (~100 years for drums in the room center in the middle layer), when modeled as elastic-plastic-failure material (Fig. 20). Buckling allows the drums to slide past each other (especially the POC within the drums).[47] Once the drums buckle, they offer little resistance to vertical room closure until a single layer is formed (i.e., the drum ensemble compresses far more than when represented as a single, isotropic material). A small difference in behavior exists between the 12-inch and 6-inch POCs in that the 12-inch POC first form two predominate layers in the room center at 200 years while the 6-inch POCs readily progresses to a mostly single layer in the room center by 200 years. The room continues to consolidate until it asymptotically reaches a maximum at ~1000 years (Fig. 21).

Whether a room is empty or filled, most compaction occurs vertically. Horizontally, the dimension in an empty room is reduced to~43% of the original 10.06 m.[49] The vertical reduction in an empty room is mostly closed by 180 years, and completely closed by 400 years. Easily compacted waste is near these values. For 6-inch POCs, the horizontal is ~44% and the vertical compaction is 95% (Fig. 21). The empty room has slightly less horizontal compaction because the vertical compaction is so rapid that it pinches off horizontal closure. A room of 12-inch POCs is noticeably less compacted at 88% of the original 3.96 m (Table IX).

Table IX. Modeled room closure from salt creep at WIPP 1000 years after emplacement

Room Contents	Horizontal Closure (%)	Vertical Closure (%)
Empty	42.7	100.0
6-inch POC	43.9	95.3
12-inch POC	40.8	88.1
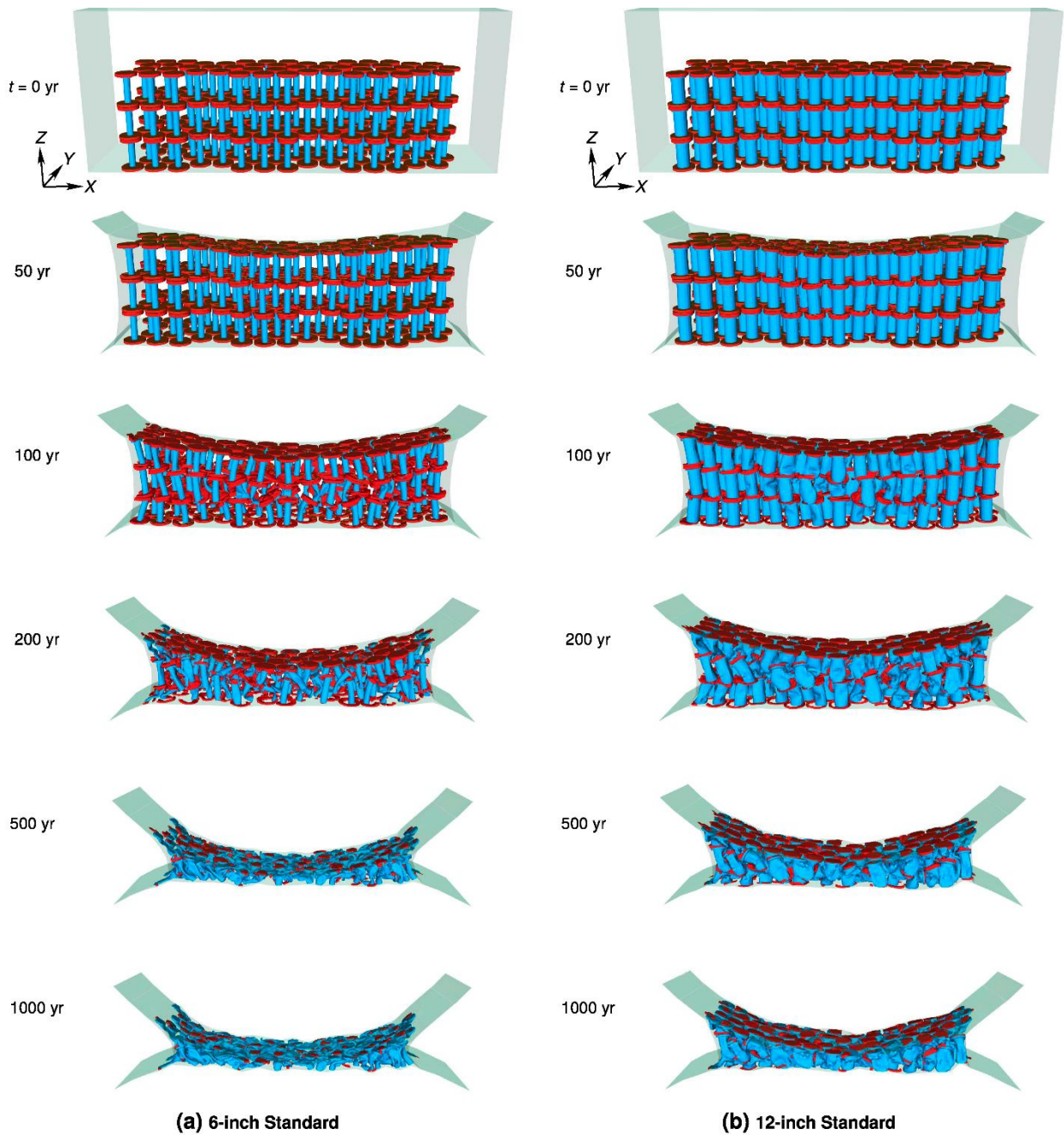
Fig. 20. Deformation of pipe overpack containers from salt creep; fiberboard, 55-gallon drums, and salt stratigraphy hidden in visualization: (a) 6-inch POCs, and (b) 12-inch POCs.[47, Figure 3-2]
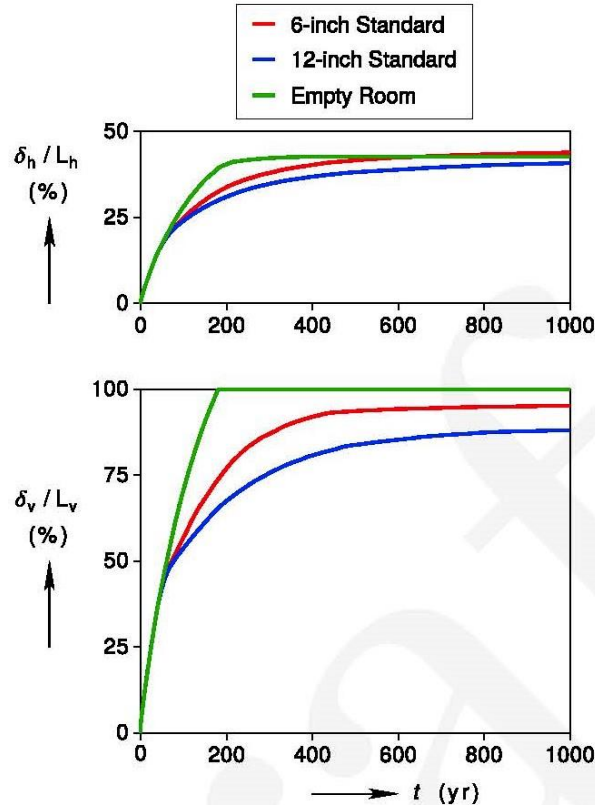
Fig. 21. Horizontal and vertical closure of WIPP disposal room empty and filled with 6-inch and 12-inch POCs.[47]

IV.C.3. Geometry of POCs in Consolidate Room at 1000 Years

At 1000 years, the minimum pitch distance between nearest neighbor centroids for 12-inch POCs is 23.3 cm, which occurred in the center of the room (Fig. 22).[47, Table 3-2] The mean and median pitch for POC is 31.5 cm. The room with 6-inch POC has a somewhat wider distribution with a mean and median pitch of 23.7; the minimum is 10.9 cm, which occurred at the room edge where two POCs buckled together.
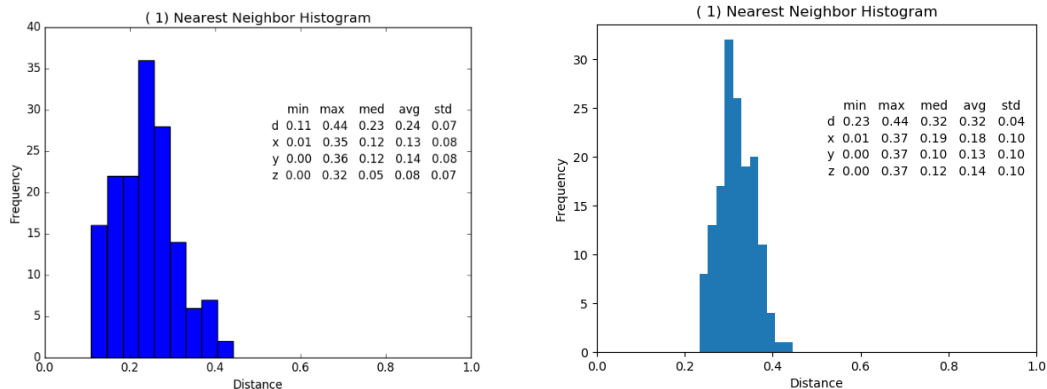
Fig. 22. Pitch distance between centroids of POCs at 1000 years in WIPP creep analysis based on first nearest neighbor (a) 6-inch POC with 23-cm average, and 11-cm minimum; and (b) 12-inch POC with 32-cm average, and 23-cm minimum.[47]
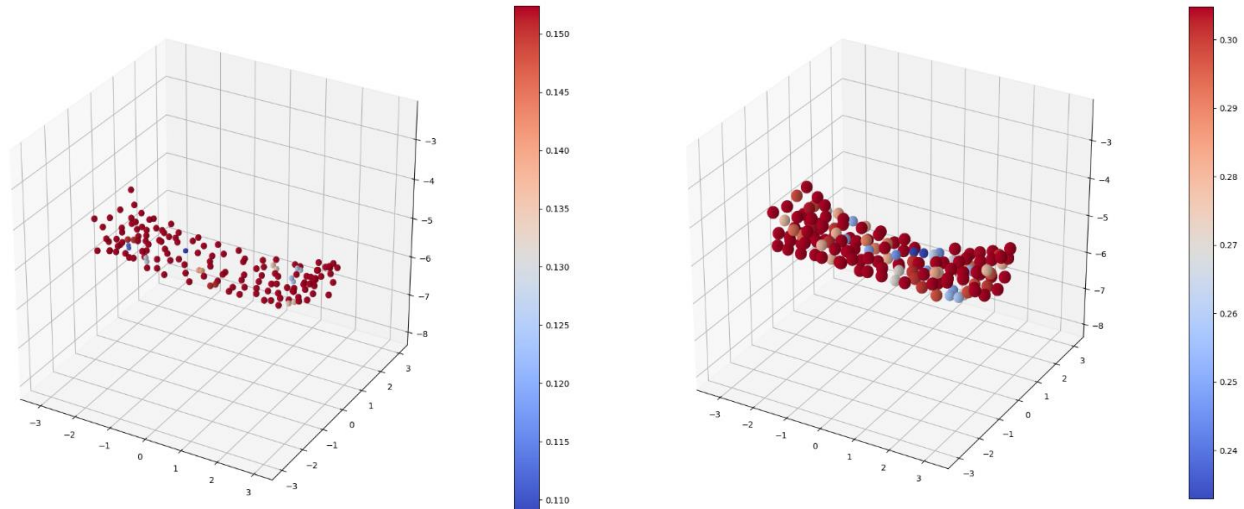
Fig. 23. Distribution of 153 spheres centered at centroids of POCs in segment of WIPP disposal room: (a) 6-inch POC with two nearest neighbors at the room edge where two buckle together; and (b) 12-inch POC with two nearest at room center.

V. CRITICALITY ANALYSIS OF PIPE OVERPACK CONTAINER ARRAY IN COMPACTED ROOMS

V.A. Criticality Analysis Assumptions

For a finite heterogeneous system, criticality depends not only on the quantity of fissile material but also on its concentration, shape, and any other material mixed with or surrounding the fissile material. Evaluating the criticality potential for a heterogeneous mixture with specific shapes and masses of fissile and other material is complex. Thus, several assumptions were made to make the analysis tractable concerning Pu waste form, moderation, shape, and materials surrounding the fissile ^{239}Pu.

V.A.1. Plutonium Waste Form

Plutonium was modeled as plutonium dioxide (PuO$_2$ with ρ_g = 11 460 kg/m^3 and 88% of density as Pu^{IV}), rather than modeled as metallic Pu or Pu with water of hydration or hydroxyl groups (i.e., PuO$_2$(OH)$_2$ • H$_2$O or Pu(OH)$_4$). For highly enriched ^{239}Pu, the mineral form only influences criticality limits when the mixture is severely under moderated.[6]

V.A.2. Plutonium Content set at Administrative Limit.

The plutonium content of a POC was set at the administrative limit of 0.2 kg Pu FME (Table V).

V.A.3. Spherical Shape

The Pu configuration was spherical to avoid making assumptions as to the initial distribution of Pu in each POC and the compaction of that material within the POC from salt creep. The ^{239}Pu density of a sphere with the inner diameter of a 12-inch POC (31.4-cm) is 12 kg/m^3; the ^{239}Pu density in a 6-inch sphere (15.8 cm) is 98 kg/m^3 (factor of 8 larger than for the 12-inch sphere). The modeling influence of salt creep was on the spacing between spheres.

V.A.2. Optimal Moderation

A POC was assumed to contain sufficient water and plastics (CH$_2$) in a volume ratio of 3 to 1 (where the plastic volume cannot be replaced with brine) for the Pu waste form to be nearly optimally moderated with hydrogen to avoid

making specific assumptions as to the pathway to criticality and the mineral form of Pu.[g] The optimum moderation was evaluated for each case analyzed.[52] For water, the optimum concentration is roughly 32 kg/m^3 and corresponds to ~22.4-cm diameter for 0.2 kg ^{239}Pu, which is <31.4-cm diameter of 12-inch POC—Fig. 6. However, the 22.4-cm diameter is greater than the 15.77-cm inside diameter of a 6-inch POC; thus, a 0.2 kg sphere of ^{239}Pu that fits inside a 6-inch pipe cannot be optimally moderated. Hence, the critical potential is reported for (a) an unconstrained diameter sphere, (b) a sphere constrained by the 6-inch pipe and, thus, not optimally moderated, and (c) a sphere constrained by a cylindrical limit.

The latter limit requires additional discussion. When a sphere is constrained by the 6-inch pipe diameter, it is possible for a cylindrical shape with diameter and height limited by the 6-inch pipe to be somewhat more reactive at small hydrogen/plutonium ratios (H/Pu) since the cylinder shape can accommodate more moderating hydrogen. In fact, the maximum H/Pu for a 6-inch sphere is ~240, the maximum H/Pu for a 6-inch cylinder is ~560, and the maximum H/Pu for an unconstrained sphere is ~800, for the range of reflector materials and spacing considered herein for repository conditions prior to 2000 years

V.A.4. Fluid mixed with Pu in Sphere

Only water or Castile brine were mixed with Pu inside the sphere in the cases reported here. Even when the situation envisioned was prior to human intrusion into the repository, Castile brine, with its lower Cl^{-1} and B^{+3} concentration compared to Salado brine (Table VIII) is used because it is conservative and avoids introducing another variable in the sensitivity analysis reported here.[52]

V.A.5. Evolution of Material in Reflector Box

The contents of the reflector sea changes to reflect the disposal room evolution through three phases described for the conceptual model: (1) salt creep compaction of containers without brine influx allow to maximum extent up to 1000 years without brine influx, (2) influx of sufficient brine for more cellulose degradation and to partially saturate pores, and (3) brine inundation to complete cellulose degradation.

V.A.6. Material in Reflector Box Surrounding Sphere

The Pu spheres (Region 1) are in a sea of reflecting material (Region 2) confined by a tightly fitting box with dimensions defined by the maximum extent of the spheres. Iron (Fe) is always modeled as rust (hematite—Fe_2O_3) even though it is present in the stainless-steel pipes and carbon-steel drums primarily as Fe^0 rather than Fe^{+3} in the first 1000 years. The oxidation state of Fe is immaterial to its behavior in reflecting neutrons in the absence of water and absorbing neutrons and dampening the potential for criticality in the presence of water. The mass of stainless steel in the pipe of the 12-inch POC is 57.3 kg (assuming the 304 stainless steel density is 7940 kg/m^3 and the volume is 7215 cm^3).[52]

Beryllium (Be), a possible component of some TRU waste because its decay contributes neutrons, is usually placed in the reflector. The Be was set at 1%wt (i.e., 1.02 kg in the 12-inch POC and 0.30 kg in the 6-inch POC). Most POCs do not have any Be and only 34 twelve-inch POCs in Panel 7 from Los Alamos National Laboratories (< 0.13%

---

[g]A hypothetical transportation condition of 75% water and 25% plastics is greatly overmoderated with concentration of ~1 kg/m^3 (H/Pu of ~6000) which is <7.2 kg/m^3 minimum critical concentration (see Table X).

by volume) report Be >1%wt. Although included for completeness, sensitivity studies showed no influence whether; mixed with the fissile material in the sphere or in the reflector box around the fissile sphere.

About 25.2 kg of fiberboard is initially present in a 12-inch POC and reduces the neutron coupling between POC until it microbially degrades. In the criticality analysis, fiberboard is modeled as cellulose ($C_6H_{10}O_5$) with a density of 224 kg/m^3.[52]

Magnesium oxide (MgO) has a large neutron scattering cross-section and thus is a good neutron reflector. MgO is emplaced above the containers but sifts down the containers sides when salt creep bursts the sacks. The MgO readily flows around and into the containers once brine inundates the disposal room; thus, MgO is mixed homogeneously with other material in the reflector box. The amount of MgO varies with the amount of salt in the cases studies but often ratio of MgO to salt around the containers is set 50/50.[52]

Salt is placed in an outer Region 3 (beyond the Region 2 reflector box) as a 10-m outer layer. Salt is also present as a neutron absorber in the Region 2 reflector box in the last of the three phases of repository conditions.[52]

V.A.7. Computational Tool

To evaluate the post-closure criticality potential of the compacted rooms, a series of models were developed with MCNP^{TM} (Monte Carlo code for solving Neutron and Photon transport equations) (v6.2)[53] using the 238 group Evaluated Nuclear Data File/B Version 7.1 (ENDF/B-VII.1) criticality library of tabulated cross-sections, which is provided in the standard release of MCNP.

V.A.8 Critical Limit

The average uncertainty in the MCNP analysis for the multiplication factor for a finite system (k^{eff}) is ~0.0006.[52, p. xiii] In geologic systems, however, factors such as variation in configuration geometry, the porosity, saturation, and host rock composition have much more influence on whether the system is critical than calculational biases and uncertainties in k^{eff}. Hence, we assume the critical limit is unity (i.e., critical limit = 1 − (calculational bias + uncertainty)), and that the system is subcritical when $k^{eff} < 1.0$ for post-closure.

V.B. Criticality Analysis of Fully Compacted Room up to 1000 years

V.B.1. Waste Conditions Inside Pipe of POC

The first phase assumed mostly dry conditions to allow maximum compaction of the room with little gas generation; hence, no brine has mixed with water inside the POC.

V.B.2. Conditions Outside Pipe

Conditions envisioned outside the containers up to 1000 years include

1. No brine between POCs spheres (i.e., fairly dry conditions so that maximum compaction occurs because little gas is generated to arrest creep closure)

2. No salt between POCs spheres because the salt may not have had time to completely encapsulate the waste

3. No MgO between POC spheres

4. Iron oxide (Fe_2O_3) (e.g., 57.2 kg of iron in 12-inch stainless steel pipe).

5. At least 60% of fiberboard dunnage remains

The fifth condition assumes the maximum rate of microbial degradation of cellulose as brine seeps into the waste to produce gases such as carbon dioxide (CO_2). The fastest rate of microbial degradation occurs when brine is readily available. Although we are assuming little microbial gas generation in the first 1000 years to allow for the maximum compaction, the fastest rate places a bound on the maximum amount of fiberboard dunnage that would be consumed over 1000 years. For the undisturbed scenario with no inadvertent intrusion, the repository exposure model for CRA-2019 calculates a range of future repository behavior predicated on features and processes (phenomena) included, and the associated uncertainty in parameters (expressed as distribution ranges). However, at least 60% of all the cellulose in the repository remains (Fig. 24).
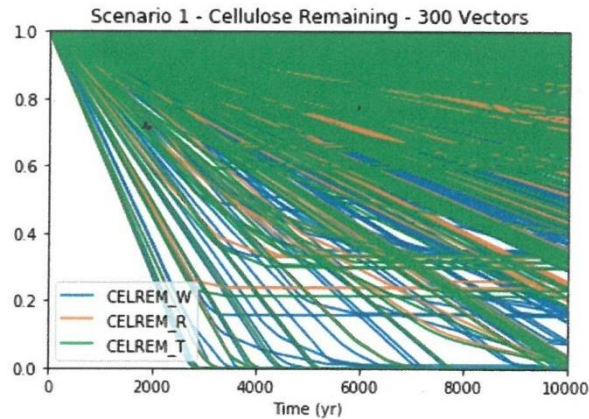
Fig. 24. Cellulose remaining in repository waste panel (CELREM_W), rest-of-repository (CELREM_R), and total repository (CELREM_T) at various times for undisturbed scenario in 300 simulations of CRA-2019

With only 60% of the initial fiberboard dunnage present in the first 1000 years, a room full of 6-inch or 12-inch POCs is subcritical (i.e., $k^{eff} < 0.961$ for 6-inch POC and <0.913 for 12-inch POC—Fig. 25). Furthermore, the reactivity of the irregular array of POC was dominated by a few POC in close proximity at the right side of the WIPP room (Fig. 26).

Three cases were also run to examine the sensitivity to type and amount of material between POC when dry. The first sensitivity case included 100% of the initial fiberboard to examine the influence of the conservative assumption on reactivity. The influence was small but differed for the 6-inch and 12-inch POC. For the 6-inch POC, more fiberboard increased reactivity 1% from 0.961 to 0.971; for the 12-inch POC, more fiberboard decreased the maximum k^{eff} 2% from 0.913 to 0.893 (Fig. 25). Evidently, as the pitch between the spheres decreases, the influence of reflector material changes.

The second sensitivity case excluded the mirror reflective boundary conditions in the y-direction down the length of the WIPP disposal room to examine how close 153 spheres sufficiently represented room reactivity. The difference was minor. For the 6-inch POC, the no-mirror boundary condition increased the maximum k^{eff} 1% from 0.961 to 0.97; for the 12-inch POC, the no-mirror boundary condition reduced the maximum k^{eff} 0.7% from 0.913 to 0.906.

The third sensitivity case modeled just salt in the reflector box around the spheres, rather than fiberboard, iron oxide, and beryllium. The results were very similar, suggesting the type of adsorbing material between POC does not have a strong influence. The maximum k^{eff} for only salt in the reflector was reduced 0.6% (from 0.961 to 0.055) for

the 6-inch POC and increased 1.8% (from 0.913 to 0.929) for the 12-inch POC. However, the location of the maximum k^{eff} noticeably shifted for the 12-inch POC from H/Pu of 1370 to 1100.
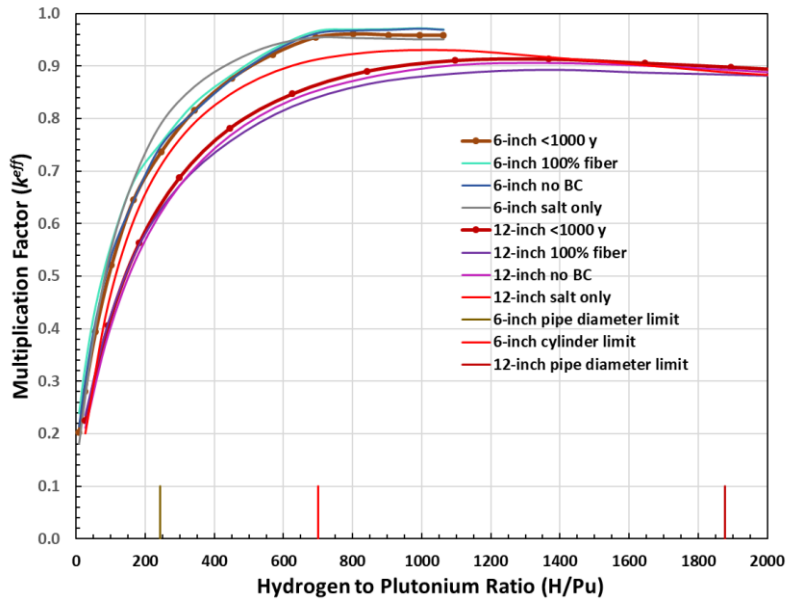
Fig. 25. Multiplication factor for compacted array of 6-inch and 12-inch POCs prior to 1000 years as represented by 153 spheres with 0.2 kg ^{239}Pu moderated only with water and plastics and reflected by iron oxide and fiberboard (60% and 100% initial mass) with and without mirror boundary conditions to model infinite extent down axis of WIPP disposal room.[52, Figures G-1 and G-2]
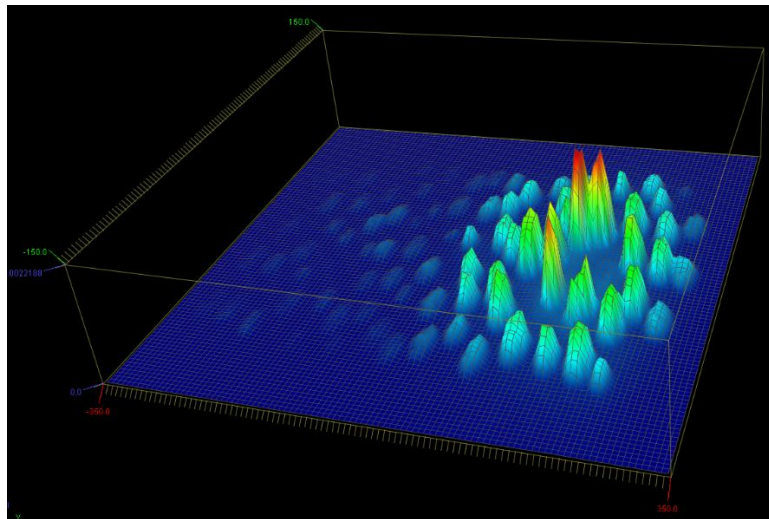
Fig. 26. Neutron tallies for 12-inch POC showing k^{eff} dominated by a few locations on right side of WIPP room segment.

V.C. Criticality Analysis of Partially Degraded Fiberboard Dunnage with Some Brine

At some point, sufficient brine enters the disposal rooms such that substantial microbial degradation of the fiberboard dunnage occurs along with more corrosion of the POC stainless and carbon steel. While the loss of the much of the fiberboard allows more neutron coupling between individual containers, the presence of Cl^{-1} and B^{+3} in

the brine dampens the reactivity. Although many combinations of brine and fiberboard can occur during the transition, one case was modeled where

1. No salt or MgO is in reflector box since the resultant gas generation arrests salt creep and prevents complete encapsulation of the drums.

2. 20% Castile brine is present in the reflector box but the containers are assumed to be sufficiently intact to prevent brine mixing with the fissile material.

3. 40% of the fiberboard remains

The presence of only 20% of the interstitial space between containers (Region 2 reflector box) filled with brine is sufficient to dominate the behavior of the POC assembly. For the 6-inch and 12-inch POCs, k^{eff} decreases 6% from 0.961 to 0.902 for 6-inch and from 0.913 to 0.855 for 12-inch (Fig. 27). The 6% decrease is noticeably greater than the 1 to 2% change in k^{eff} in the sensitivity studies observed prior to 1000 years (Fig. 25).
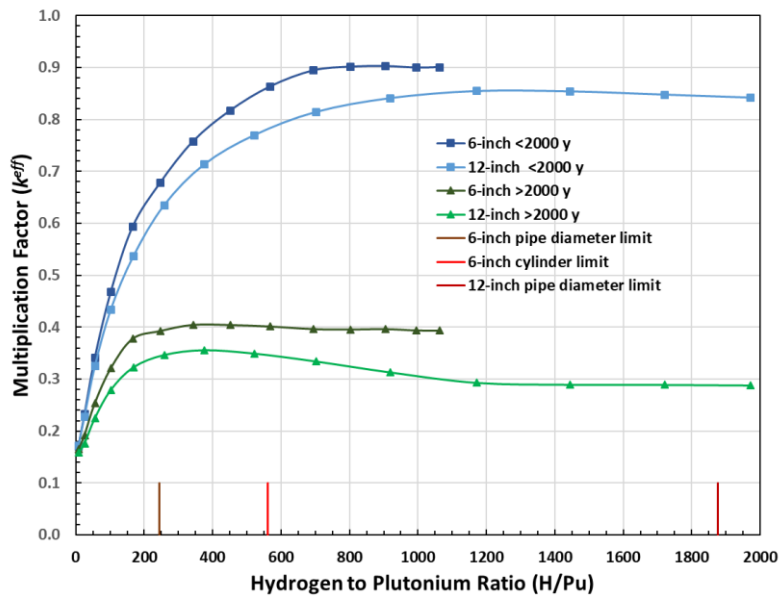
Fig. 27. Multiplication factor for compacted array of 6-inch and 12-inch POCs prior to 2000 years when some brine resides between POCs and after 2000 years when degradation has occurred such that brine resides inside the POC.[52, Figures G-1 and G-2]

V.D. Criticality Analysis of Fully Degraded Fiberboard with Brine Inundation

The final compaction phase modeled in the criticality analysis is between 2000 and 10,000 years where

1. All fiberboard dunnage has degraded

2. Salt and MgO is present between the remnants of POCs

3. Castile brine dominates absorbed fluid within $^{239}PuO_2$ waste (i.e., containers have completely degraded)

The reactivity of the POC room ensemble continues to decrease as more brine is mixed with the POCs (Fig. 27) The k^{eff} decreases ~60% from the first compaction phase without brine; specifically, from 0.961 to 0.405 for 6-inch POCs and from 0.913 to 0.356 for 12-inch POCs.

VI. CRITICALITY ANALYSIS OF CH AND RH CONTAINERS
VI.A. POC Behavior Bounds Standard CH-TRU Drum Behavior

The maximum fissile limit in any one standard CH-TRU drum is 0.2 kg Pu FME (Table V). The ^{239}Pu concentration is 2.0 kg/m^3 for a sphere with a 0.57-m internal diameter of a drum, like the POC criticality analysis. Alternatively, the density in any one drum is 0.94 kg/m^3 in 0.2137 m^3 (internal dimensions of 55-gallon drum—Fig. 10) for^{239}Pu uniformly dispersed throughout the waste. Based on the porosity reduction for the CCA-1996 (Fig. 16), salt creep could mechanically compact the uniformly dispersed waste in one drum to a higher Pu density of 2.2 kg/m^3 (i.e., 2.4•0.94 kg/m^3 where the factor 2.4 is discussed in §IV.B.1), which is similar to that of the spherical concentration.

The behavior of 6-inch POCs likely bounds standard CH-TRU drum behavior because of three reasons. First, both containers are structurally weak and thus allow for the maximum compaction from salt creep. Second, the 98-kg/m^3 fissile concentration of a compacted sphere constrained by the inside diameter of a 6-inch POC is greater than the 2-kg/m^3 Pu concentration of a compacted sphere constrained by the inside diameter of a 55-gallon drum, each at the administrative limit of 0.2 kg Pu FME. Third, the 1.4 kg Pu FME transportation limit in the 6-inch POCs is 77% greater than the 0.325 kg Pu FME transportation limit in every 7-pack (in a HalfPACT), or 14-pack (in TRUPACT-II) of 55-gallon drums (Table V). Hence, replacing 6-inch POCs in a room with CH-TRU 55-gallon drums, which have the same areal footprint (Table VI) will reduce room reactivity.

VI.B. Fissile Concentration Less in Large Drums and Containers

A similar rationale applies to larger drums (i.e., 85-gallon, 100-gallon drums), which all have a similar footprint and the same transportation limit of 0.325 Pu FME; thus, room reactivity will certainly be less than for the 6-inch POC. Furthermore room reactivity will be less than 55-gallon drums, because the initial fissile concentration is smaller because of the large volume (0.31 m^3 for 85-gallon drum and 0.38 m^3 for 100-gallon drums—Table VI) yet same 0.2-kg Pu FME administrative limit (Table V). The larger containers also have a smaller initial fissile concentration even though the transportation limit is 0.325 kg Pu FME. The standard waste box (1.35 m^3), large standard waste box (7.39 m^3), and the 10-drum overpack (2.05 m^3) have initial concentrations of 0.24 kg/m^3, 0.044 kg/m^3, 0.159 kg/m^3, respectively (Table V). The final fissile density will also likely be less because compaction is not easily increased from that of the smaller standard 55-gallon drums, as demonstrated by the difference in compaction from 6-inch POCs and 12-inch POCs (Fig. 20). Thus, criticality is not possible from compacting large CH-TRU waste containers.

VII. RH-TRU CONTAINERS AND CRITICALITY CONTROL CONTAINERS
VII.A. Neutronic Isolation of RH-TRU Canisters Placed in Room Wall

As noted in §III.D.6, 2005 containers in 719 RH-TRU payload canisters (i.e., often 3 containers per canister) have been placed in room walls at WIPP. The 0.66-m diameter canisters are emplaced in 0.7 m diameter boreholes spaced 2.4 m apart centerline to centerline (Fig. 13 and Fig. 28a).

The 2.4 spacing (with 1.7 m of salt) is sufficient to neutronically isolate the canisters from each other (Appendix A); thus, they cannot function as a heterogeneous array (Fig. 28b). Hence, the canister fissile mass limits are sufficient to prevent criticality. That is, the canister content is limited to 0.315 kg FME Pu without ^{240}Pu (Table VII), which is < 5.3 kg when optimally moderated in Salado brine, <3.3 kg when optimally moderated Castile brine, and < 0.5 kg when optimally moderated in water.[5]
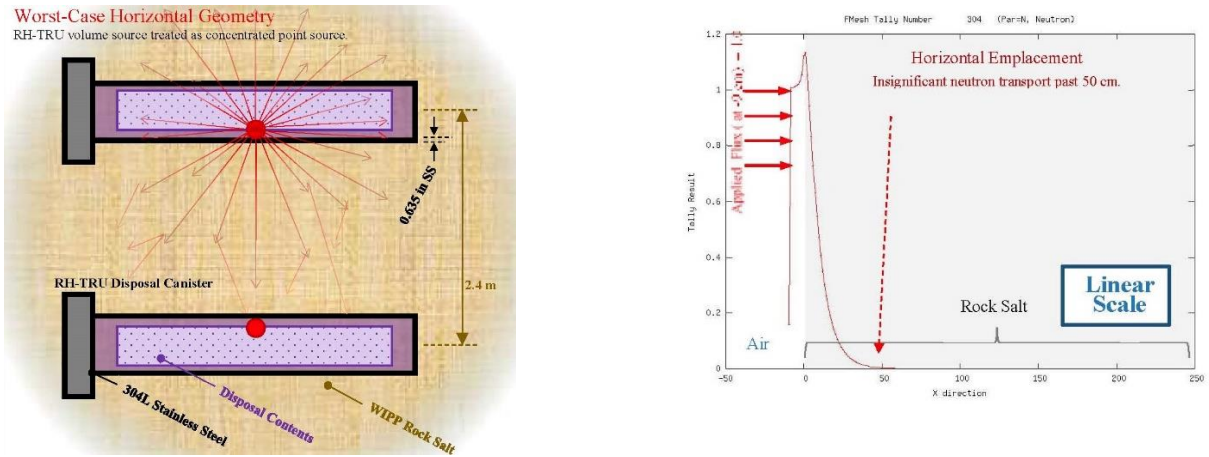
Fig. 28. Calculation of neutron communication between RH-TRU payload containers emplaced horizontally in WIPP salt with contents modeled as single neutron source using 1-D planar flux in MCNP without absorption credit taken for stainless steel (a) conceptual model, and (b) results showing salt isolation (Appendix A).

VII.B. POC Behavior Bounds RH-TRU Shielded Container Behavior

The 2.54 cm of lead and 0.794 cm of carbon steel in a shielded drum with RH-TRU (Fig. 29a) is sufficient to drop the surface exposure dose from γ radiation to that of CH-TRU; however, 35% of neutrons are able to penetrate (Fig. 29b) and so an array of shielded drums disposed in a disposal room is not neutronically isolated by the lead shielding.
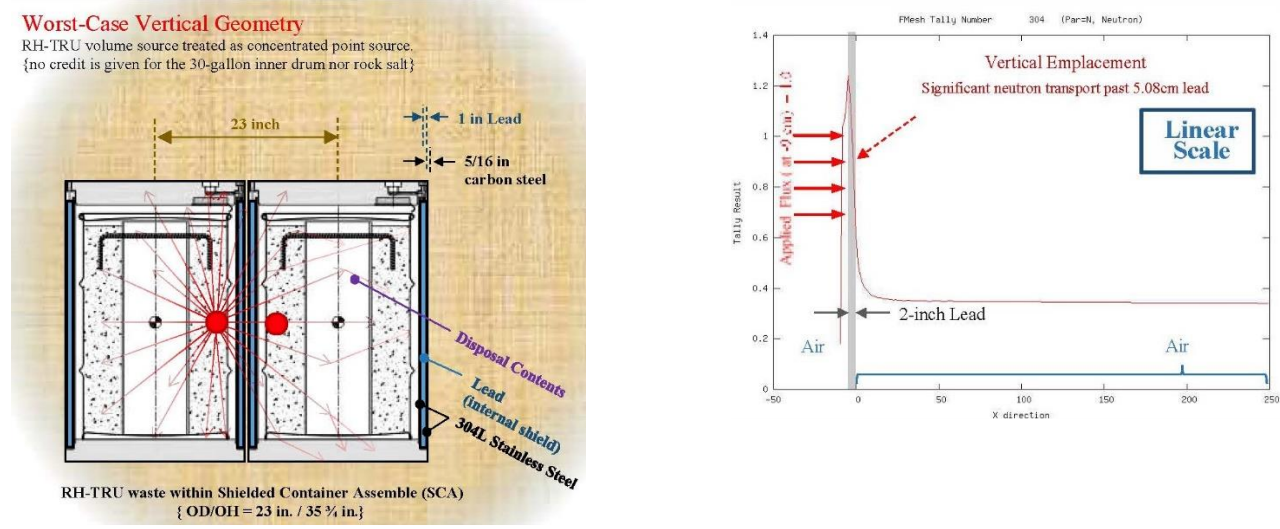
Fig. 29. Calculation of neutron communication between RH-TRU shielded containers emplaced in WIPP disposal rooms with contents modeled as single neutron source using 1-D planar flux in MCNP without absorption credit taken for carbon steel drum (a) conceptual model, and (b) results showing neutron flux reduced only 65% (Appendix A).

The behavior of 12-inch POCs, however, conservatively bound RH-TRU shielded container behavior because of three reasons. First, both containers are structurally stiff and similar dimensions and thus shielded containers would behave similarly to the 12-inch from salt creep. Second, the 12-kg/m^3 fissile concentration of a compacted sphere inside a 12-inch POC is greater than the 2.8-kg/m^3 fissile concentration of a sphere inside a shielded container, each

with 0.2 kg Pu FME. Third, the fissile mass of 1.4 kg Pu FME for the POC is 77% greater than 0.325 kg Pu FME for the 3-pack, each with a similar footprint (3.52 m^2 versus 3.31 m^2–Table VI).

VII.C. Current Low ^{239}Pu Concentration in Shielded Containers for RH-TRU

The current situation for the RH-TRU shielded drum is far from critical. The 27 drums from ANL have an average uranium mass of 0.0047 kg of U at 11.7% enrichment (i.e., 0.000555/0.117 from §III.D.6) and uranium concentration of 0.064 kg/m^3 in sphere (i.e., 0.0047 U $kg/0.073$ m^3). The combined uranium mass of 0.128 kg (i.e., 27* 0.0047) is much less than 7.5 kg, which is the critical mass for 15% enriched uranium in water and where we are comparing with uranium critical limits since most of the ^{239}Pu FME derives from ^{235}U.[5]

VI.D. Physical Criticality Control for Non-Pit Surplus Plutonium in Criticality Control Containers

Non-pit surplus ^{239}Pu is likely to be oxidized to PuO_2 and mixed with a concrete-like material to produce a waste form that would be shipped in critical control container (CCC). Each CCC contains up to 0.38 kg ^{239}Pu at a solid concentration of 185 kg/m^3 in a small cylinder with a diameter of 15.4 cm and height of ~11.0 cm, depending on waste matrix composition and additives (Fig. 10). A defined waste form creates the opportunity for engineered options, such as limiting water content to less than 10% and limiting polyethylene bagging to less than 0.40 kg to reduce neutron moderation. Furthermore, current plans are to add at least 50 g B_4C to the ^{239}Pu mixture in each CCC makes criticality highly unlikely even if all the cylinders of surplus Pu mass in a disposal room are assembled together without any material between cylinders, as discussed in a supporting report.[8]

VIII. SUMMARY

Compaction of transuranic (TRU) waste by salt creep cannot cause criticality after closure of the Waste Isolation Pilot Plant (WIPP), an operating repository in bedded salt for geologic disposal of TRU waste from atomic energy defense activities, based on the qualitative low-probability rationale presented here. Furthermore, criticality has not been included in the performance assessment for the 2019 Compliance Recertification of WIPP based on combining this rationale with the rationale that hydrologic and geochemical conditions also cannot sufficiently concentration fissile plutonium (^{239}Pu) and uranium (^{235}U) elsewhere within the WIPP disposal system (as presented in a companion memorandum[7]).

Herein, the probability of criticality is notionally conceived as the sum of the probability of salt-creep sufficiently compacting four categories of containers disposing TRU waste: (1) pipe overpack containers, (2) drum and box containers, (3) criticality control containers (none yet emplaced), and (4) canisters and shielded containers. The first three categories are for contact-handled TRU waste. The last category is for remote-handled TRU waste. The probability of criticality from compaction is very low for these four container categories because criticality cannot occur for a representative salt-creep compaction calculation with bounding fissile loading in the container and bounding estimates of material present in and about the container, as discussed below.

VIII.A. Constraints on Pipe Overpack Container Criticality in Repository

VIII.A.1. Pipe Overpack Containers

CH-TRU waste from cleaning up the Rocky Flats plant in Colorado was sent to WIPP and placed in Panels 1 and 2 in ~17 000 12-inch pipe overpacks (POCs).[22] Since that time ~10 000 more POCs from various sources have been sent to WIPP. Although representing 15% of the total number of containers, the POCs represent a small portion of the total volume of TRU waste received at WIPP. As the volume is currently measured using the internal volume of outer most container, 75 800 m^3 has been received at WIPP, of which 1270 m^3 is in POCs (1.7%). The current contents of POCs consist mostly of cellulose (73% by volume). Other contents include 2%vol plastics, 7%vol iron-based metals, 2%vol other metal alloys 14%vol other inorganic material, and 3% solidified inorganic material. Of the 1270-m^3 waste volume disposed in POCs at WIPP, standard 12-inch POC represents 99.9%vol. No standard 6-inch POCs have been used but are authorized for disposal and so included in the criticality evaluation. Other POCs use either a variation of the 12-inch (0.1%) or the 6-inch POC (0.01% and, thus, are represented by the two standard POCs in the criticality analysis.

VIII.A.2. Salt Creep Analysis of Room Filled with Discrete Pipe Overpack Containers

High-fidelity salt creep simulations were conducted of a room filled with 153 discrete POCs to predict a representative final configuration. The four POC components (internal stainless-steel pipe, its plywood stabilizer on the top and bottom, the fiberboard dunnage, and outer 55-gallon carbon steel drum shell) were discretely modeled with individual elastic-plastic-failure material models.[47; 49] Salt creep was modeled with an updated Munson-Dawson model that matched vertical closure rates measured at WIPP. [50; 51] Although the model was reasonably realistic, several conservative assumptions were employed to promote more compaction and facilitate the numerical computations: (a) the stainless steel pipes were empty; thus, structural stiffening from some forms of TRU was omitted; (b) plywood was assigned a weak failure strength, (c) container elements were deleted from the analysis once they become severely distorted or the material fractured (e.g., plywood quickly splintered and thus not much of the plywood elements remain

at 1000 years—Fig. 30). With 153 discrete POCs, the calculation progressed in a feasible amount of time (2.5 weeks) yet produced a wide variety of deformed spacing between POCs.

Shortly after the room ceiling contacts the POC drums in the simulations, the POC drums begin to buckle. Buckling allows the POCs to slide past each other such that containers in upper layers are thrust into the bottom layer Once the containers buckle, they offer little resistance to vertical room closure until mostly a single layer is formed in the room center. The room continues to consolidate until it asymptotically reaches a maximum at ~1000 years (Fig. 30). For 6-inch POCs, the horizontal compaction is ~44% of the original 10.08 m width and the vertical compaction is 95% of the original 3.96 m height. A room of 12-inch POCs is noticeably less compacted at 88%. The final coordinate positions of the centroids of each POC are used in subsequent criticality calculations.

(a) 6-inch Standard   **(b) 12-inch Standard**
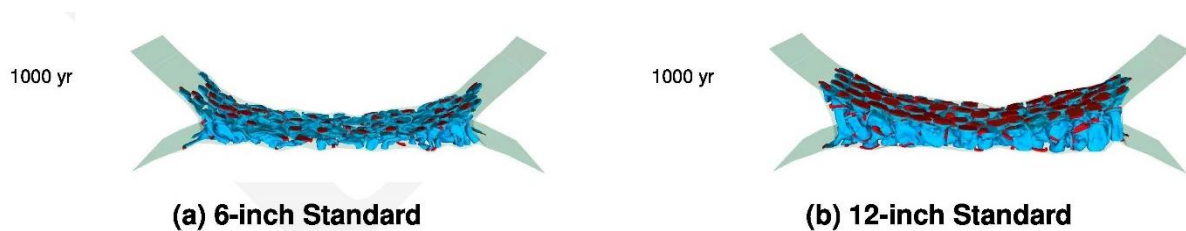
Fig. 30. Deformed individual inner pipes of the standard pipe overpack container in a representative WIPP disposal room consolidated from salt creep at final 1000-year configuration; the outer drum, fiberboard dunnage on sides, and detailed bedded salt stratigraphy are included in the analysis but removed in the visualization; the red elements represent the plywood, which stabilizes the pipe during transport, that is conservatively removed when excessively deformed (i.e., splintered and failed).[47, Figure 3-2]

VIII.A.3. Rock Fall Analysis of Room Filled with Discrete Pipe Overpack Containers

During the first 20 years of room closure, some rock fall may occur along with rapid salt creep closure. A discrete rock fall model was constructed to evaluate the potential of rock fall scattering and clustering POCs and, thereby, potentially producing a reactive POC configuration prior to full compaction from salt creep. Several conservative assumptions were made to produce a bounding case: (a) one large right-triangular-shaped block with one thick side is used to promote some moment and uneven impact, (b) the large block is not allowed to break into pieces, (c) each layer of POCs is offset by 2.54 cm to promote minor instability; (c) rock fall occurred immediately so that the largest free-fall distance exists; and (d) the large polypropolyene sacks holding magnesium oxide are omitted to increase the free-fall distance and avoid dissipating the rock fall shock. As in the salt creep analysis, the four POC components are discretely modeled with individual elastic-plastic-failure material models; however, stainless steel, carbon steel, and plywood parameters, which are based on slow strain rate experiments, are not increased to more appropriately model shock conditions. Furthermore, the plywood strength is reduced 80% to promote greater inner pipe movement, and the minimum yield strength of stainless and carbon steel was used.

In the roof-fall simulations, the salt block lands almost flat, bounces slightly, and settles on top of the drum ensemble, causing less than 5% drum deformation, without noticeably changing the disposed configuration of the POCs. Consequently, large salt block falls shortly after disposal are not likely to cause collapse and major clustering of drums prior to later salt creep.

VIII.A.4. Material around POCs as WIPP Disposal Room Evolves over 10 000 Years

As documented for operations,[18; 19] an infinite array in the x- and y-directions of uncompacted POC containers, each with 0.2 kg of Pu fissile mass equivalent (FME) and reflected by 62 cm of MgO on the top of a stack of 3 containers and 300-cm salt above the MgO and bottom of containers, is subcritical at emplacement because of the initial, uncompacted spacing between drums (58-cm outer diameter and 88 cm outer height—Fig. 6).

Because spacing is so important, the maximum opportunity for criticality occurs at maximum room closure from salt creep. Yet, criticality analysis shows that a maximally compacted array of POCs is not critical when material in and around the container is included for three phases of WIPP disposal room evolution: (1) initial phase of salt creep with no brine present (thus avoiding gas generation by metal corrosion and cellulose degradation) and thereby allowing the maximum compaction of containers up to 1000 years; (2) a transitional phase with influx of some brine to partially saturate pores and initiate metal corrosion and cellulose degradation up to 2000 years; and then (3) a final phase with the influx of more brine that fully saturates containers to complete metal corrosion and cellulose degradation followed by partial drying sometime before the end of the 10 000-year regulatory period.

The rationale is primarily focused on the evolution of repository conditions prior to humans unknowingly intruding into WIPP (i.e., undisturbed conditions). Inadvertent intrusion, a disruptive condition required by the Environmental Protection Agency in their disposal regulations, does not produce additional conditions conducive to criticality from compaction, unless the inadvertent intrusion also intersects a brine pocket in the Castile Formation below the WIPP repository. To conveniently include this intrusion condition, Castile brine was conservatively used throughout the criticality analysis since it has less boron and chloride to curtail criticality than brine from the Salado Formation, which hosts the WIPP repository (Table VIII).

VIII.A.5. Fiberboard and Iron Isolates Pipe Overpack Containers while Repository Dry up to 1000 Years

Maximum room closure from salt creep in the first 1000 years occurs when (a) no gas from waste degradation and container corrosion is generated, or (b) generated gas readily and continuously leaks out of the repository. The later situation cannot occur (a) for permeabilities measured for the salt and anhydrite layers that host the WIPP repository, or (b) continuously over 1000 years from a short inadvertent human intrusion event borehole. No gas is generated if no metal corrosion or microbial degradation of organics (primarily cellulose and some plastics and rubber) occurs. In turn, no degradation implies that the general integrity of the inner stainless pipe is maintained and fiberboard (cellulose) dunnage in the POC remains. As with any material that separates the POCs, the fiberboard dunnage provides neutronic isolation between containers, even when it is compacted. Similarly, the iron in the inner stainless pipe absorbs some neutrons and the general integrity of the pipe limits the size of fissile material shapes.

A compacted array of POCs is subcritical in a criticality analysis of a disposal room with three regions, defined in a model using MCNP (Monte Carlo code for solving neutron and photon transport equations), version 6.2 with ENDF/B- VII.I cross-section library. Region 1 is represented with (a) 153 spheres, (b) sphere spacing calculated by salt-creep modeling described above (§VIII.A.2), (c) sphere diameter constrained by distance to the nearest neighboring sphere, (d) each sphere contains 0.2 kg of fissile plutonium (^{239}Pu) that is moderated with hydrogen-bearing water (H_2O) and plastic (CH_2) in a volume ratio of 3 to 1 (where the plastic volume cannot be replaced with brine). The spheres of Region 1 are in a sea of reflecting material (Region 2) with dimensions defined by the maximum extent of the compacted spheres. The reflecting material in Region 2 consists of (e) iron from POC containers, (f) 60%

of fiberboard (cellulose) dunnage, and (g) 1%wt beryllium. Around the box of Region 2 is the box of Region 3 that consists of 10 m of salt (Fig. 31).

A maximum fissile content of 0.2 kg in each sphere is used to match administrative limits. Water and plastic are used in the first 1000 years to match transportation accident conditions,[h] and 153 spheres are used to match the high-fidelity modeling of 153 discrete POCs to represent typical compaction from salt creep. However, a repeating boundary condition was applied in the y-direction of the room to represent a full room. The 60% of fiberboard dunnage is used under the conservative assumption that microbial degradation occurs at the maximum rate even though brine is not present to promote degradation.
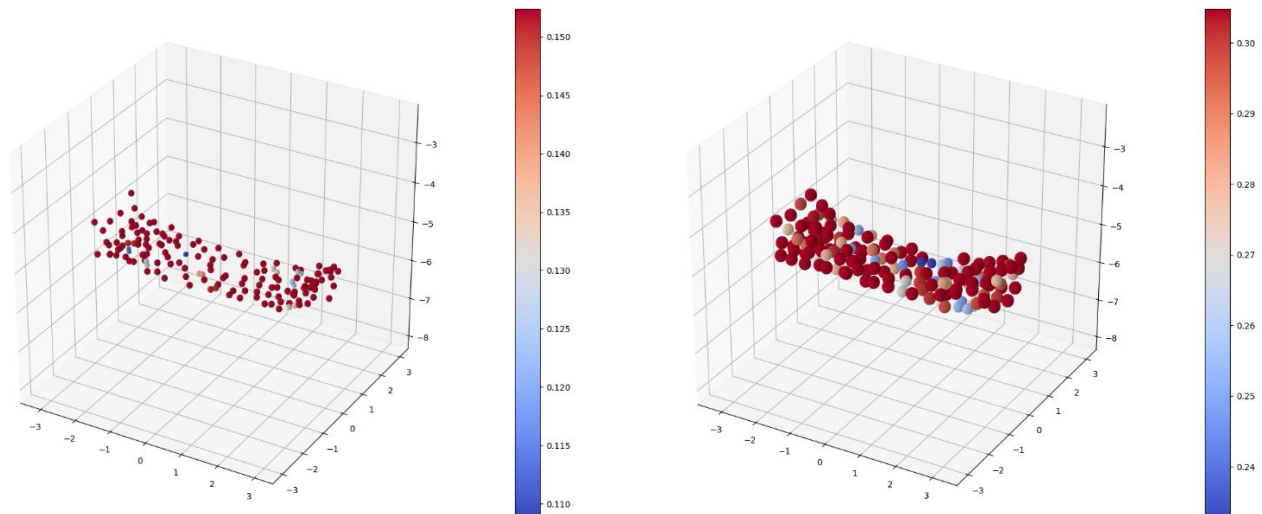
Fig. 31. Distribution of 153 spheres centered at centroids of POCs in WIPP disposal room with the full width (x-direction), full height (z-direction), and a segment in the y-direction: (a) 6-inch POC with two nearest neighbors at the room edge where two buckle together; and (b) 12-inch POC with two nearest at room center.

A sphere is used for the 12-inch pipe because its minimum surface area minimizes neutron leakage and, thus, maximizes reactivity. The optimum moderation is used for the 12-inch pipe to also maximize reactivity. Both assumptions make it possible to avoid specifying how the configuration occurred.

However, the 6-inch pipe poses a unique situation. An optimally moderated sphere cannot fit inside a 6-inch pipe that maintains its integrity in the first 2000 years. Yet, when a sphere is constrained by the 6-inch pipe diameter, it is possible for a cylindrical shape with diameter and height limited by the 6-inch pipe to be somewhat more reactive at small hydrogen/plutonium ratios (H/Pu) since the cylinder shape can accommodate more moderating hydrogen. Hence, the neutron multiplication factor (k^{eff}) for room filled with 6-inch POCs is reported at (a) an sphere with unconstrained diameter, which occurs at H/Pu of ~800 H/Pu;[i] (b) a sphere constrained by the 6-inch pipe diameter, which occurs at H/Pu of ~240 and, thus, not optimally moderated; and (c) a sphere constrained by a cylindrical limit, which occurs at H/Pu ~560, (Fig. 32). Specifically, a deformed array of 6-inch POCs is subcritical when unconstrained

---

[h] Assuming POCs are fully moderated with water and plastics is extremely conservative but one of the extreme assumptions for transportation.
[i] The maximum k^{eff} occurs at a H/Pu ratio of ~1200 (diameter of ~22.5 cm), while the H/Pu ratio at a diameter of 31.4 cm (inner diameter of a 12-inch sphere) occurs at ~1880 (Fig. 32).

($k^{eff} < 0.96$) (Table XI); when compared to a cylinder ($k^{eff} < 0.92$); and, significantly so, if the sphere diameter is constrained by the inner diameter of the inner 6-inch pipe ($k^{eff} < 0.72$) (Fig. 32). A deformed array of 12-inch POCs is also subcritical ($k^{eff} < 0.91$).

VII.A.6. Brine and Iron Adsorb Neutrons and Fiberboard Isolates POCs up to 2000 Years

A compacted array of POCs becomes less critical when brine enters a fully compacted disposal room that supports microbial degradation of the fiberboard up to 2000 years. Specifically, a deformed array of 6-inch POCs is less critical ($k^{eff} < 0.90$), and significantly so, when constrained by the diameter of the inner 6-inch pipe ($k^{eff} < 0.67$) (Fig. 32). A deformed array of 12-inch POCs is also less critical ($k^{eff} < 0.85$). These results are based on MCNP analysis of a compacted array of POCs as represented in Region 1 by (a) 153 spheres (b) sphere spacing calculated from salt-creep modeling, (c) sphere diameter constrained by distance to nearest neighboring sphere, (d) 0.2-kg ^{239}Pu sphere contents moderated with water and plastics. The reflector material in Region 2 still includes iron oxide but has changed to 40% fiberboard dunnage and adds Castile brine. The Castile brine only occupies 20% of the available volume representing the interstitial space between POCs.
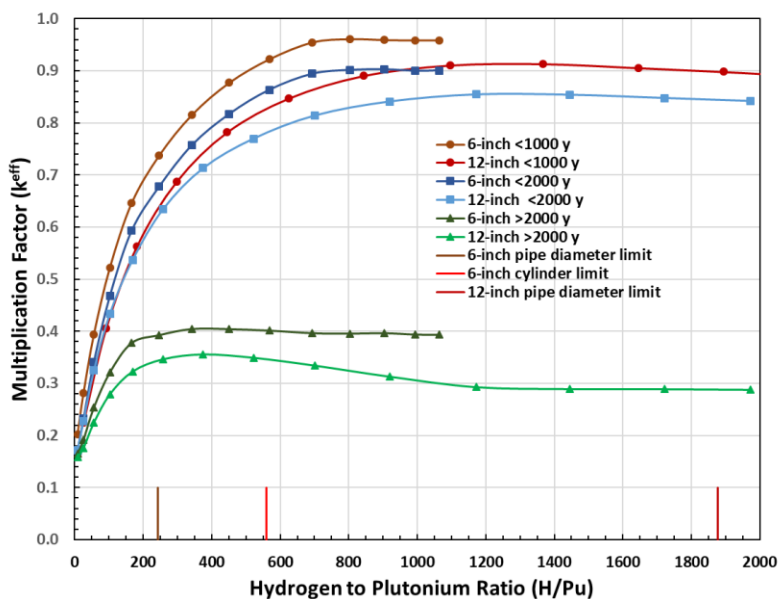
Fig. 32. Maximum multiplication factor of 6-inch and 12-inch pipe overpack containers vary from 0.96 and 0.91, respectively, for repository conditions prior to 1000 years to 0.90 and 0.85 for conditions prior to 2000 years and to 0.40 and 0.36 for conditions after 2000 years.[52, Figures G-1 & G-2]

VIII.A.7. Neutrons Adsorbed by Brine Around Pipe Overpack Containers After 2000 Years

A compacted array of POCs is far from critical when brine mixes with the ^{239}Pu sphere contents as would occur after full brine inundation (possibly after inadvertent human intrusion) with subsequent drying sometime before the end of the 10 000-year regulatory period. Specifically, an analysis of a deformed array of 6-inch POCs is far from critical ($k^{eff} < 0.40$) (Fig. 32). A deformed array of 12-inch POC is also far from critical ($k^{eff} < 0.35$). Hence, criticality will not occur in a room full of POCs from physical compaction, especially if brine is present. Similar to other phases, Region 1 includes (a) 153 spheres, (b) sphere spacing calculated from salt creep modeling, (c) sphere diameter constrained by distance to nearest neighboring sphere, (d) spheres containing 0.2 kg of fissile ^{239}Pu moderated with

plastics. However, the water in Region 1 is replaced with Castile brine. The Region 2 reflector consists of iron oxide, magnesium oxide, salt, and 20% of interstitial porosity filled with Castile brine.

VIII.A.8 Mixing 6-inch and 12-inch POCs and bounding reactivity for other containers

The reduction in reactivity between the 6-inch POC and 12-inch POC remains fairly consistent for the 3 repository phases (Fig. 32). Consequently, if a 7-pack of 12-inch POCs replaces a 7-pack of 6-inch POCs in a disposal room full of 6-inch POCs (with each 7-pack at the maximum fissile content of 1.4 kg Pu FME), the room reactivity will likely decrease proportional to the number of 6-inch and 12-inch 7-pack POCs because the footprints, heights, and maximum fissile content are identical.

Furthermore, the room reactivity of 6-inch and the 12-inch POCs bound the reactivity of all other container groupings disposed at WIPP except the criticality control containers, because the disposal footprints for all containers are similar; yet, the allowable fissile mass in other container groupings is reduced 77% from 1.4 kg to 0.325 kg Pu FME (Table X). Specific, examples are presented for the RH-TRU shielded containers and CH-TRU drums and boxes in the following sections.

Table X. Transportation fissile limits for shipping casks, administrative fissile limits for individual containers, and bundled volumes and footprints of TRU containers used at WIPP.

Payload Container					Bundle for Shipping and Disposal				Shipping Cask	
Type [a]	Admin Fissile Limit (kg)	Diameter Width × Length (cm)	Height (cm)	Waste Volume (m³)	Count	Waste Volume (m³)	Enclosure Diameter (cm)	Approx Footprint Area (m²)	Type	Transport Fissile Limit[b] (kg)
6-inch pipe overpack container	0.2	15.7	65.4	0.012	7-Pack	0.089	183	3.52	HalfPACT	1.400
					Two 7-Pack	0.177			TRUPACT	2.800
12-inch pipe overpack container	0.2	31.4	64.6	0.049	7-Pack	0.34	183	3.52	HalfPACT	1.400
					Two 7-Pack	0.68			TRUPACT	2.800
Shielded container	0.2	51.8	75.6	0.117[c]	3-Pack	0.35	178	3.31	HalfPACT	0.325
100-gallon drum	0.2	76.2	83.3	0.385	3-Pack	1.16	175	3.21	HalfPACT	0.325
85-gallon drum-tall	0.2	66.0	97.2	0.324	4-Pack	1.30	176	3.23	HalfPACT	0.325
55-gallon drum	0.2	57.2	84.5	0.216	7-Pack	1.51	183	3.52	HalfPACT	0.325
					Two 7-Pack				TRUPACT	0.325
Standard waste box	0.325	138×175	93.5	1.88	One	1.88		2.33	HalfPACT	0.325
85-gallon drum-short	0.2	68.9	84.5	0.315	Two 4-Pack	2.52	182	3.48	TRUPACT	0.325
10-drum overpack[d]	0.325	174.6	184.5	4.37	One	4.37	181	3.43	TRUPACT	0.325
Large waste box 2	0.325	166×265	168.4	7.38	One	7.38		4.39	TRUPACT	0.325

[a] Containers ordered by waste volume in the shipping and disposal bundle.
[b] Baseline Pu FME limits listed; limits change if waste has > 1 wt% Be/BeO (e.g., TRUPACT transport limit reduced to 0.1 kg Pu FEM); if waste machine compacted at 60 MPa (e.g., TRUPACT transport limit reduced to 0.25 kg Pu FME when waste is machine compacted), or drums and waste boxes contain ^{240}Pu (e.g., TRUPACT transport limit increased to 0.38 kg Pu FME if 0.025 kg ^{240}Pu is present).
[c] Volume refers to 30-gallon inner container.
[d] 10-drum overpack can overpack 55-gal and 85 gal drums or be loaded directly; directly loaded volume listed.

VIII.B. Salt Isolates RH-TRU Canisters and POC Behavior Bounds Shielded Container Behavior

The activity of RH derives mostly from fission products and the Pu fissile mass equivalent derives mostly from ^{235}U. As of April 2019, 719 RH-TRU payload canisters (1% by total volume) have been emplaced in disposal room walls. The RH-TRU payload canisters, which can contain up to 0.37 kg ^{239}Pu base on the transportation limit (Table VII), are isolated neutronically by the 1.7 m of salt (2.4 m centerline spacing) between boreholes.

As of April 2019, 27 shielded containers from Argonne National Laboratory have been emplaced in WIPP disposal rooms. The behavior of 12-inch POCs conservatively bound RH-TRU shielded container behavior because

of three reasons. First, both containers are structurally stiff with the same outer dimensions of individual containers; thus, shielded containers would behave similarly to the 12-inch from salt creep. Second, the 12-kg/m^3 fissile concentration of a compacted sphere inside an individual 12-inch POC is greater than 2.8-kg/m^3 fissile concentration for a compacted sphere inside an individual shielded container (assuming each contains the administrative limit of 0.2 kg Pu FME). Third, the transportation fissile mass limit of 1.4 kg Pu FME for the 7-pack POC is 77% greater than 0.325 kg Pu FME limit for the 3-pack of the shielded container; yet, the 3.5-m^2 disposal footprint of a 7-pack of 12-inch POCs is similar to the 3.3-m^2 footprint of a 3-pact of shielded containers (Table X). If one or more 12-inch POCs are replaced in a room with k^{eff} of ~0.91, then the room reactivity will decrease.

VIII.C. Insufficient Compaction of Initially Low Concentration of Fissile Material in Waste Drums
VIII.C.1. Standard CH-TRU Waste

Standard CH-TRU waste consists of a variety of debris contaminated with TRU radionuclides. The estimated composition in CCA-1996 consisted of cellulose (~30% by volume), plastics and rubber (15%), metal (22%), sludges (26%), and sorbents (7%). As of April 2019, CH-TRU waste has mostly been disposed in 55-gallon drums (27% of total volume of 75 800 m^3), standard waste boxes (33%), large waste boxes (2%), super-compacted waste in 100-gallon drums (18%), and ten-drum overpacks (18%). Five 85-gallon-tall containers have also been used.

VIII.C.2. Low Concentrations of Fissile Material in Waste Drums

The maximum fissile administrative limit in any one standard CH-TRU drum is 0.2 kg Pu FME (Table V). For ^{239}Pu uniformly dispersed throughout the waste, the average ^{239}Pu density is 0.94 kg/m^3 in 0.21 m^3 (internal dimensions of 55-gallon drum). Salt creep may increase concentration in a standard 55-gallon CH-TRU drum by a factor of 2.4 to 2.2 kg/m^3, based on an average initial waste porosity of 0.643 and final room porosity of 0.243 (2.4= $\rho_i/\rho_f = (1 - \phi_f) / (1 - \phi_i)$. Alternatively, the fissile concentration is 2.0 kg/m^3 for a sphere confined by the inner diameter of a 55-gallon drum, which similar to the approach for POCs and avoids specifying how the configuration occurred.

The behavior of 6-inch POCs likely bounds standard CH-TRU drum behavior because of three reasons. First, both containers are structurally weak and thus allow for the maximum compaction from salt creep. Second, the compacted 98-kg/m^3 fissile concentration of a sphere inside a 6-inch POC is much greater than the compacted 2-kg/m^3 fissile concentration of a sphere inside a standard CH-TRU drum, conservatively assuming that each 55-gallon CH-TRU drum contains the administrative limit of 0.2 kg Pu FME. Third, the 1.4 kg Pu FME transportation limit in a 7-pack of 6-inch POCs is 77% greater than the 0.325 kg Pu FME transportation limit in 7-pack (in a HalfPACT), or 14-pack (in TRUPACT-II) of 55-gallon drums with the same footprint, height; yet, the 3.5-m^2 disposal footprint of a 7-pack of 12-inch POCs is similar to the 3.3-m^2 footprint of a 3-pact of shielded containers (Table X). Replacing one or all 6-inch POCs with 55-gallon drums in a room initially filled with 6-inch POCs at k^{eff} of ~ 0.96, will reduce room reactivity (Table XI).

VIII.C.3. Low Concentrations of Fissile Material in Larger Drums and Standard Boxes

A similar rationale applies to larger drums which all have a similar footprint and same transportation limit of 0.325 Pu FME (Table X); thus, the room reactivity will certainly be less than for 6-inch POCs. Furthermore, room reactivity will be less than 55-gallon drums because the initial fissile concentration is smaller in larger drums because of the larger volume (i.e., 0.31 m^3 for 85-gallon and 0.38 m^3 for100-gallon drums) and same administrative limit of

0.2 kg Pu FME (Table IV). The initial fissile concentration is also smaller for large containers even though the transportation limit is slightly larger at 0.325 kg Pu FME (i.e., standard waste box with 1.35 m^3, large standard waste box with 7.39 m^3, and 10-drum overpack with 2.05 m^3). The final fissile density will also likely be less for the larger drums and boxes because compaction is not easily increased from that of smaller standard 55-gallon drums, as demonstrated by the difference in compaction from 6-inch POCs and 12-inch POCs (Fig. 20).

VIII.D. Physical Criticality Control for Non-Pit Surplus Plutonium in Criticality Control Overpack

In April 2011, DOE decided to process ~0.6 MT of miscellaneous surplus Pu and send it to WIPP. In April 2016, DOE decided to dispose of 6.0 MT of non-pit Pu at WIPP. The 6.6 MT of miscellaneous and non-pit Pu has been added to the CRA-2019 inventory; however, it has not been shipped.

Non-pit surplus ^{239}Pu is likely to be oxidized to PuO_2 and mixed with a concrete-like material to produce a waste form that would be shipped in critical control container (CCC) and overpack. Each CCC would contain up to 0.38 kg ^{239}Pu at a solid concentration of 184 kg/m^3 in a small cylinder with an inner diameter of 15.4 cm and height of ~11.0 cm. A defined waste form creates the opportunity for engineered options, such as limiting water to less than 10% and polyethylene bagging content to less than 0.4 kg, to help prevent criticality. Furthermore, current plans are to add 50 g B_4C to the ^{239}Pu defined waste form in each CCC, which makes criticality highly unlikely even if all the cylinders of surplus Pu mass in a disposal room are assembled together without any material between cylinders (Table XI).

Table XI. Rationale for Low Probability of Criticality from Compaction in WIPP Repository

Container	Rationale for Salt-Creep Compaction Not Causing Criticality

Pipe Overpacks	**Fiberboard and Iron Isolates Pipe Overpack Containers while Repository Dry**
	1. *Initial Waste Emplacement in Repository*
	 Rectangular array of *6-inch and 12-inch* pipe overpack containers (POCs) represented by spheres with 0.2 kg fissile plutonium (^{239}Pu) is subcritical when initially emplaced with a POC centroid pitch spacing of 58 cm (drum diameter) horizontally and 88 cm vertically.
	2. *Compacted Array in Repository for Undisturbed Conditions without Brine up to 1000 Years:*
	 For compacted array of POCs represented with (a) spheres, (b) sphere pitch calculated from salt-creep modeling, (c) sphere diameter constrained by nearest neighbor, (d) 0.2-kg ^{239}Pu contents moderated with water and plastics, (e) stainless steel iron reflection, and (f) 60% of fiberboard (cellulose) dunnage reflection (assuming maximum microbial cellulose degradation rate):
	  i. 6-inch deformed array is subcritical ($k^{eff} < 0.96$)
	  ii. 12-inch deformed array is subcritical ($k^{eff} < 0.91$)

Pipe Overpacks	**Brine and Iron in Pipe Overpacks Greatly Reduces Reactivity when Repository Later Saturated**
	1. *Compacted Array in Repository for Undisturbed Conditions with Brine Influx up to 2000 Years*
	 For compacted array of POCs represented with (a) spheres, (b) spacing calculated from salt-creep modeling, (c) diameter constrained by nearest neighbor, (d) 0.2-kg ^{239}Pu contents moderated with water and plastics, (e) stainless steel iron reflection, (f) 20% of interstitial porosity between POCs filled with Castile brine as disposal room transitions from dry to some brine that supports microbially degradation such that (g) 40% of fiberboard dunnage reflection remains:
	  i. 6-inch deformed array is less critical ($k^{eff} < 0.90$)
	  ii. 12-inch deformed array is less critical ($k^{eff} < 0.85$)
	2. *Compacted Array for Undisturbed/Disturbed Conditions with Brine Inundation after 2000 Years*
	 For compacted array of POCs represented with (a) spheres, (b) spacing calculated from salt-creep modeling, (c) diameter constrained by nearest neighbor, (d) 0.2-kg ^{239}Pu contents moderated by Castile brine and plastics, (e) iron, magnesium oxide, and salt reflection, and (f) 20% of interstitial porosity filled with Castile brine as would occur after brine inundation and then drying sometime before the end of the 10 000-year regulatory period:
	  i. 6-inch deformed array is much less critical ($k^{eff} < 0.40$)
	  ii. 12-inch deformed array is much less critical ($k^{eff} < 0.36$)
	3. For a mixture of 6-inch and 12-inch POCs, room reactivity will reduce proportional to number of 6-inch POCs replaced with 12-inch POCs, because fissile content, height, and footprint are identical.

RH-TRU Canisters and RH-TRU Shielded Drums	**Salt Isolates RH-TRU Canisters and POC Behavior Bounds Shielded Container Behavior** 1. RH-TRU canisters disposed in room walls are neutronically isolated by 1.7 m of salt between boreholes. 2. Behavior of 12-inch POCs bound behavior of RH-TRU shielded containers because: (1) both containers of similar size and structurally stiff and thus will compact similarly from salt creep; (2) compacted sphere Pu concentration of 12 kg/m^3 for 12-inch POC greater than 2.8 kg/m^3 for shielded containers, each with 0.2 kg Pu FME; and (3) 12-inch POC room reactivity is greater than shielded container because the 1.4 kg Pu FME transportation limit in the 7-pack of 12-inch POCs is 77% greater than 0.325 kg for 3-pack shielded containers with similar footprint (3.5 m^2 versus 3.3 m^2); hence, replacing one or all 12-inch POCs in a room with RH-TRU shield containers will reduce room reactivity.
CH-TRU Drums	**Insufficient Compaction of Initially Low Fissile Concentration in Waste Drums and Boxes** 1. The behavior of 6-inch POCs likely bounds standard CH-TRU drum behavior because (1) both containers are structurally weak and thus allow for the maximum salt creep compaction; (2) the Pu compacted concentration in sphere of 98 kg/m^3 for 6-inch POC > ~2 kg/m^3 for waste drum, each bound by the inner container diameter and with 0.2 Pu FME; and (3) the 1.4 kg Pu FME transportation limit in the 6-inch POCs is 77% greater than 0.325 kg Pu FME for 7-pack of 55-gallon drums, each with the same footprint (3.5 m^2); hence, replacing 7-pack of 6-inch POCs with 7-pack of 55-gallon CH-TRU drums will reduce room reactivity. 2. A similar rationale applies to larger drums which all have a similar footprint and same transportation limit of 0.325 Pu FME; thus, the room reactivity will be less than for 6-inch POCs. 3. Room reactivity will also be less than 55-gallon drums because (1) the initial fissile concentration is smaller in larger drums because of the larger volume but same administrative limit of 0.2 kg Pu FME. The initial fissile concentration is also smaller for large containers even though the transportation limit is slightly larger at 0.325 kg Pu FME; and (2) the final fissile density will be less because compaction is not likely to increase for larger containers, similar to the observed less compaction of 12-inch POCs than 6-inch POCs.
Criticality Control Containers	**Physical Criticality Control in Criticality Control Containers** Non-pit surplus Pu mixed with concrete components to produce a waste form of 184 kg/m^3(380 Pu FGE in 2.35×10^{-3} m^3) in a CCC container, but adding 50 g B$_4$C to Pu mixture ensures criticality is highly unlikely.

ACKNOWLEDGEMENTS

REFERENCES

1. R. P. RECHARD, L. C. SANCHEZ, H. R. TRELLUE and C. T. STOCKMAN, "Unfavorable Conditions for Nuclear Criticality Following Disposal of Transuranic Waste at the Waste Isolation Pilot Plant," *Nuclear Technology*, **136**(*1*), 99-129 (2001).

2. R. P. RECHARD, L. C. SANCHEZ, C. T. STOCKMAN and H. R. TRELLUE, "Consideration of Nuclear Criticality When Disposing of Transuranic Waste at the Waste Isolation Pilot Plant," SAND99-2898, Sandia National Laboratories (2000).

3. R. P. RECHARD, "Probability and Consequences of Nuclear Criticality at a Geologic Repository--I: Conceptual Overview for Screening," *Nuclear Technology*, **190**(*2*), 97-126 (2015).

4. DOE (US DEPARTMENT OF ENERGY), "Surplus Plutonium Disposition, Record of Decision," *Federal Register*, **81**(*65*), 19588-19594 (2016).

5. R. P. RECHARD, L. C. SANCHEZ, M. OLGVUN and G. RYBA, "Fissile Mass and Concentration Necessary for Criticality in Geologic Media near Bedded Salt Repository, Memorandum to Paul E. Shoemaker, 8880; Todd Zeitler, 8862; Ross Kirkes, 8883; November 2019," Sandia National Laboratory (2019).

6. R. P. RECHARD, L. C. SANCHEZ, P. K. MCDANIEL, J. HUNT and G. BROADOUS, "Fissile Mass and Concentration Criteria in Geologic Media near Bedded Salt Repository " *International High-Level Radioactive Waste Management Conference, April 14-18, 2019*, *Knoxville, TN*, La Grange Park, IL: American Nuclear Society (2019).

7. R. P. RECHARD and E. STEIN, "Hydrologic and Geochemical Constraints on Criticality in Geologic Media near Bedded Salt Repository; Memorandum to Paul E. Shoemaker, 8880; Todd Zeitler, 8863; Ross Kirkes, 8883; November 2019," Sandia National Laboratories (2019).

8. E. M. SAYLOR and J. M. SCAGLIONE, "Nuclear Criticality Safety Assessment of Potential Plutonium Disposition at the Waste Isolation Pilot Plant," ORNL/TM-2017/751/R1, Oak Ridge National Laboratory (2018).

9. EPA (US ENVIRONMENTAL PROTECTION AGENCY), "40 CFR Part 191: Environmental Standards for the Management and Disposal of Spent Nuclear Fuel, High-Level and Transuranic Radioactive Wastes: Final Rule," *Federal Register*, **50**(*182*), 38066-38089 (1985).

10. EPA (US ENVIRONMENTAL PROTECTION AGENCY), "40 CFR Part 191: Environmental Radiation Protection Standards for the Management and Disposal of Spent Nuclear Fuel, High-Level and Transuranic Radioactive Wastes, Final Rule," *Federal Register*, **58**(*242*), 66398-66416 (1993).

11. EPA (US ENVIRONMENTAL PROTECTION AGENCY), "40 CFR Part 194: Criteria for the Certification and Re-Certification of the Waste Isolation Pilot Plant's Compliance with the 40 CFR Part 191 Disposal Regulations; Final Rule," *Federal Register*, **61**(*28*), 5224-5245 (1996).

12. R. P. RECHARD, "Historical Background on Performance Assessment for the Waste Isolation Pilot Plant," *Reliability Engineering and System Safety*, **69**(*1-3*), 5-46 (2000).

13. EPA (US ENVIRONMENTAL PROTECTION AGENCY), "40 CFR Part 197: Public Health and Environmental Radiation Protection Standards for Yucca Mountain, Nevada; Proposed Rule," *Federal Register*, **70**(*161*), 49014 (2005).

14. EPA (US ENVIRONMENTAL PROTECTION AGENCY), "40 Cfr Part 197: Public Health and Environmental Radiation Protection Standards for Yucca Mountain, Nevada; Final Rule," *Federal Register*, **73**(*200*), 61256:61289 (2008).

15. NRC (US NUCLEAR REGULATORY COMMISSION), "Yucca Mountain Review Plan, Final Report," NUREG-1804, REV 2, Office of Nuclear Material Safety and Safeguards, US Nuclear Regulatory Commission (2003).

16. EPA (US ENVIRONMENTAL PROTECTION AGENCY), "Compliance Application Guidance for 40 Cfr 194," EPA-402-R-95-014, Office of Radiation and Indoor Air, US Environmental Protection Agency (1996).

17. ANSI (AMERICAN NATIONAL STANDARDS INSTITUTE), "An American National Standard for Nuclear Criticality Safety in Operations with Fissionable Materials Outside Reactors," ANSI/ANS-8.1-2014, American National Standards Institute (2014).

18. DOE (US DEPARTMENT OF ENERGY), "Waste Isolation Pilot Plant Documented Safety Analysis," DOE/WIPP 07-3372, US Department of Energy, Carlsbad Field Office (2016).

19. NWP (NUCLEAR WASTE PARTNERSHIP), "Nuclear Criticality Safety Evaluation for Contact-Handled Transuranic Waste Containers at the Waste Isolation Pilot Plant," WIPP-016, Revision 5, Nuclear Waste Partnership (2015).

20. PUB. L. 102-579, "Waste Isolation Pilot Plant Land Withdrawal Act. (106 Stat. 4777)," (1992).

21. B. M. BUTCHER, "A Summary of the Sources of Input Parameter Values for the Wipp Final Porosity Surface Calculations," SAND97-0796, Sandia National Laboratories (1997).

22. B. Y. PARK and F. D. HANSEN, "Determination of the Porosity Surfaces of the Disposal Room Containing Various Waste Inventories for WIPP PA," SAND2005-4236, Sandia National Laboratories (2005).

23. DOE (US DEPARTMENT OF ENERGY), "Title 40 CFR Part 191: Compliance Certification Application for the Waste Isolation Pilot Plant," DOE/CAO-1996-2184. Vol. I-XXI, DOE Carlsbad Area Office (1996).

24. C. D. LEIGH, J. TRONE and B. FOX, "TRU Waste Inventory for the 2004 Compliance Recertification Application Performance Assessment Baseline Calculation," ERMS 541118, Sandia National Laboratories (2005).

25. B. CRAWFORD, D. GUERIN, S. LOTT, W. MCINROY, J. MCTAGGART and G. D. VAN SOEST, "Performance Assessment Inventory Report--2008," INV-PA-08, Revision 0, Los Alamos National Laboratory, Carlsbad Operations (2009).

26. G. D. VAN SOEST, "Performance Assessment Inventory Report - 2012," INV-PA-12, Rev. 0; LA-UR-12-26643, Los Alamos National Laboratory Carlsbad Operations (2012).

27. G. D. VAN SOEST, "Performance Assessment Inventory Report--2018," INV-PA-18, Revision 0, Los Alamos National Laboratory (2018).

28. DOE (US DEPARTMENT OF ENERGY), "Notice of Intent to Prepare a Supplemental Environmental Impact Statement for Surplus Plutonium Dispostion at the Savannah River Site," *Federal Register*, **72**(*59*), 14543-14546 (2007).

29. DOE (US DEPARTMENT OF ENERGY), "Yucca Mountain Repository License Application, Safety Analysis Report," DOE/RW-0573, Office of Civilian Radioactive Waste Management, US Department of Energy (2008).

30. DOE (US DEPARTMENT OF ENERGY), "Draft Surplus Plutonium Disposition Supplemental Environmental Impact Statement," DOE/EIS-0283-S2, Office of Environmental Managment, US Department of Energy (2012).

31. NRC (US NUCLEAR REGULATORY COMMISSION), "Certificate of Compliance for Radioactive Material Package RH-TRU 72-B," 71-9212, US Nuclear Regulatory Commission (2011).

32. DOE (US DEPARTMENT OF ENERGY), "RH-TRU 72-B Safety Analysis Report," Rev. 4, Carlsbad Area Field Office, US Department of Energy (2006).

33. DOE (US DEPARTMENT OF ENERGY), "Transuranic Waste Acceptance Criteria for the Waste Isolation Pilot Plant," DOE/WIPP-02-3122, Rev 8, Carlsbad Field Office, US Department of Energy (2016).

34. DOE (US DEPARTMENT OF ENERGY), "TRUPACT-II Safety Analysis Report," Revision 23, US Department of Energy, Carlsbad Field Office (2013).

35. DOE (US DEPARTMENT OF ENERGY), "CCP Transuranic Authorized Methods for Payload Control (CCP-CH-TRAMPAC)," CCP-PO-003, Rev. 13, Carlsbad Field Office, US Department of Energy (2013).

36. G. R. KIRKES, ""POC Data as of June 1 2019.xlsx" Excel Spreadsheet Showing All Emplaced Pipe Overpack Containers, Emplacement Location, and Waste Information as of June 1, 2019.," ERMS 571584, Sandia National Laboratories (2019).

37. AREVA, "Criticality Control Overpack Criticality Analysis for TRUPACT-II and HalfPACT," 01937.01.M009-1, Revision O, AREVA Federal Services (2012).

38. NWP (NUCLEAR WASTE PARTNERSHIP), "Criticality Control Overpack," CCO-DWG-001, Revision 3, Nuclear Waste Partnership (2015).

39. J. J. DUDERSTADT and L. J. HAMILTON, *Nuclear Ractor Analysis*, John Wiley & Sons, (1976).

40. DOE (US DEPARTMENT OF ENERGY), "RH-TRAMPAC," Revision O, Carlsbad Field Office, US Department of Energy (2006).

41. D. E. MUNSON, A. F. FOSSUM and P. E. SENSENY, "Advances in Resolution of Discrepancies between Predicted and Measured in Situ WIPP Room Closures," SAND88-2948, Sandia National Laboratories (1989).

42. L. BRUSH, H, "Test Plan for Laboratory and Modeling Studies of Repository and Radionuclide Chemistry for the Waste Isolation Pilot Plant," SAND90-0266, Sandia National Laboratories (1990).

43. E. COTWORTH, "Letter to Dr. Ines Triay, Acting Manager Carlsbad Field Office Us Department of Energy, from Elizabeth Cotworth, Director Office of Air and Radiation," US Environmental Protection Agency (2005).

44. C. M. STONE, "SANTOS - a Two-Dimensional Finite Element Program for the Quasistatic, Large Deformation, Inelastic Response of Solids," SAND90-0543, Sandia National Laboratories (1997).

45. C. M. STONE, "Final Disposal Room Structural Response Calculations," SAND97-0795, Sandia National Laboratories (1997).

46. B. M. BUTCHER, T. W. THOMPSON, R. G. VANBUSKIRK and N. C. PATTI, "Mechanical Compaction of Waste Isolation Pilot Plant Simulated Waste," SAND90-1206, Sandia National Laboratories (1991).

47. B. REEDLUNN and J. E. BEAN, JR, "Simulations of Pipe Overpack Container Compaction at the Waste Isolation Pilot Plant, ," SAND2019-12111, Sandia National Laboratories (2019).

48. SNL (SANDIA NATIONAL LABORATORIES), "Sierra/Solid Mechanics User's Guide. 4.50," SAND2018-10673, Sandia National Laboratories (2018).

49. B. REEDLUNN and J. BEAN, J.E., "Simulations of Canister Compaction at the WIPP," *US/German Workshop: Salt Repository Research, Design, & Operation, September 10-11, 2018*, *Hanover, Germany. SAND2018-9828C*, *September*, (2018).

50. B. REEDLUNN, "Enhancements to the Munson-Dawson Model for Rock Salt," SAND2018-12601, Sandia National Laboratories (2018).

51. B. REEDLUNN, "Joint Project Iii on the Comparison of Constitutive Models for the Mechanical Behavior of Rock Salt; Reinvestigation into Isothermal Room Closure Predictions at the Waste Isolation Pilot Plant." In *The Mechanical Behavior of Salt IX*, J.H. S. FAHLAN, F.D.H. HANSEN, S. HEUSERMANN, K.-H. LUX, AND W. MINKLEY Ed. BGR (Federal Institute for Geosciences and Natural Resources) (2018).

52. B. D. BRICKNER, "Post-Closure Nuclear Criticality Evaluations Involving 6- and 12-Inch Pipe Overpack Tru Waste Containers at the Waste Isolation Pilot Plant," ORNL/TM-2019/1222, Oak Ridge National Laboratory (2019).

53. C.J. Werner, et al., eds., MCNP® User's Manual, Code Version 6.2, LA-UR-17-29981, Los Alamos National Laboratory (2017).

Appendix A: Radiation Transport Calculations for Neutrons from WIPP Remote-Handled Transuranic Waste through Rock Salt

![Sandia National Laboratories logo] **Sandia National Laboratories**

date :   October 17, 2019

to: File

from: L.C. Sanchez, Org 08845, MS 0779, PH-(505) 844-1369

subject: Radiation Transport Calculations for Neutrons from WIPP Remote-Handled TRansUranic Waste thru Rock Salt

EXECUTIVE SUMMARY

Radiation transport calculations were performed to compute the possible "cross talk" – the neutron transport between fissile mass assembles disposed within the host-rock (*e.*g., rock salt) of the Waste Isolation Pilot Plant (WIPP). These calculations analyzed the neutron transport between adjacent Remote-Handled TRansUranic (RH-TRU) waste containers that are placed in two configurations – a) horizontally at 2.4 *m* apart within the host-rock, or b) side-by-side (see Figure ES-1). The results from conservative 1D radiation calculations indicated the following:

1) Horizontal Case – the large separation distance between adjacent containers results in insignificant neutron transport between containers because the WIPP host rock (Salado rock salt) serves as a good neutron absorber (see Figure ES-2a).

2) Vertical Case – there is significant neutron transport between adjacent containers because: a) there is essential no host rock (rock salt – a good neutron absorber) between them, and b) the internal lead shielding material, which is excellent for shielding x-rays and gammas, is not as good of a neutron absorber for high-energy neutrons (see Figure ES-2b).
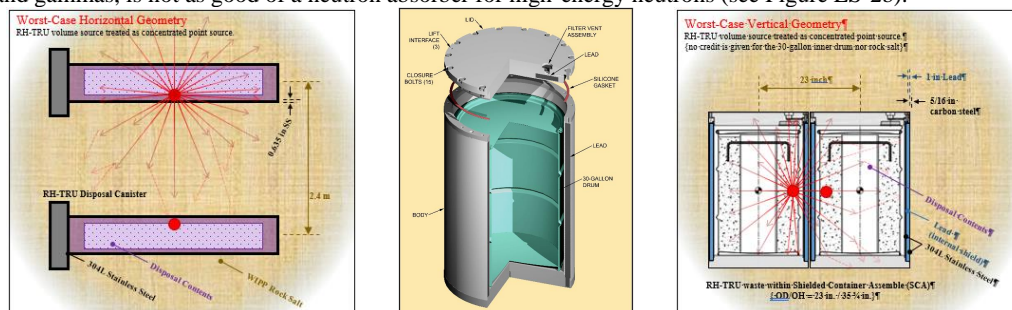
Figure ES-1. Cross sectional geometry of RH-TRU waste containers containing plutonium waste packages using following conditions: (a) horizontal emplacement of RH-TRU – separation pitch = 2.4 meters, (b) lead shield used for vertical emplacement (1-inch internal lead shielding within each 55-gallon DOT-spec drum), and (c) vertical emplacement (side-by-side layout). Worst-case, conservative assumption were as follows: (a) no shielding credit for waste container materials (just lead for vertical case), (b) all fissile mass within a container is treated as a single point source located nearest to that from adjacent container, (c) all of emitted neutrons are model with a neutron spectrum for Pu239 (Watt fission spectrum for induced fissions), and (d) neutrons are modeled as a simple 1-dimensional planar flux (no credit for $1/(4\pi \text{Radius}^2)$ spatial divergence).
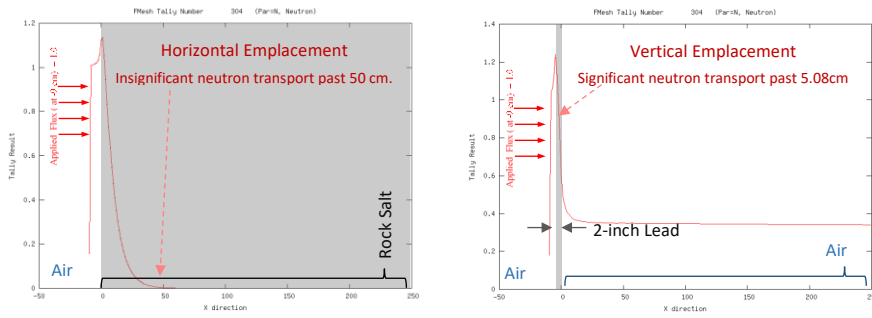
Figure ES-2. Normalized 1-D radiation transport computational results showing (a) significant neutron attenuation by host rock for horizontal wall emplacement, and b) minor neutron attenuation (~ 60%) for vertical room emplacement ().]

INTRODUCTION

Remote-Handled TRansUranic (RH-TRU) is to be disposed within the Waste Isolation Pilot Plant (WIPP) – a deep geologic waste repository for TRU waste generated by the U.S. nuclear weapons complex. The waste can be disposed in two configurations:

1) horizontally at 2.4-meter pitch spacing in the host rock (located in the WIPP Salado formation) comprised of rock salt, and

2) vertically within 55-gal DOT spec metal drums with an added 1 inch of internal lead shielding (for attenuation of x-rays and gammas).

Simple one-dimensional neutron shielding (*e*.g., neutron radiation transport) calculations were performed to find out if neutron "cross-talk" (neutron transport from the fissile material with a container to the fissile material of the adjacent container) is significant. The obtained computational results are presented in this memo.

Geometry

RH-TRU waste is disposed within WIPP in one of the two configurations:

1) Horizontal Case (see Figure 1) – RH-TRU waste is disposed within RH-72B canisters directly into host rock (WIPP/Salado rock salt) at a 2.4 meter spacing (Ref. [RE19]). For conservative analysis purposes, all the neutrons emitting (fissile) materials in a canister (U-233, U-235, Pu-239, *etc*.,) are assumed to be a point source located closest to its nearest neighbor. The neutron flux is modeled as a one-dimensional planar flux (directional) between the fissile masses (*e*.g., the $1/(4\pi Radius^2)$ spatial divergence was not included).

2) Vertical Case (see Figure 2) – RH-TRU waste is placed in the inner 30-gal cavity within a 55-gal DOT-7A spec drum (see Figure 3 and Table 1 for the DOT drum geometry and dimensions). This special DOT container has a 1-inch internal lead shield for x-ray and gamma attenuation (note: while lead is a good shield for photons, it is not a good shielding material for neutrons – unless the neutrons are thermalized). These drums are placed side-by-side within waste rooms within the WIPP repository.
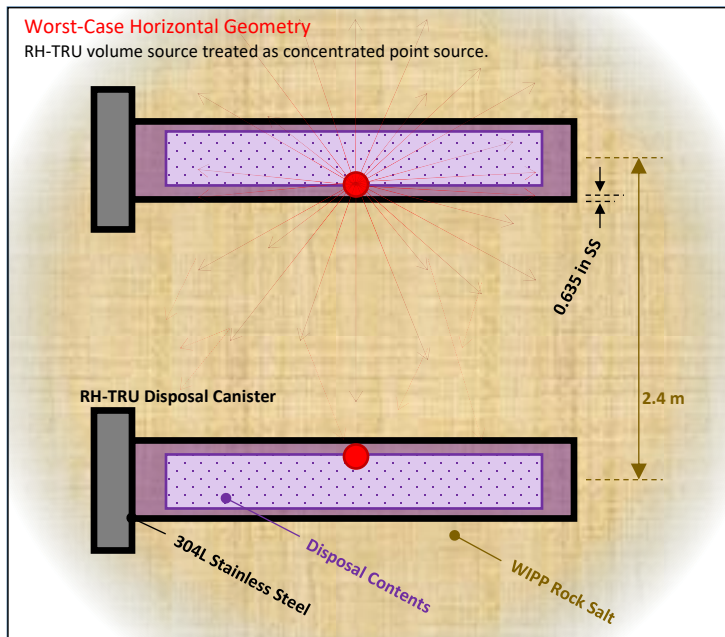
Figure 1. Horizontal Emplacement Geometry– RH-72B inner container (bounding case) for neutron radiation transport calculations (*e*.g., calculations to determine the possible cross talk of neutrons from a RH-TRU disposal canister to its immediate near neighbor RH-TRU canister). Substantial distance exist between the disposal canisters which is filled with rock salt, which can absorb neutrons. For modeling simplicity, no credit was given to shielding due to internal canister contents and the neutron flux was modeled as 1-D planar fluxes.
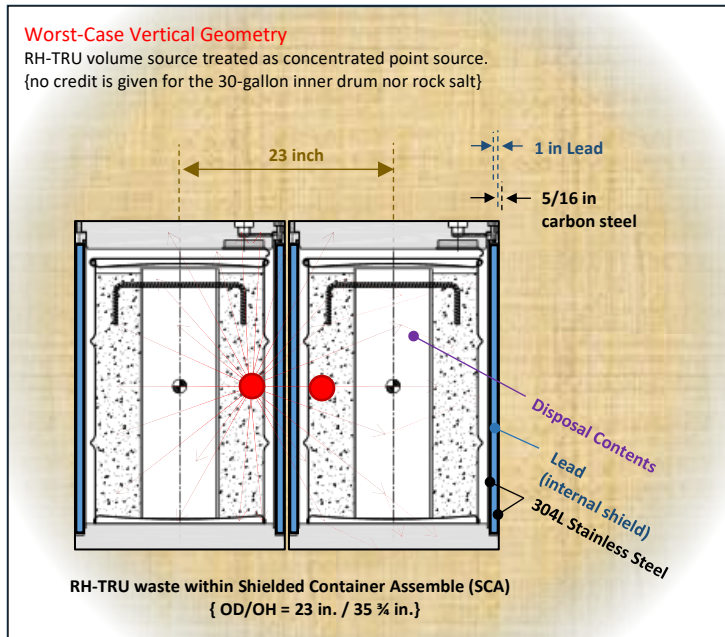
Figure 2. Vertical Emplacement – lead shielded DOT Spec 7A drums/30-gallon payload (bounding case) for neutron radiation transport calculations (*e.g.*, calculations to determine the possible cross talk of neutrons from a "shielded container assemble (SCA)" to its immediate near neighbor SCA). Lead shielding is used internally within the SCAs (only the 2-inch thick region of lead is modeled in the radiation transport calculations). No credit is taken for the small amount of rock salt that may creep between containers, nor is credit taken for the 30-gallon payload inner drum construction (see Figure 3 for details) and neutron fluxes were modeled as 1-D planar fluxes.
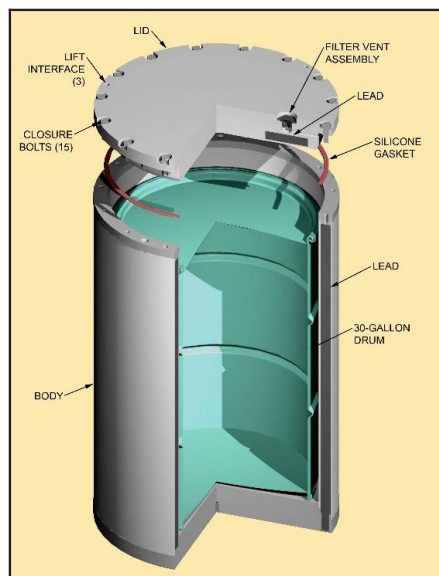
Figure 3. WIPP RH-TRU disposal option (taken from Ref. [DA08, pg. 2-3]). The shielded container is used for direct load – solids, any particles size (*e.g.*, fine power to debris, metal waste cans, *etc.*). Radiation transport analysis only considers the 1-inch lead internal shielding per drum; it does not take into account internal 30-gallon drum payload which is filled with concrete.

Table 1. Shielded Container Dimensions and Components (Ref. [DA08, pg. 2-4])

Dimension	Approximate Measurement (inches)	
	Inside Dimension (in.)	Outside Dimension (in.)
Height	29 ¾	35 3/4
Diameter	20 3/8	**23**

Shielded Container Component	Material	Temperature Range (°F)
Lid, base, flange, inner shell, outer shell, alignment pins, filter shield cap	Carbon steel	-40 to 2750
Body annular lead and filter shield plug	Lead **(nominal 1 inch thick per drum**, Ref. [DA08, pg. 2-1])	<620
Closure bolts and socket set screw	Alloy steel	-40 to 2750
Gasket	Silicone rubber	-65 to 400

RH-TRU Inventory

Information for the RH-TRU radionuclide inventory is presented in Appendix B. Abbreviated information table is contained in Table 2 below. From this table it can be identified that key contributors to the radionuclide inventory are: Sr-90 & Cs-137 for curie content (radioactivity) and U-235 & U-238 for mass content. Also, the fissile loading of plutonium is only 69.5 kg-FGE – this corresponds to an average Pu fissile mass loading[j] of only ~ 9.81E-03 (kg-FGE/m^3) = 2.04 grams of FGE-Pu239 per 55-gallon drum). From a nuclear criticality viewpoint, this value is insignificant by orders of magnitude.

---

[j] WIPP has a RH-TRU disposal volume of 0.25 million *cu.ft*., This corresponds to 7,080 m^3 or 34,002 drum equivalents (nominal). The average plutonium concentration is only 69.5/7,080 = 9.81E-03 (kg-FGE/m^3) = 2.04 (gm-FGE/55-gal drum).

Table 2. Remote Handled – TRansUranic (RH-TRU) Waste Radionuclide Inventory [a]					
(not included in this table are the large masses of non-radioactive materials that are present in the RH-TRU waste matrix)					
Fissile Radionuclide	**Radioactivity** [b]		**Mass** [c]		**239Pu FGE** [d]	**Enrichment**
	(Ci)	**(Ci%)**	**(kg)**	**(wt%)**	**(kg-FGE)**	**(wt%)** [e]
U232	8.87E+00	< 0.01%	4.02E-04	< 0.01%	0.00E+00	
U233	1.72E+01	< 0.01%	1.78E+00	0.02%	1.61E+00	
U234	9.70E+00	< 0.01%	1.56E+00	0.01%	0.00E+00	
U235	1.85E+00	< 0.01%	8.56E+02	**8.16%**	5.51E+02	
U236	2.53E-01	< 0.01%	3.91E+00	0.04%	0.00E+00	
U238 [f]	3.13E+00	< 0.01%	9.31E+03	**88.76%**	0.00E+00	
Uranium Nuclides only, sum =			1.02E+04		5.52E+02	
Uranium Only Enrichment =						**5.43 wt%**
Np237	6.96E+00	< 0.01%	9.88E+00	0.09%	1.48E-01	
Pu238	2.25E+04	3.96%	1.31E+00	0.01%	1.48E-01	
Pu239	4.22E+03	0.74%	6.80E+01	0.65%	**6.80E+01**	
Pu240	3.16E+03	0.56%	1.39E+01	0.13%	3.13E-01	
Pu241	4.53E+04	7.98%	4.37E-01	0.00%	9.82E-01	
Pu242	1.59E+01	< 0.01%	4.04E+00	0.04%	3.03E-02	
Pu244	2.82E-02	< 0.01%	1.56E+00	0.01%	0.00E+00	
Plutonium Nuclides only, sum =			8.93E+01		6.95E+01	
Plutonium Only Enrichment =						**77.83 wt%**
Uranium + Plutonium Nuclides only, sum =			1.03E+04		6.22E+02	
Uranium + Plutonium Only Enrichment =						**6.05 wt%**
others (transuranics)						
Am241	1.30E+04	2.29%	3.79E+00	0.04%	7.09E-02	
Am243	4.12E+02	0.07%	2.06E+00	0.02%	2.66E-02	
Cm244	3.32E+04	5.85%	4.10E-01	0.00%	3.69E-02	
others (non-transuranics) of interest						
Sr-90	1.96E+05	**34.52%**	1.42E+00	0.01%	0.00E+00	
Cs-137	2.50E+05	**44.03%**	2.88E+00	0.03%	0.00E+00	
Th-229	8.74E-01	< 0.01%	4.14E-03	0.00%	0.00E+00	
Th-230	2.26E+00	< 0.01%	1.10E-01	0.00%	0.00E+00	
Th-232	2.26E-02	< 0.01%	2.05E+02	**1.96%**	0.00E+00	
total sum =	5.68E+05		1.05E+04		9.28E+02	
Uranium + Plutonium + Others Enrichment =						**5.93 wt%**

a) RH-TRU inventory data obtained from Ref. [DOETRU18]. For more detail on the values in this table, see Appendix B.
b) The fission yield products Sr-90 and Cs-137 are the major contributors to the radioactivity inventory of the WIPP bound RH-TRU. Note, since these radionuclides have short half-lives, they have very small associated masses.
c) The RH-TRU mass inventory is dominated by uranium (mostly U-238 & U-235). Overall, RH-TRU has a waste matrix average enrichment of only ~5.9 wt%.
d) FGE – fissile gram equivalent (Pu-239 mass equivalent), see Table A-2 for FGE factors.
e) The most significant information from this table is that the plutonium radionuclides have a large enrichment (~78 wt%). This is of importance for hypothetical scenarios that envision plutonium becoming soluble in groundwater and then transport to a location where it would precipitate out. Also, of concern, is that at this large of an enrichment there is the possibility of positive reactive feedback for a criticality assembly.
f) Since U-238 has a very long half-life, these few curies of radioactivity correspond to a large mass inventory.

Source Term Neutron Spectrum

The neutrons emitted from WIPP TRU waste are due to three sources:
1) *Induced Fissions* (key effect)
   These fissions produced neutrons via neutron-chain reactions. The spectrum of the neutron can be represented by the Watt fission spectrum (Ref. [PE13, pg.11-3], with coefficients; a= 0.966 (MeV), b= 2.842 (MeV^{-1})).
2) *Spontaneous Fissions* (minor effect)
   These fissions are due to the spontaneous fission half-life of Pu239 (fissile radionuclides have a spontaneous fission half-life in addition to their α-emitting half-life). The neutrons emitted by this process contribute to the nuclide INRAD

(intrinsic radiation). The spectrum of the neutron can be represented by the Watt fission spectrum (Ref. [PE13, pg.11-4], with coefficients; a= 0.885247 (MeV), b= 3.80269 (MeV^{-1})).

3) (α,n) *Reactions* (minor effect)

When alpha emitting radionuclides (actinides) are combined (*e.g.*, in very close proximity) with some low-z materials, the combination can become a neutron source (such as; Pu-Be, Po-Li, Po-B, and Ra-Be). This is because the alpha particles that are emitted from actinides (Pu-239, in this case) are released at high enough energies and only a small fraction of them can overcome the coulomb barrier of a low-z nucleus and can then emit a neutron via a (α,n) reaction. The released neutrons will have a high-energy spectrum, see Figure 4 for an example. Even though this is a "hard neutron spectrum", the intensity (source strength) of the neutrons is low unless this neutron source is specially constructed (note: the max range of alphas within plutonium is ~3E-4 cm = 2.28E-04 cm in plutonium, see Figure 5). At most, less than 1 in 10,000 alphas emitted from plutonium could result in an emitted neutron (see Table 3).
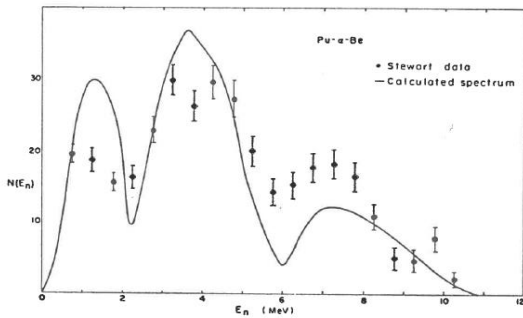
Figure 4. Pu-α-Be neutron spectrum (taken from Ref. [SH98, *pg*. 7-8]). This spectrum is mostly likely for Pu-238 (a very commonly used neutron source in industry) but would be acceptable for Pu-239 and other Pu isotopes.}
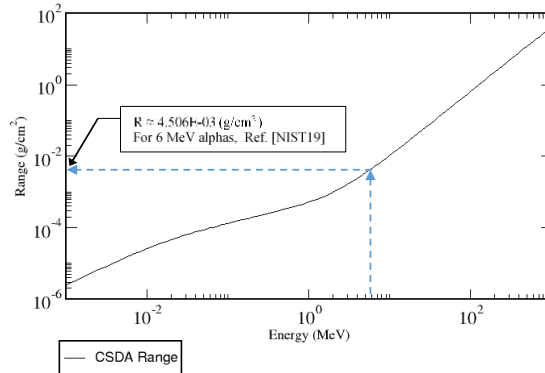
Figure 5. Bounding Range for alpha (helium ions) particles (taken from Ref. [NIST19]). Using the NIST/ASTR tool it was identified that 6 MeV alphas have an areal density range of 4.506E-03 (g/cm^2) – for plutonium with density = 19.8 (gm/cm^3), the Range$_{max}$ (a=6 MeV) = 4.506E-03/19.8 = 2.28E-04 cm.

Table 3. Characteristics of Selected Radioactive Neutron Sources
(Note: for neutron flux calculations, the neutron yield value can be bounded by a value of 1.5E+07 (n/sec) per *Ci*)

Source	Reaction	Half-life	Average Neutron Energy (MeV)	Yield per Bq (n/sec)	Yield per Ci (n/sec/per *Ci*)
^{210}Po-Be	α, n	138.4 d	4.2	6.8E-05	2.5E+06
^{226}Ra-Be	α, n	1620 yr	4.0	3.51E-04	1.3E+07
^{238}Pu-Be	**α, n**	**86.4 yr**	**4.5**	**6.2E-05**	**2.3E+06**
^{241}Am-Be	α, n	458 yr	4.5	5.9E-05	2.2E+06
^{210}Po-B	α, n	138.4 d	B10: 6.3 B11: 4.5	1.6E-05	6.0E+05
^{124}Sb-Be	γ, n	60 d	0.024	3.5E-05	1.3E+06

a) Data taken from Ref. [SH98, pg. 7-12].

b) For (α,n) reactions, yields are an indefinite function of target material and emitter mixing.

From a nuclear sub-criticality standpoint, only induced fissions are of concern, since neutrons from spontaneous and (*α*,n) serve as constant additional sources of neutrons (*e.g.*, steady-state extraneous sources, see the radiation transport and the neutron criticality equations in Figures 6 and 7). Because the enrichment of WIPP RH-TRU plutonium is high (~78 ^{wt} %), its neutron spectrum (χ distribution) can be represented by Equation 3, the Watt fission spectrum (theoretical spectrum for neutron-induced fissions) showed in Figure 8. Radiation transport calculations were performed with the analog Monte Carlo code^k: MCNP^{TM} Version 6.1 (Ref. [PE13]) and treating the fissile material as

---

[k] Note -- This version of the Boltzmann transport equation for neutral particles allows us to estimate the criticality constant for systems that are critical or near critical conditions. It is an energy and direction dependent integral-differential equation that is complicated to solve for materials

100 ^{wt}% enriched Pu-239. As a quality check, the Watt spectrum for Pu239 (both induced- and spontaneous-fissions) was compared to the spectrum from a 95.2 ^{wt}% enriched Pu239 reactor called Jezebel (Ref. [FR99, pg. 77]) – this is presented in Figure 9.

Figure 6. Time independent radiation transport equation (*aka* Boltzmann transport equation) used to model neutrons where Φ= flux, Σ= macroscopic cross section, and χ= fast fission spectrum (see Figure 8).

Figure 7. Nuclear criticality analysis equation with k_{eff} (criticality constant) used for "neutron balance" of radiation transport equation}.

Watt Fission Spectrum equation: $\quad f(E) = C \exp(-E/a) \sinh\left(\sqrt{bE}\right)$ $\qquad$ (*Eq. 3*)

(*aka* χ-distribution for fission source term in radiation transport equation)

Figure 8. Fission neutron spectrum (*aka* chi distribution for fast fission neutrons from fissile assemblies) used for radiation transport / nuclear criticality analysis. The coefficients for this theoretical spectrum are; a= 0.966 (MeV), b= 2.842 (MeV^{-1}) – these are values for both induced- and spontaneous-fissions of Pu239.

---

with significant variation in properties due to position, energy, direction, and time. The numerical method used to solve this equation is an "analog Monte Carlo" method which monitors each individual neutron from birth to death – it is not a "non-analog" code that propagates uncertainty thru computational models.
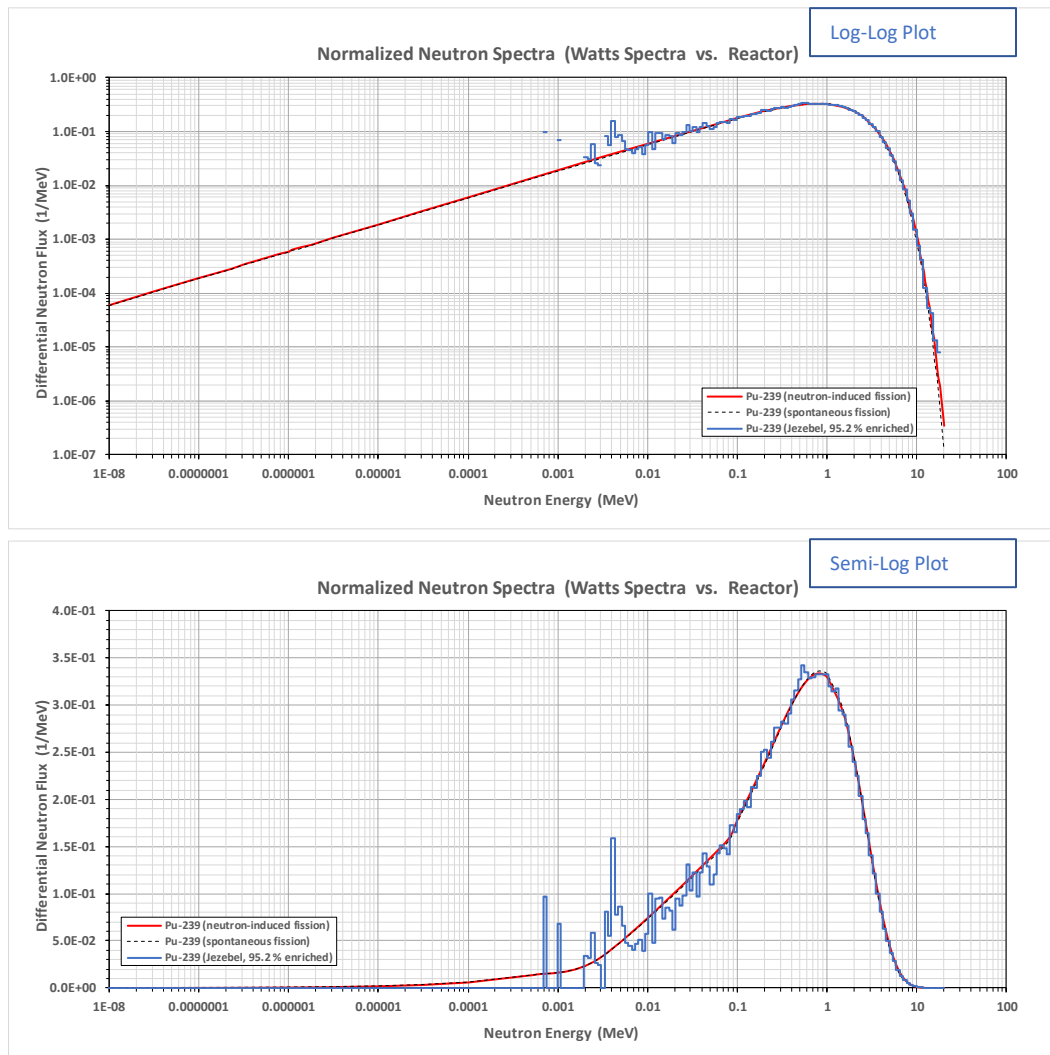
Figure 9. Comparison of neutron spectra from: Jezebel (95.2^{wt}% enriched Pu239 reactor), 100% Pu239 induced fission, and 100% Pu239 spontaneous fission[l]. The neutron spectrum for WIPP TRU waste (~78^{wt}% enriched, see Table 2) can be conservatively bounded by the Pu239 induced spectrum.

Radiation Transport / Nuclear Criticality Equations

As mention previously, radiation transport analyses use the Boltzmann Transport equation (BTE) for neutral <u>particles</u> (the Boltzmann Fokker-Planck equation is used for charged particles). When there are significant scattering events, particle transport theories such as BTE replace <u>wave</u> theories – *e.g.*, the wave nature of the particles is not important for modeling the transport and mean-free-paths of the particles (quantum mechanical wave properties are taken into account and are hidden within the nuclear and atomic cross sections used in the BTE).

---

[l] The neutron spectrum (differential neutron fluence) for Jezebel was computed using the code: MCNP^{TM} 6.1 with input model data from Ref. [FR99, *pg*. 77] along with the ENDF/B-VII.1 nuclear cross section library. The emitted fission neutron spectrum was modeled as "neutron-induced" Pu239 spectrum using Watt fission spectrum coefficients of $a = 0.966$ and $b = 2.842$ (see Ref. [PE13, pg. 11-3). Not included in this plot comparison is the neutron spectrum from (α,n) reactions – the contribution from these reactions is considered to be small.

This radiation transport equation is a seven-dimensional Louisville-type transport equation (3-space, 2-angle, 1-energy, & 1-time) – see Figure 10 below. For detailed models this is computational expensive to solve via Monte Carlo codes (analog MC analysis) – for the analyses used for this memo, only a simple slab geometry was used along with a planar incident nuclear flux. Key to the use of the transport code MCNP™ 6.1, was the nuclear cross section libraries that were used – discussion of their data/formats in available from Ref. [BNL09]. It is important to note that all the calculations in this memo used the ENDF/B-VII.1 nuclear cross section library, this is the latest recommended library by the Cross Section Evaluation Working Group (CSEWG, see Ref. [BNL19]). The reason why the choice of the library is important, is because the previous ENDF/B-VII.0 version contained some data corruption problems (a few of the nuclear cross section values were somehow misplaced into data file locations meant for other nuclides).

$$\nabla \cdot \widehat{\Phi}(r,E,\widehat{\Omega}) + \Sigma_t(r,E)\,\widehat{\Phi}(r,E,\widehat{\Omega}) \quad = \quad S +$$

$$\frac{\chi(E)}{4\pi}\int_0^{4\pi} d\widehat{\Omega}'\int_0^{\infty} dE'\,\overline{\nu\Sigma_f}(r,\acute{E})\,\widehat{\Phi}(r,E',\widehat{\Omega}') \quad + \quad \int_0^{4\pi} d\widehat{\Omega}'\int_0^{\infty} dE'\,\Sigma_s(r,E \xrightarrow{\cdot} E,\widehat{\Omega}' \to \widehat{\Omega})\,\widehat{\Phi}(r,E',\widehat{\Omega}')$$

(Eq. 4)

Key Terms:
$\widehat{\Phi}(r,E,\widehat{\Omega})$ = angular flux
$\Sigma_t(r,E)$ = macroscopic cross section = n σ
n = atom density
σ = microscopic cross section

Figure 10. Boltzmann transport equations (*aka* the "Transport equation" or the "Radiation transport" equation) has 5 major components (divergence, removal, external, fission, and scattering kernel terms). This equation is simply the continuity equation for particles that do not interact with themselves – *i.e.*, an equation of state (EOS) is not needed. Solutions to this equation will provide the energy dependent flux (differential flux, *aka* "neutron spectra") at specified locations. Desired reaction rates (absorbed doses, nuclear heating rates, ionization, *etc*.) are computed by folding (multiplying on an energy-by-energy dependent basis) the computed fluxes with "response functions" (flux-to-dose conversion factors). Response functions are determined from codes such as QASPR, which solve the momentum and energy equations to determine radiation damage effects.

All the computational results presented in this memo were obtained with the radiation transport code MCNP™6.1 (Ref. [PE13]). Coupled neutron/photon transport calculations (without bremsstrahlung) were performed for all the naturally occurring elements (no radioactive nuclides) that also have existing nuclear cross sections included in the standard cross sections libraries that are distributed with MCNP 6.1. The identification of: 1) the available nuclear cross sections, 2) the elements (and the abundance fractions of their stable nuclides) and 3) the calculated atom densities (needed as input for radiation transport codes) are all presented in the data memo: LCS_memo_5199 (see Ref. [SA18]^m).

---

[m] Important note: all the computed atom density values are based on nuclear data (atomic weights, atom abundances, *etc*.,) obtained from a standard nuclear engineering reference: the "Chart of the Nuclides", Seventeenth Edition, Revised 2009 (Ref. [BA09]).

Rock Salt Composition and Atom Densities (number densities)

In order to perform radiation transport or nuclear criticality calculations, atom densities or weight fractions are required for each of the nuclides present in the material regions. Mineral composition for WIPP rock salt were obtained from Ref. [BR90] – this reference contains the individual mass densities (theoretical mineral densities) and weight percentages for five minerals contained within the rock salt. Unfortunately, the reference does not include the bulk density (mixture density) for the rock salt, which is needed for computing atom densities. The bulk density was determined/reversed-engineered by converting the weight percentages into volume percentages and then used to compute the bulk mass density, which then is used for determining the atom densities of all the nuclides in the WIPP rock salt. The calculations used to ultimately compute the WIPP rock salt atom densities are presented in this section in the following tables:

Table	Description
4	Composition and Calculation of Bulk Mass Density of WIPP Rock Salt
5	Calculation of Atom Fractions of WIPP (Rock) Salt
6	Atom Number Densities of Rock Salt Minerals by Nuclide

Table 4. Composition and Calculation of Bulk Mass Density of WIPP/Salado Rock Salt [a]

(the purpose of this table is to convert mineral weight fractions to volume fractions,
which can then be used to determine the bulk density of the WIPP rock salt)

Item	Name [b]	Mineral [c] Density (gm/cm³)	Mineral [d] Wt Frac (Dry) (--) dry only	WtFrac/Density (Dry) (see Equation B-1) (cm³/gm) dry only	Volume Fraction [e] (Wet, 100% sat) (--)	Partial [f] Density (Wet, 100% sat) (gm/cm³)
1	Halite	2.165	0.9323	0.43062	0.9323	2.0183
2	Anhydrite	2.61	0.015325	0.00587	0.0127	0.0332
3	Gypsum	2.32	0.015325	0.00661	0.0143	0.0332
4	Magnesite	3.009	0.015325	0.00509	0.0110	0.0332
5	Polyhalite	2.775	0.015325	0.00552	0.0120	0.0332
6	Corrensite (clay)	2.8	0.0064	0.00229	0.0049	0.0139
(7)	1.28 vol% Porosity (void)	0	0			
7	Porosity (with water)	1.0			0.0128	0.0128
		sum =	1.000	0.456	1.0000	**2.178** [g]

a) Ref. [BR90] is missing the mass density (bulk density) of the WIPP rock salt, thus this table was generated to compute that value (*e.g.*, the sum of the "partial densities").

b) Mineral composition values for WIPP rock salt were obtained from Ref. [BR90, pg. 21]. (Also, see Appendix D.)

c) Mass density values for the five (5) minerals that comprise WIPP rock salt were obtained from Ref. [CRC91]. Mass density for the clay (corrensite) was obtained from Ref. [RE19]. Mass density for water was set at 1.0 (gm/cm³) – which is slightly conservative compared to the value of 0.99707 at NTP conditions. Salado rock salt porosity taken from Ref. [RE19].

d) Mineral weight fractions taken from Ref. [BR90 *pg.* 81] – minerals 2 thru 5 were assumed in the report to have about equal weight contributions, minor minerals (such as basanite, quartz, and various clay minerals) were included as corrensite clay. Note, the mineral weight fractions were for WIPP Salado rock salt with a porosity of 1.28 vol% (Ref. [RE19]) without the presence of water in the pores.

e) The equation used to determine the volume fractions is given by:

$$\text{Volume Fraction (i)} = \frac{Weight\ Fraction\ (i)}{\sum_{j=1}^{n} Weight\ Fraction\ (j) * \frac{\rho_i}{\rho_j}} = \frac{Weight\ Fraction\ (i)\ /\ \rho_i}{\sum_{j=1}^{n}\ (Weight\ Fraction\ (j)\ /\ \rho_j)} \qquad (\rho = \text{density of species } i) \qquad (Eq.\ 1)$$

Volume Fraction (i) with porosity = (1.0 – *porosity*) * Volume Fraction (i) without porosity   (*Eq.* 2)

f) Partial density (*aka* "particular density") is the mass of a specific species (mineral) per unit *mixture* volume. The summation of the partial densities results in the "bulk density" of the mixture – in this case = **2.178** gm/cm³.

g) The Salado rock salt bulk (mixture) density is 2.178 (gm/cm³) if the 1.28 vol% porosity is filled with water (100% saturation). If the rock salt is dry (zero saturation) then the bulk density is 2.165 (gm/cm³).

Table 5. Calculation of Atom Fractions of WIPP/Salado Rock Salt
(these atom fractions are based on the rock salt bulk density & mineral partial densities from Table1)

Item	Mineral Name [a]	Chemical [a] Composition	Mass [b] Density (gm/cm^3)	Weight [c] Percent (wt %)	Partial [d] Density (gm/cm^3)	ATWT [e] {mineral} (AMU)	Theo Mineral Density [f] (#m/b-cm)	Atom Percent (at %)
1	Halite	NaCl	2.165	93.23 wt %	2.0183	58.44277	2.08E-02	86.75%
2	Anhydrite	CaSO$_4$	2.61	1.5325 wt %	0.0332	136.11900	1.47E-04	1.84%
3	Gypsum	CaSO$_4$ 2(H$_2$O)	2.32	1.5325 wt %	0.0332	172.13876	1.16E-04	2.90%
4	Magnesite	MgCO$_3$	3.009	1.5325 wt %	0.0332	84.29770	2.37E-04	2.47%
5	Polyhalite	K$_2$MgCa$_2$(SO$_4$)$_4$2(H$_2$O)	2.775	1.5325 wt %	0.0332	602.84136	3.31E-05	2.14%
6	Corrensite	H$_{28}$O$_{31}$Na$_{0.2}$Mg$_5$Al$_3$Si$_6$K$_{0.2}$Ca$_{0.6}$Fe$_3$	2.8	0.64 wt %	0.0139	1099.01835	7.59E-06	1.22%
7	Water		1.0	0.0128 wt %	0.0128	18.00988	4.28E-04	2.68%
			sum =	100.0 wt %	**2.178**		sum =	100.00 at %

a) Mineral compositions for WIPP/Salado rock salt were identified in Ref. [BR90, *pg*. 21]. Not shown are minor minerals such as basanite, quartz, and various clay minerals.
b) Mass density values for the five (5) minerals that comprise WIPP rock salt were obtained from Ref. [CRC91].
c) Mineral weight fractions taken from Ref. [BR90 *pg*. 81] – minerals 2 thru 5 were assumed in the report to have about equal weight contributions, minor minerals were not included.
d) Partial densities taken from Table C-1 – originally computed using weight fractions published in Ref. [BR90, *pg*. 81].
e) Atomic weight values for mineral composition taken from Table C-5 (last row entries).
f) Theoretical mineral density = mineral density x Avogadro constant / ATWT (*ex*. halite = 2.0183 x 0.6022 / 58.44277 = 2.08E-02).

Table 6. Atom Number Densities of Salado Rock Salt Minerals by Nuclide
(the atom densities to be used in radiation transport code are shown in blue font)

Item	Symbol	Theoretical Atom Density (a) {each mineral} (#/b-cm)							Bulk Mixture Atom Density (b) {includes all minerals} (#/b-cm)							
		1 Halite	2 Anhydrite	3 Gypsum	4 Magnesite	5 Polyhalite	6 Corrensite	7 Water	1 Halite	2 Anhydrite	3 Gypsum	4 Magnesite	5 Polyhalite	6 Corrensite	7 Water	Total Roll-Up Values
1	H (nat)															
2	H-1			3.2462E-02		1.1087E-02	4.2955E-02	6.6868E-02			4.6422E-04		1.3256E-04	2.1256E-04	8.5591E-04	5.9677E-04
3	H-2			3.7335E-06		1.2752E-06	4.9404E-06	7.6907E-06			5.3391E-08		1.5246E-08	2.4447E-08	9.8441E-08	6.8637E-08
4	C (nat)				2.1496E-02							2.3701E-04				2.3701E-04
5	O (nat)															
6	O-16		4.6076E-02	4.8580E-02	6.4331E-02	4.9777E-02	4.7447E-02	3.3357E-02		5.8570E-04	6.9471E-04	7.0931E-04	5.9512E-04	2.3478E-04	4.2697E-04	2.5848E-03
7	O-17		1.7552E-05	1.8505E-05	2.4505E-05	1.8961E-05	1.8074E-05	1.2706E-05		2.2311E-07	2.6463E-07	2.7020E-07	2.2670E-07	8.9435E-08	1.6264E-07	9.8463E-07
8	O-18		9.4686E-05	9.9831E-05	1.3220E-04	1.0229E-04	9.7503E-05	6.8548E-05		1.2036E-06	1.4276E-06	1.4576E-06	1.2230E-06	4.8248E-07	8.7741E-07	5.3118E-06
9	F-19															
10	Na-23	2.2309E-02					3.0686E-04		2.0798E-02							2.0798E-02
11	Mg (nat)															
12	Mg-24				1.6980E-02	2.1897E-03	6.0596E-03					1.8722E-04	2.6179E-05	2.9985E-05		2.1340E-04
13	Mg-25				2.1496E-03	2.7721E-04	7.6714E-04					2.3701E-05	3.3143E-06	3.7961E-06		2.7016E-05
14	Mg-26				2.3667E-03	3.0521E-04	8.4462E-04					2.6095E-05	3.6490E-06	4.1795E-06		2.9744E-05
15	Al-17						4.6028E-03									
16	Si-nat															
17	Si-28						8.4897E-03									
18	Si-29						4.3129E-04									
19	Si-30						2.8464E-04									
20	S-nat															
21	S-32		1.0969E-02	7.7097E-03		1.0533E-02				1.3943E-04	1.1025E-04		1.2593E-04			3.7561E-04
22	S-33		8.6603E-05	6.0873E-05		8.3163E-05				1.1009E-06	8.7051E-07		9.9428E-07			2.9656E-06
23	S-34		4.9075E-04	3.4494E-04		4.7126E-04				6.2382E-06	4.9329E-06		5.6342E-06			1.6805E-05
24	S-36		1.1547E-06	8.1163E-07		1.1088E-06				1.4678E-08	1.1607E-08		1.3257E-08			3.9542E-08
25	Cl-nat															
26	Cl-35	1.6901E-02							1.5756E-02							1.5756E-02
27	Cl-37	5.4077E-03							5.0413E-03							5.0413E-03
28	K-nat															
29	K-39					5.1704E-03	2.8617E-04						6.1816E-05	1.4161E-06		6.1816E-05
30	K-40					6.4867E-07	3.5902E-08						7.7554E-09	1.7766E-10		7.7554E-09
31	K-41					3.7314E-04	2.0652E-05						4.4611E-06	1.0219E-07		4.4611E-06
32	Ca-nat															
33	Ca-40		1.1194E-02	7.8681E-03		5.3746E-03	8.9241E-04			1.4229E-04	1.1252E-04		6.4258E-05	4.4159E-06		3.1907E-04
34	Ca-42		7.4710E-05	5.2513E-05		3.5871E-05	5.9561E-06			9.4968E-07	7.5096E-07		4.2887E-07	2.9473E-08		2.1295E-06
35	Ca-43		1.5589E-05	1.0957E-05		7.4847E-06	1.2428E-06			1.9815E-07	1.5669E-07		8.9485E-08	6.1496E-09		4.4433E-07
36	Ca-44		2.4087E-04	1.6931E-04		1.1565E-04	1.9203E-05			3.0619E-06	2.4212E-06		1.3827E-06	9.5023E-08		6.8657E-06
37	Ca-46		4.6188E-07	3.2465E-07		2.2177E-07	3.6823E-08			5.8713E-09	4.6427E-09		2.6514E-09	1.8221E-10		1.3165E-08
38	Ca-48		2.1593E-05	1.5178E-05		1.0368E-05	1.7215E-06			2.7448E-07	2.1705E-07		1.2395E-07	8.5184E-09		6.1548E-07
39	Ti-nat															
40	Ti-46															
41	Ti-47															
42	Ti-48															
43	Ti-49															
44	Ti-50															
45	Fe-nat															
46	Fe-54						2.6904E-04									
47	Fe-56						4.2233E-03									
48	Fe-57						9.7534E-05									
49	Fe-58						1.2980E-05									
	Sum =	4.4618E-02	6.9283E-02	9.7396E-02	1.0748E-01	8.5936E-02	1.1814E-01	1.0031E-01	4.1595E-02	8.8069E-04	1.3928E-03	1.1851E-03	1.0274E-03	4.9197E-04	1.2840E-03	4.6081E-02

a) Theoretical densities are given by;   Atom density (i) $= \dfrac{Mass\ Density(i) * Avogadro\ Constant}{ATWT(i)}$ (Eq. 3)

b) Bulk (mixture) densities given by;   Bulk atom density (i) = volume fraction (i) * theoretical atom density   (Eq. 4)

Computational Results

Neutron shielding (radiation transport) calculations were performed with MCNP™ version 6.1 using the geometry models shown in Figures 10 and 11. The neutron energy spectrum was modeled as "induced fission" neutrons from Pu-239 in a planar flux. The computational results indicated the following:[n]

1) Horizontal Case – the large separation distance between adjacent containers results in insignificant neutron transport between containers because the host rock (rock salt) serves as a good neutron absorber.

2) Vertical Case – there is significant neutron transport between adjacent containers because: a) there is essential no host rock (rock salt – a good neutron absorber) between them, and b) the internal lead shielding material, which is excellent for shielding x-rays and gammas, is not as a good neutron absorber for neutrons.

Computational modeling assumptions and obtained results are presented in this section in the following:

Item   Description
Table 7   Computational Modeling Assumptions/Conservatisms

Table 7. Computational Modeling Assumptions/Conservatisms		
Horizontal Displacement (note – HD corresponds to RH-TRU canisters that are placed individually within rock salt with 2.4 meter spacings)		
Item	Name	Description
H1	N-spectrum	The neutron energy spectrum for plutonium fissile material is complex. It has contributions from spontaneous fissions, induced fissions, and neutrons from (α,n) reactions (see Ref. [NASA72] for discussion). For simplicity, the emitted neutron flux from the RH-TRU waste matrix is upper bounded as mono-energetic with energy = 4.5 MeV.
H2	Point Source	The exact geometry of the disposal waste is not known (nor the radionuclide distribution within the waste matrix). A very conservative model was used, in which the neutron source term is treated as a point source located closest to the container inner wall (see Figure 1 for location).
H3	Normalized Planar Flux	The neutrons emitted from the source are treated as a planar flux emitted at the waste container's inner surface. This is conservative since the radial emission of neutrons is not considered. However, if wanted, the $1/(4 \pi \text{ radius}^2)$ geometry divergence can be added after the fact.
H4	No Container Shield Material	Credit for shielding by the disposal container was not considered – the shielding by the container materials (metals) is insignificant in comparison to the neutron absorption due to the host rock (rock salt) that surrounds the container. Note, the centerline-to-centerline spacing of the horizontal disposal option is 2.4 meters – computational results presented in Figure 10 confirm this.
Vertical Displacement (note – VD corresponds to RH-TRU waste place internally within "Shielded Container Assemblies" (see Figure 2). These SCA have 1 inch thick internal lead shielding which is used to significantly shield the gamma radiation emitted from the RH-TRU waste matrix (e.g., shielded down to CH-TRU levels). This allows the SCAs to be co-disposed/co-mingled with CH-TRU drums within WIPP.)		
V1	N-spectrum	Same as H1.
V2	Point Source	Same as H2 (see Figure 2 for vertical geometry).
V3	Normalized Planar Flux	Same as H3.
V4	Only Lead Shield Material	Credit for the carbon steel materials of the SCA are not modelled – these metal shells are thin compared to the lead shield region. For simplicity, the only SCA material modeled was the 1 inch thick internal lead shield.

---

[n]   The input and output files for MCNP are archived in the Central Files for CRA-2019 in the directory /nfs/data/CVSLIB/WIPP_EXTERNAL/CRA19_crit/FILES
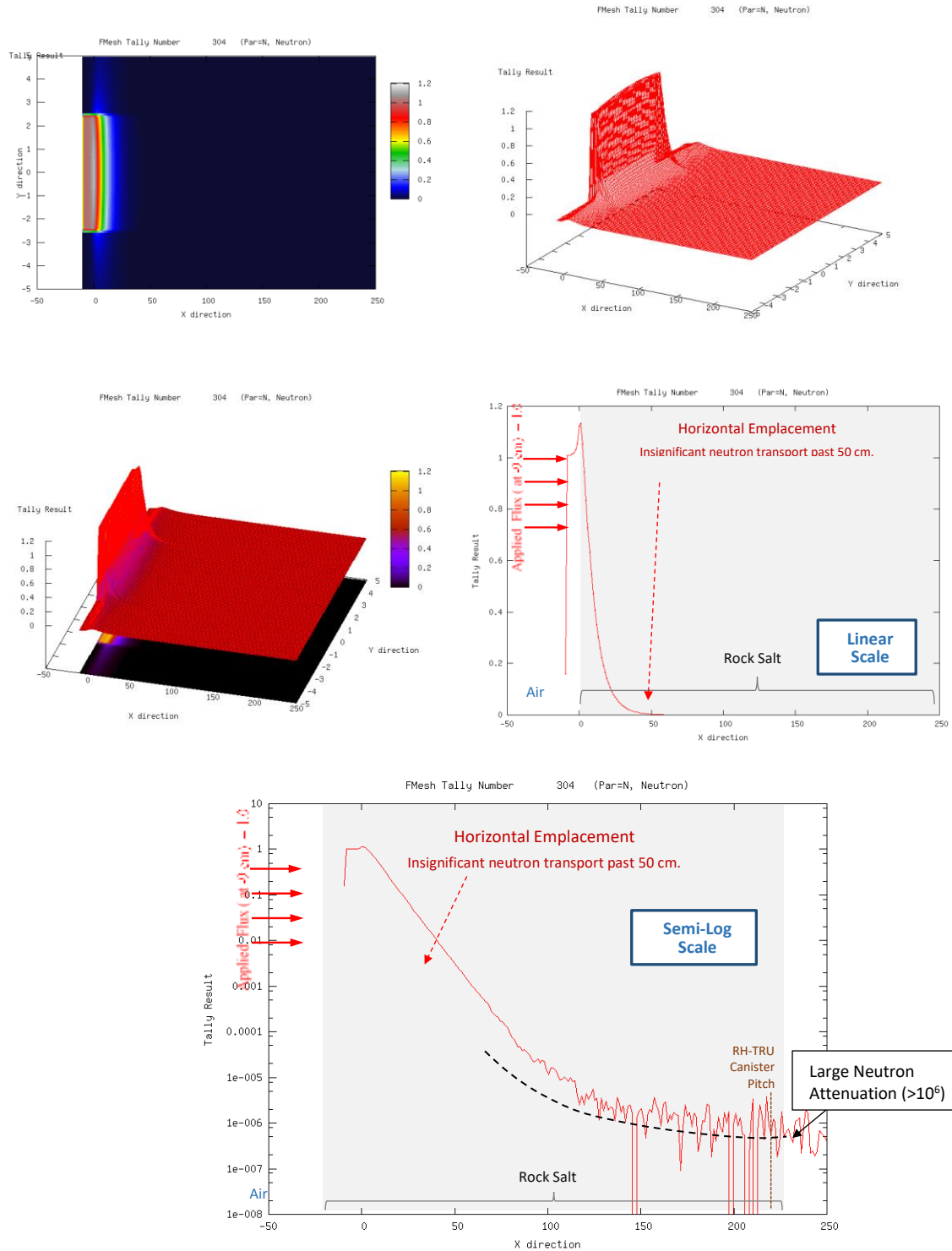
Figure 10. Horizontal Case – Normalized 1-D radiation transport computational results for RH-TRU waste emplacement within WIPP/Salado rock salt (see Figure 1 for model geometry). These results indicate that the host rock is good neutron absorber, this results in insignificant neutron transport (neutron "cross-talk") between adjacent waste canisters. Additional calculations not shown here were performed with 4.5 MeV mono-energetic neutrons, but they did not change the results significantly.
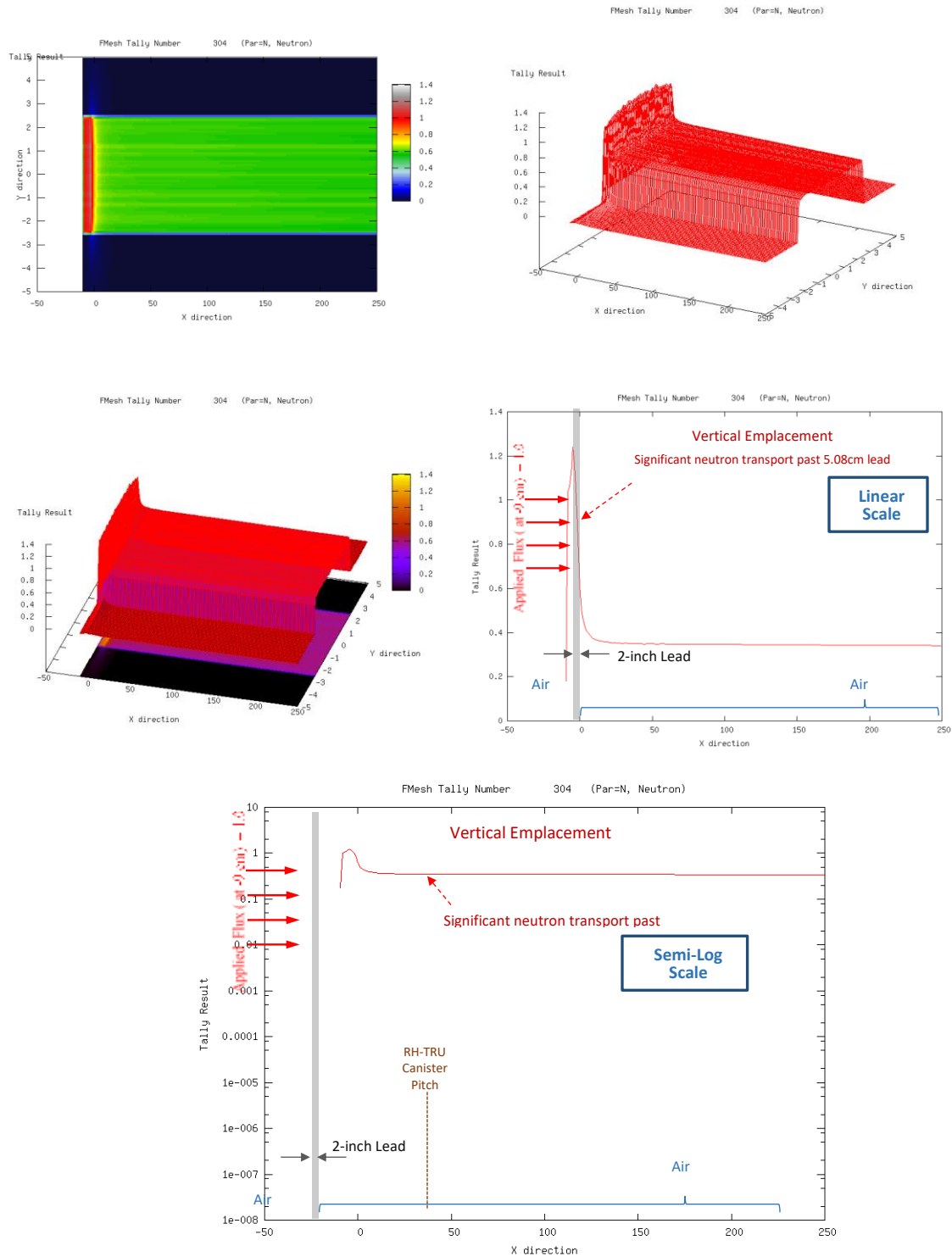
Figure 11. Vertical Case – Normalized 1-D radiation transport computational results for RH-TRU waste emplacement within lead shielded DOT-7 spec drums (see Figure 2 for model geometry). These results indicate that the lead shielding does not provide enough neutron attenuation – *e*.g., there is significant neutron transport (neutron "cross-talk") between adjacent waste canisters – ~40% neutron attenuation thru the lead shield. Additional calculations not shown here were performed with 4.5 MeV mono-energetic neutrons, but they did not change the results significantly.

REFERENCES

[ANSI81] American National Standards Institute/American Nuclear Society (ANSI/ANS), 1981, "Nuclear Criticality Control of Special Actinide Elements," ANSI/ANS-8.15-1981, American National Standards Institute/American Nuclear Society, Washington, D.C.

[ANSI98] American National Standards Institute/American Nuclear Society (ANSI/ANS), 1998, "Nuclear Criticality Safety in Operations with Fissionable Materials Outside Reactors," ANSI/ANS-8.1-1998, American National Standards Institute/American Nuclear Society, Washington, D.C.

[BA09] "Chart of the Nuclides, Nuclides and Isotopes", Seventeenth Edition, Revised 2009, E.M. Baum, et al, Bechtel Marine Propulsion Corporation, Knolls Atomic Power Laboratory, 2009.

[BR90] Brush, L.H., "Test Plan for Laboratory and Modeling Studies of Repository and Radionuclide Chemistry for the Waste Isolation Pilot Plant", SAND90-0266, Sandia National Laboratories, Albuquerque, New Mexico, September 1990 (see pp. 21 and 81). {web address: http://infoserve.sandia.gov/sand_doc/1990/900266.pdf, access date: 2019.08.05} [Note: on page 81, the following weight percentages were identified for rock salt; 93.2 ^{wt}% halite, 1.7 ^{wt}% anhydrite, 1.7 ^{wt}% gypsum, 1.7 ^{wt}% magnesite, and 1.7 ^{wt}% polyhalite. The mass density for the WIPP rock salt was not reported, this requires the conversion of weight fractions into volumes fractions and then determination of the rock salt mass density.]

[CO13] J.L. Conlin (*et al.*), "Release of ENDF/B-VII.1-based Continuous Energy Neutron Cross Section Data Tables for MCNP", LA-UR-13-20240, Los Alamos National Laboratory, 2013, (Intended for: 2013 ANS Annual Meeting, 2013-06-16 (Atlanta, Georgia, United States), {web address: https://mcnp.lanl.gov/pdf_files/la-ur-13-20240.pdf , access date: 2019.07.25}.

[CO14] J.L. Conlin (*et al.*), "Listing of Available ACE Data Tables", LA-UR-13-21822, Los Alamos National Laboratory, 2014-06-26 (rev.4), {web address: https://laws.lanl.gov/vhosts/mcnp.lanl.gov/pdf_files/la-ur-13-21822v4.pdf , access date: 2019.07.25}.

[CRC91] CRC Handbook of Chemistry and Physics, 72nd Ed., D.R. Lide (Editor); CRC Press, Inc., Boca Raton, Florida, 1991.

[DA08] "Shielded Container Type A Evaluation Report", ECO Bo: 11834, Revision: 0, Brad Day, Washington TRU Solutions LLC, 06/11/08, {web address: https://19january2017snapshot.epa.gov/sites/production/files/2015-05/documents/6_shieldedcontainertypea_evalrpt.pdf , access date: 2019.08.02}. [Shielded containers (DOT 7A Type A packaging) are typically shipped in three pack configurations within the HalfPACT Type B packaging

[DOEHP] U.S. Department of Energy (DOE), HalfPACT Shipping Package Safety Analysis Report, current revision, USNRC Certificate of Compliance 71-9279, U.S. Department of Energy, Carlsbad Field Office, Carlsbad, New Mexico. (Identified as reference #4, page 1-1 of Ref [DA08].

[DOETRU18] "Los Alamos National Laboratory, Carlsbad Operations, Performance Assessment Inventory report -- 2018", INV-PA-18, Revisions 0, Effective Date: 12/20/2013. [*aka* PAIR report.]

[FR99] Frankle, S.C., "A Suite of Criticality benchmarks for Validating Nuclear Data", LA-13594 (Editor: P.W. Mendius), Los Alamos National Laboratory, April 1999. [Note, there are MCNP input files for several Jezebel-Pu reactor configurations – only the 95.2 % enriched reactor is of concern in this memo (*e.g*., 95.2^{wt}% Pu239 & 4.5^{wt}% Pu240), see page 77 of the report. Also, the input file presents on this page is incorrect, an extra input block delimitator (blank line) was accidentally inserted in the DATA section of the input.] {Web address: http://lib-www.lanl.gov/cgi-bin/getfile?00326791.pdf, access date: 2019.09.19].

[LANL18] "WIPP Performance Assessment Inventory Report" -- 2018, Los Alamos National Laboratory Carlsbad Operations, INV-PA-18, Revision 0, Effect Date: 12/20/2018 (the controlled version of this document is on the LCODocs website (https://lcodocs.lanl.gov/), printed copy may not be the current version). [WARNING -- do not use DOE Annual TRU Waste Inventory Report -- link: https://wipp.energy.gov/library/TRUwaste/DOE-TRU-18-3425_Rev_0.pdf, DOE/TRU-18-3425, Rev 0, Nov 2018 (this report does not have value decayed to the 2033 closure timeframe).]

[NIST19] National Institute of Standards and Technology, Web Site for ASTAR Program {web address: https://physics.nist.gov/cgi-bin/Star/ap_table.pl , access date: 2019.04.17}. [Access is available via Firefox and not Windows Explorer.]

[PE13] (OUO/ECI) – "MCNP6^{TM} User's Manual", Version 1.0, Manual Rev. 0, D.B. Pelowitz, *et al*, May 2013 – (OUO).

[RE19] Personal communications with R.P. Rechard (Org 08842), Subject: "WIPP RH-TRU Horizontal Emplacement", July 2019.

[RHTRAM14] "RH-TRAMPAC", Revision 3, October 2014, {web address: https://www.nrc.gov/docs/ML1432/ML14323A652.pdf , access date: 2019.09.21}.

[NASA72] Taherzadeh, M., "Neutron Radiation Characteristics of Plutonium Dioxide Fuel", NASA Technical Report 32-1555, National Aeronautics and Space Administration, Jet Propulsion Laboratory, California Institute of Technology, Pasadena, California, June 1, 1972.

[NIST19] National Institute of Standards and Technology, Web Site for ASTAR Program {web address: https://physics.nist.gov/cgi-bin/Star/ap_table.pl , access date: 2019.04.17}. [Access is available via Firefox and not Windows Explorer.]

[SA17] SNL Memo from L.C. Sanchez (SNL Org 08845), To: File (SNL Org 12345), Dated December 13, 2017, Subject: "Identification of Standard ENDF Nuclear Cross Sections Distributed with MCNPTM6.1", [A copy of this memo can be obtained from Org 08845.]

[SH98]   Shleien, B, Slaback, Jr., L.A., and Birky, B.K.; Handbook of Health Physics and Radiological Health, Third Edition, Williams and Williams (A Waverly Company), Baltimore, 1998.

[ST85]   Stein, C. L. (1985). Mineralogy in the Waste Isolation Pilot Plant (WIPP) Facility Stratigraphic Horizon. SAND85-0321, Sandia National Laboratories, Albuquerque, NM. {Web address: : https://prod-ng.sandia.gov/techlib-noauth/access-control.cgi/1985/850321.pdf , access date: 2019.09.19}

Reading Material for Information on the ENDF Nuclear Cross Sections

[BNL09] "ENDF-6 Formats Manual, Data Formats and Procedures for the Evaluated Nuclear Data File ENDF/B-VI and ENDF/B-VII", CSEWG, M. Herman and A. Trkov (Editors), CSEWG Document ENDF-102, Report BNL-90365-2009, June 2009, [web address: https://www.bnl.gov/isd/documents/70393.pdf , access date: 2019.09.19]. {Note: the ENDF/B-VII.1 library is the latest recommended evaluated nuclear data file released by the Cross Section Evaluation Working Group (CSEWG) on December 22, 2011 for use in nuclear science and technology applications – for more information see Ref. [BNL19].}

[BNL19] "ENDF/B-VII.1 Evaluated Nuclear Data Library", BNL web site – discusses cross section library contents and identifies that the ENDF/B-VII.1 is the latest recommended evaluated nuclear data file by the Cross Section Evaluated Working Group (CSEWG). {web address: https://www.nndc.bnl.gov/endf/b7.1/ , access date: 2019.09.19.}

[WE17]   MCNP® User's Manual, Code Version 6.2, C.J. Werner, et al., Editors, LA-UR-17-29981, Los Alamos National Laboratory, October 27, 2017.

LCS:08845:lcs/(2019-5224Rev6)
Copy to:
MS-0779,   Day File   [Dept. 08845]

Appendix B -- WIPP RH-TRU Radionuclide Inventory

RH-TRU Inventory

The Waste Isolation Pilot Plant (WIPP) is a deep-geological waste disposal repository for transuranic waste which can contain up to 6.2×10^6 *cu.ft.* (= 175,564 m^3) of TRU waste, of which 0.25×10^6 *cu.ft.* (= 7,079 m^3)[o] could be remote-handled transuranic waste (RH-TRU). The maximum RH-TRU fissile loading is 370 grams within horizontal containers that are spaced 2.4 *m* apart within rock salt for horizontal emplacement and some vertical containers that contain 1 inch of internal lead shielding.

The RH-TRU waste for disposal in WIPP contains high-enriched plutonium (HEPu), but it also contains much more mass of uranium which is much lower in fissile enrichment. When these fissile nuclides are co-mingled/co-disposed with the rest of the RH-TRU waste matrix, the fissile concentration is very small and not of much concern. The only exception would be a hypothetical long timescale scenario in which plutonium could selectively be separated from uranium (via solubility in groundwater) and deposited separately in concentrated amounts (precipitation at external locations). Data from Table B-1 can be used to illustrate the above discussion. From this table it can be identified that plutonium by itself is ~ 78 ^{wt}% enriched, but when co-mingled with uranium and other actinides its inventory is ~9 ^{wt}%. Even more important, the total RH-TRU plutonium mass is only 69.5 kg-FGE – this corresponds to an average Pu fissile mass loading[p] of only ~ 9.81E-03 (kg-FGE/m^3). From a nuclear criticality viewpoint, this value is insignificant by multiple orders of magnitude.

In order to perform neutron radiation shielding calculations, information of the fissile source isotopic distribution is needed. WIPP inventory values for RH-TRU waste were obtained from the DOE database (Ref. [LANL18]) and were processed using the flowchart shown in Figure B-1 which produced the following tables:

Item	Description
Table B-1	WIPP Remote-Handled Transuranic (RH-TRU) Waste Inventory
Table B-2	WIPP RH-TRU Fissile Gram Equivalent (FGE) Waste Inventory
Table B-3	WIPP RH-TRU Fissile Gram Equivalent (FGE) Enrichments (by Element)
Table B-4	Remote-Handled TRansUranic (RH-TRU) Waste Radionuclide Inventory

The results from these table indicate that WIPP RH-TRU waste is highly enriched with an average plutonium enrichment of ~78 ^{wt}%.
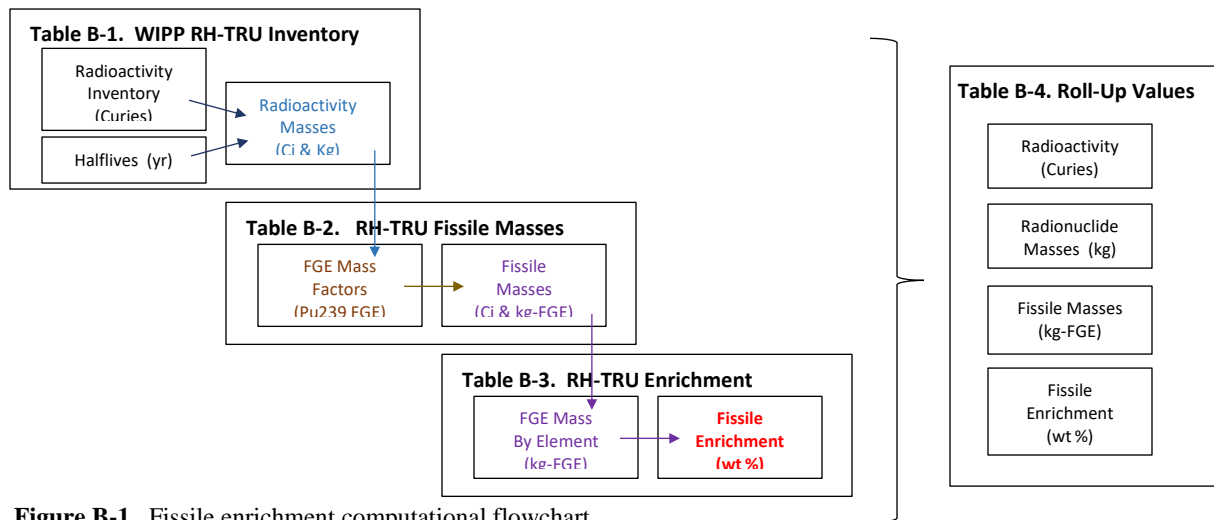
Figure B-1. Fissile enrichment computational flowchart.

---

[o] RH-TRU volume is approximately 1,474 55-gallon (nominal) drum equivalents (out of a total of 810,730 drum equivalents for WIPP).

[p] WIPP has a RH-TRU disposal volume of 0.26 million *cu.ft.*, This corresponds to 7,080 m^3 or 34,002 drum equivalents (nominal). The average plutonium concentration is only 69.5/7,080 = 9.81E-03 (kg-FGE/m^3).

Radionuclide	Radioactivity		Half-Life	Mass	
	(Ci)	(Ci%)	(yr)	(kg)	(kg%)
U-232	8.87E+00	0.00%	6.98E+01	4.02E-01	0.00%
U-233	1.72E+01	0.00%	1.59E+05	1.78E+00	0.02%
U-234	9.70E+00	0.00%	2.46E+05	1.56E+00	0.01%
U-235	1.85E+00	0.00%	7.04E+08	8.56E+02	**8.16%**
U-236	2.53E-01	0.00%	2.34E+07	3.91E+00	0.04%
U-238	3.13E+00	0.00%	4.47E+09	9.31E+03	**88.76%**
Np-237	6.96E+00	0.00%	2.14E+06	9.88E+00	0.09%
Pu-238	2.25E+04	3.96%	8.77E+01	1.31E+00	0.01%
Pu-239	4.22E+03	0.74%	2.41E+04	6.80E+01	**0.65%**
Pu-240	3.16E+03	0.56%	6.56E+03	1.39E+01	**0.13%**
Pu-241	4.53E+04	7.98%	1.43E+01	4.37E-01	0.00%
Pu-242	1.59E+01	0.00%	3.75E+05	4.04E+00	0.04%
Pu-244	2.82E-02	0.00%	8.11E+07	1.56E+00	0.01%
Am-241	1.30E+04	2.29%	4.33E+02	3.79E+00	0.04%
Am-242		0.00%	1.41E+02	0.00E+00	0.00%
Am-243	4.12E+02	0.07%	7.37E+03	2.06E+00	0.02%
Cm-243		0.00%	2.91E+01	0.00E+00	0.00%
Cm-244	3.32E+04	5.85%	1.81E+01	4.10E-01	0.00%
Cm-245		0.00%	8.50E+03	0.00E+00	0.00%
Cm-247		0.00%	1.56E+07	0.00E+00	0.00%
Cf-249		0.00%	3.51E+02	0.00E+00	0.00%
Cf-251		0.00%	9.00E+02	0.00E+00	0.00%
others					
Sr-90	1.96E+05	**34.52%**	2.88E+01	1.42E+00	0.01%
Cs-137	2.50E+05	**44.03%**	3.01E+01	2.88E+00	0.03%
Th-229	8.74E-01	0.00%	7.40E+03	4.14E-03	0.00%
Th-230	2.26E+00	0.00%	7.56E+04	1.10E-01	0.00%
Th-232	2.26E-02	0.00%	1.40E+10	2.05E+02	1.96%
sum =	5.68E+05	100.00%		1.05E+04	100.00%

Table B-1. WIPP Remote-Handled TRansUranic (RH-TRU) Waste Inventory
(radioactivity values taken from Ref. [DOETRU18], values rounded to three digits)

Table B-2. WIPP RH-TRU Fissile Gram Equivalent (FGE) Waste Inventory
(radioactivity values taken from Ref. [DOETRU18], values rounded to three digits)

Radionuclide	Mass (kg)	Pu-239 FGE Factor [a]	FGE Radioactivity (Ci)	FGE Radioactivity (Ci%)	FGE Mass (kg)	FGE Mass (kg%)
U-232	4.01E-04		0.00E+00	0.00%	0.00E+00	0.00%
U-233	1.78E+00	**9.00E-01**	1.55E+01	0.01%	**1.61E+00**	**0.26%**
U-234	1.56E+00		0.00E+00	0.00%	0.00E+00	0.00%
U-235	8.56E+02	**6.43E-01**	1.19E+00	0.00%	**5.51E+02**	**88.53%**
U-236	3.91E+00		0.00E+00	0.00%	0.00E+00	0.00%
U-238	9.31E+03		0.00E+00	0.00%	0.00E+00	0.00%
Np-237	9.88E+00	1.50E-02	1.04E-01	0.00%	1.48E-01	0.02%
Pu-238	1.31E+00	1.13E-01	2.54E+03	2.27%	1.48E-01	0.02%
Pu-239	6.80E+01	**1**	4.22E+03	3.77%	**6.80E+01**	**10.93%**
Pu-240	1.39E+01	2.25E-02	7.11E+01	0.06%	3.13E-01	0.05%
Pu-241	4.37E-01	2.25E+00	1.02E+05	90.99%	9.82E-01	0.16%
Pu-242	4.04E+00	7.50E-03	1.19E-01	0.00%	3.03E-02	0.00%
Pu-244	1.56E+00		0.00E+00	0.00%	0.00E+00	0.00%
Am-241	3.79E+00	1.87E-02	2.43E+02	0.22%	7.09E-02	0.01%
Am-242	0.00E+00	3.46E+01	0.00E+00	0.00%	0.00E+00	0.00%
Am-243	2.06E+00	1.29E-02	5.31E+00	0.00%	2.66E-02	0.00%
Cm-243	0.00E+00	5.00E+00	0.00E+00	0.00%	0.00E+00	0.00%
Cm-244	4.10E-01	9.00E-02	2.99E+03	2.67%	3.69E-02	0.01%
Cm-245	0.00E+00	1.50E+01	0.00E+00	0.00%	0.00E+00	0.00%
Cm-247	0.00E+00	5.00E-01	0.00E+00	0.00%	0.00E+00	0.00%
Cf-249	0.00E+00	4.50E+01	0.00E+00	0.00%	0.00E+00	0.00%
Cf-251	0.00E+00	9.00E+01	0.00E+00	0.00%	0.00E+00	0.00%
others						
Sr-90	1.42E+00		0.00E+00	0.00%	0.00E+00	0.00%
Cs-137	2.88E+00		0.00E+00	0.00%	0.00E+00	0.00%
Th-229	4.14E-03		0.00E+00	0.00%	0.00E+00	0.00%
Th-230	1.10E-01		0.00E+00	0.00%	0.00E+00	0.00%
Th-232	2.05E+02		0.00E+00	0.00%	0.00E+00	0.00%
sum =	1.05E+04		1.12E+05	100.00%	**6.22E+02**	100.00%

a) Pu-239 Fissile Gram Equivalent (FGE) correction factors taken from Ref. [RHTRAM14, Table 5.1-1, pp. 5.1-9 – 5.1-14], original references: [ANSI81] and [ANSI98]. Some waste sites conservatively assigned Pu-239 FGE factors of unity (1.00) to both U-233 and U-235.

Table B-3. WIPP RH-TRU Fissile Gram Equivalent (FGE) Enrichments (by Element)					
Radionuclide	**Uranium Only**		**Plutonium Only**		**U + Pu Only**	
	U mass (kg)	**FGE (kg-fge)**	**Pu mass (kg)**	**FGE (kg-fge)**	**U+Pu mass (kg)**	**FGE (kg-fge)**
U-232	4.02E-04	0.00E+00			4.02E-04	0.00E+00
U-233	1.78E+00	1.61E+00			1.78E+00	1.61E+00
U-234	1.56E+00	0.00E+00			1.56E+00	0.00E+00
U-235	8.56E+02	5.51E+02			8.56E+02	5.51E+02
U-236	3.91E+00	0.00E+00			3.91E+00	0.00E+00
U-238	9.31E+03	0.00E+00			9.31E+03	0.00E+00
Np-237					9.88E+00	1.48E-01
Pu-238			1.31E+00	1.48E-01	1.31E+00	1.48E-01
Pu-239			6.80E+01	6.80E+01	6.80E+01	6.80E+01
Pu-240			1.39E+01	3.13E-01	1.39E+01	3.13E-01
Pu-241			4.37E-01	9.82E-01	4.37E-01	9.82E-01
Pu-242			4.04E+00	3.03E-02	4.04E+00	3.03E-02
Pu-244			1.56E+00	0.00E+00	1.56E+00	0.00E+00
sum =	1.02E+04	5.52E+02	8.93E+01	6.95E+01	1.03E+04	6.22E+02
enrichment =		**5.43^{wt}%**		**77.83 ^{wt} %**		**6.05 ^{wt} %**
mass loading =	0.078	(kg/m^3)	**9.81E-03**	**(kg/ m^3)**	8.78E-02	(kg/ m^3)

Fissile Radionuclide	Radioactivity [b]		Mass [c]		^{239}Pu FGE [d]	Enrichment
	(Ci)	(Ci%)	(kg)	(wt%)	(kg-FGE)	(wt%) [e]
U232	8.87E+00	< 0.01%	4.02E-04	0.00%	0.00E+00	
U233	1.72E+01	< 0.01%	1.78E+00	0.02%	1.61E+00	
U234	9.70E+00	< 0.01%	1.56E+00	0.01%	0.00E+00	
U235	1.85	< 0.01%	8.56E+02	**8.16%**	5.51E+02	
U236	2.53E-01	< 0.01%	3.91E+00	0.04%	0.00E+00	
U238 [f]	3.13E+00	< 0.01%	9.31E+03	**88.76%**	0.00E+00	
Uranium Nuclides only, sum =			1.02E+04		5.52E+02	
Uranium Only Enrichment =						**5.43%**
Np237	6.96E+00	< 0.01%	9.88E+00	0.09%	1.48E-01	
Pu238	2.25E+04	3.96%	1.31E+00	0.01%	1.48E-01	
Pu239	4.22E+03	0.74%	6.80E+01	0.65%	**6.80E+01**	
Pu240	3.16E+03	0.56%	1.39E+01	0.13%	3.13E-01	
Pu241	4.53E+04	7.98%	4.37E-01	0.00%	9.82E-01	
Pu242	1.59E+01	< 0.01%	4.04E+00	0.04%	3.03E-02	
Pu244	2.82E-02	< 0.01%	1.56E+00	0.01%	0.00E+00	
Plutonium Nuclides only, sum =			8.93E+01		6.95E+01	
Plutonium Only Enrichment =						**77.83%**
Uranium + Plutonium Nuclides only, sum =			1.03E+04		6.22E+02	
Uranium + Plutonium Only Enrichment =						**6.05%**
others (transuranics)						
Am241	1.30E+04	2.29%	3.79E+00	0.04%	7.09E-02	
Am242		0.00%	0.00E+00	0.00%	0.00E+00	
Am243	4.12E+02	0.07%	2.06E+00	0.02%	2.66E-02	
Cm243		0.00%	0.00E+00	0.00%	0.00E+00	
Cm244	3.32E+04	5.85%	4.10E-01	0.00%	3.69E-02	
Cm245		0.00%	0.00E+00	0.00%	0.00E+00	
Cm247		0.00%	0.00E+00	0.00%	0.00E+00	
Cf249		0.00%	0.00E+00	0.00%	0.00E+00	
Cf251		0.00%	0.00E+00	0.00%	0.00E+00	
others (non-transuranics)						
Sr-90	1.96E+05	**34.52%**	1.42E+00	0.01%	0.00E+00	
Cs-137	2.50E+05	**44.03%**	2.88E+00	0.03%	0.00E+00	
Th-229	8.74E-01	< 0.01%	4.14E-03	0.00%	0.00E+00	
Th-230	2.26	< 0.01%	1.10E-01	0.00%	0.00E+00	
Th-232	2.26E-02	< 0.01%	2.05E+02	**1.96%**	0.00E+00	
Total sum =	5.68E+05		1.05E+04		6.22E+02	
Uranium + Plutonium + Others Enrichment =						**5.93%**

Table B-4. Remote Handled – TRansUranic (RH-TRU) Waste Radionuclide Inventory[a]
(not included in this table are the large masses of non-radioactive materials
that are present in the RH-TRU waste matrix)

a) RH-TRU inventory data obtained from Ref. [DOETRU18]. .

b) The fission yield products Sr-90 and Cs-137 are the major contributors to the radioactivity inventory of the WIPP bound RH-TRU. Note, since these radionuclides have short half-lives they have very small associated masses.

c) The RH-TRU mass inventory is dominated by uranium (mostly U-238 & U-235). Overall, RH-TRU has an average enrichment of only ~8.4 wt%.

d) FGE – fissile gram equivalent (Pu-239 mass equivalent).

e) The significant information from this table is that the plutonium radionuclides have a large enrichment (~78 wt%). This is of importance for hypothetical scenarios that envision plutonium becoming soluble in groundwater and then transport to a location where it would precipitate out. Also, of concern is that at this large of an enrichment there is the possibility of positive reactive feedback for a criticality assembly.

f) Since U-238 has a very long half-life, these few curies of radioactivity correspond to a large mass inventory.

REFERENCES

[ANSI81] American National Standards Institute/American Nuclear Society (ANSI/ANS), 1981, "Nuclear Criticality Control of Special Actinide Elements," ANSI/ANS-8.15-1981, American National Standards Institute/American Nuclear Society, Washington, D.C.

[ANSI98] American National Standards Institute/American Nuclear Society (ANSI/ANS), 1998, "Nuclear Criticality Safety in Operations with Fissionable Materials Outside Reactors," ANSI/ANS-8.1-1998, American National Standards Institute/American Nuclear Society, Washington, D.C.

[DOETRU18] "Los Alamos National Laboratory, Carlsbad Operations, Performance Assessment Inventory report -- 2018", INV-PA-18, Revisions 0, Effective Date: 12/20/2013. [*aka* PAIR report.]

[LANL18] "WIPP Performance Assessment Inventory Report" -- 2018, Los Alamos National Laboratory Carlsbad Operations, INV-PA-18, Revision 0, Effect Date: 12/20/2018 (the controlled version of this document is on the LCODocs website (https://lcodocs.lanl.gov/), printed copy may not be the current version). WARNING -- do not use DOE Annual TRU Waste Inventory Report -- link: https://wipp.energy.gov/library/TRUwaste/DOE-TRU-18-3425_Rev_0.pdf, DOE/TRU-18-3425, Rev 0, Nov 2018 (this report does not have value decayed to the 2033 closure timeframe).

[RHTRAM14] "RH-TRAMPAC", Revision 3, October 2014, {web address: https://www.nrc.gov/docs/ML1432/ML14323A652.pdf , access date: 2019.09.21}.

Appendix C – WIPP Rock Salt Atom Densities

In order to perform radiation transport or nuclear criticality calculations, atom densities or weight fractions are required for each of the nuclides present in the WIPP/Salado rock salt minerals. Mineral composition for the rock salt were obtained from Ref. [BR90] – this reference contains the individual mass densities (theoretical mineral densities) and weight percentages for five minerals contained within the rock salt. Unfortunately, the reference does not include the bulk density (mixture density) for the rock salt, which is needed for computing atom densities. The bulk density was determined by converting the weight percentages into volume percentages and then used to compute the bulk mass density, which then is used for determining the atom densities of all the nuclides in the WIPP rock salt. The calculations used to ultimately compute the WIPP rock salt atom densities are produced according to the flowchart in Figure B-1 which produced the following tables"

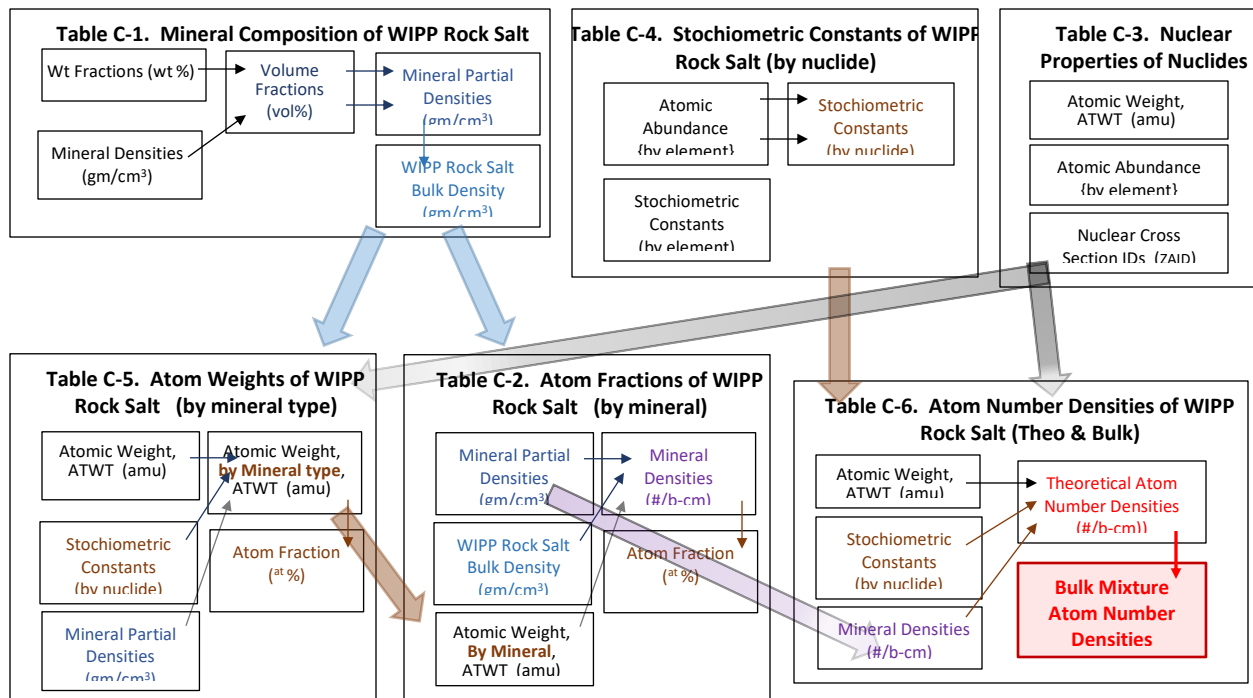| Table	Description
C-1	Composition and Calculation of Bulk Mass Density of WIPP/Salado Rock Salt
C-2	Calculation of Atom Fractions of WIPP/Salado Rock Salt
C-3	Nuclear Properties of Nuclides in WIPP/Salado Rock Salt
C-4	Atomic Properties of WIPP/Salado Rock Salt Minerals by Element & Nuclide
C-5	Atomic Weights and Atom Percent Abundance of Nuclides within Rock Salt Minerals
C-6	Atom Number Densities of WIPP/Salado Rock Salt Minerals by Nuclide

Figure C-1. WIPP rock salt atom density computational flowchart.

Table C-1. Composition and Calculation of Bulk Mass Density of WIPP/Salado Rock Salt [a]
(the purpose of this table is to convert mineral weight fractions to volume fractions,
which can then be used to determine the bulk density of the WIPP rock salt)

Item	Name [b]	Mineral [c] Density	Mineral [d] Wt Frac (Dry)	WtFrac/Density (Dry) (see Equation B-1)	Volume Fraction [e] (Wet, 100% sat)	Partial [f] Density (Wet, 100% sat)
		(gm/cm^3)	(--) dry only	(cm^3/gm) dry only	(--)	(gm/cm^3)
1	Halite	2.165	0.9323	0.43062	0.9323	2.0183
2	Anhydrite	2.61	0.015325	0.00587	0.0127	0.0332
3	Gypsum	2.32	0.015325	0.00661	0.0143	0.0332
4	Magnesite	3.009	0.015325	0.00509	0.0110	0.0332
5	Polyhalite	2.775	0.015325	0.00552	0.0120	0.0332
6	Corrensite (clay)	2.8	0.0064	0.00229	0.0049	0.0139
(7)	1.28 ^{vol}% Porosity (void)	0	0			
7	Porosity (with water)	1.0			0.0128	0.0128
		sum =	1.000	0.456	1.0000	**2.178** [g]

a) Ref. [BR90] is missing the mass density (bulk density) of the WIPP rock salt, thus this table was generated to compute that value (*e.g*, the sum of the "partial densities").
b) Mineral composition values for WIPP rock salt were obtained from Ref. [BR90, pg. 21]. (Also, see Appendix B.)
c) Mass density values for the five (5) minerals that comprise WIPP rock salt were obtained from Ref. [CRC91]. Mass density for the clay (corrensite) was obtained from Ref. [RE19]. Mass density for water was set at 1.0 (gm/cm^3) – which is slightly conservative compared to the value of 0.99707 at NTP conditions. Salado rock salt porosity taken from Ref. [RE19].
d) Mineral weight fractions taken from Ref. [BR90 *pg*. 81] – minerals 2 thru 5 were assumed in the report to have about equal weight contributions, minor minerals (such as basanite, quartz, and various clay minerals) were included as corrensite clay. Note, the mineral weight fractions were for WIPP Salado rock salt with a porosity of 1.28 ^{vol}% without the presence of water in the pores.
e) The equation used to determine the volume fractions is given by:

$$\text{Volume Fraction (i)} = \frac{Weight\ Fraction\ (i)}{\sum_{j=1}^{n} Weight\ Fraction\ (j) * \frac{\rho_i}{\rho_j}} = \frac{Weight\ Fraction\ (i)\ /\ \rho_i}{\sum_{j=1}^{n}\ (Weight\ Fraction\ (j)\ /\ \rho_j)} \quad (\rho = \text{density of species } i) \qquad (Eq.\ \text{C-1})$$

$$\text{Volume Fraction (i) with porosity} = (1.0 - porosity) * \text{Volume Fraction (i) without porosity} \qquad (Eq.\ \text{C-2})$$

f) Partial density (*aka* "particular density") is the mass of a specific species (mineral) per unit *mixture* volume. The summation of the partial densities results in the "bulk density" of the mixture – in this case = **2.178** gm/cm^3.
g) The Salado rock salt bulk (mixture) density is 2.178 (gm/cm^3) if the 1.28 ^{vol}% porosity is filled with water (100% saturation). If the rock salt is dry (zero saturation) then the bulk density is 2.165 (gm/cm^3).

Table C-2. Calculation of Atom Fractions of WIPP/Salado Rock Salt
(these atom fractions are based on the rock salt bulk density & mineral partial densities from Table1)

Item	Mineral Name [a]	Chemical [a] Composition	Mass [b] Density	Weight [c] Percent	Partial [d] Density	ATWT [e] {mineral}	Theo Mineral Density [f]	Atom Percent
			(gm/cm^3)	(^{wt}%)	(gm/cm^3)	(AMU)	(#m/b-cm)	(^{at}%)
1	Halite	NaCl	2.165	93.23 ^{wt}%	2.0183	58.44277	2.08E-02	86.75%
2	Anhydrite	CaSO$_4$	2.61	1.5325 ^{wt}%	0.0332	136.11900	1.47E-04	1.84%
3	Gypsum	CaSO$_4$ 2(H$_2$O)	2.32	1.5325 ^{wt}%	0.0332	172.13876	1.16E-04	2.90%
4	Magnesite	MgCO$_3$	3.009	1.5325 ^{wt}%	0.0332	84.29770	2.37E-04	2.47%
5	Polyhalite	K$_2$MgCa$_2$(SO$_4$)$_4$2(H$_2$O)	2.775	1.5325 ^{wt}%	0.0332	602.84136	3.31E-05	2.14%
6	Corrensite	H$_{28}$O$_{31}$Na$_{0.2}$Mg$_5$Al$_3$Si$_6$K$_{0.2}$Ca$_{0.6}$Fe$_3$	2.8	0.64 ^{wt}%	0.0139	1099.01835	7.59E-06	1.22%
7	Water		1.0	0.0128 ^{wt}%	0.0128	18.00988	4.28E-04	2.68%
			sum =	100.0 ^{wt}%	**2.178**		*sum* =	100.00 ^{at}%

a) Mineral compositions for WIPP/Salado rock salt were identified in Ref. [BR90, *pg*. 21]. [Not shown are minor minerals such as basanite, quartz, and various clay minerals.]
b) Mass density values for the five (5) minerals that comprise WIPP rock salt were obtained from Ref. [CRC91].
c) Mineral weight fractions taken from Ref. [BR90 *pg*. 81] – minerals 2 thru 5 were assumed in the report to have about equal weight contributions, minor minerals were not included.
d) Partial densities taken from Table C-1 – originally computed using weight fractions published in Ref. [BR90, *pg*. 81].
e) Atomic weight values for mineral composition taken from Table C-5 (last row entries).
f) Theoretical mineral density = mineral density x Avogadro constant / ATWT (*ex*. halite = 2.0183 x 0.6022 / 58.44277 = 2.08E-02).

Table C-3. Nuclear Properties of Nuclides Within WIPP/Salado Rock Salt
(note: ZAIDs are presented for the rock salt nuclides, only carbon has a ZAID for natural abundances)

Item	Symbol	Name	Atomic Weight, ATWT [a] (AMU)	Atomic Percent Abundance [a] {by element} (%)	Nuclear Cross Section ID [b] (ZAID)
1	H (nat)	Hydrogen	1.00794		
2	H-1			99.99%	1001.80c
3	H-2			0.01%	1002.80c
4	C (nat)	Carbon	12.0107	100.00%	6000.80c
5	O (nat)	Oxygen	15.994		
6	O-16			99.76%	8016.80c
7	O-17			0.04%	8017.80c
8	O-18			0.21%	**8016.80c** [c]
9	F-19	Fluorine	18.9984032	100.00%	9019.80c
10	Na-23	Sodium	22.98976928	100.00%	11023.80c
11	Mg (nat)	Magnesium	24.305		
12	Mg-24			78.99%	12024.80c
13	Mg-25			10.00%	12025.80c
14	Mg-26			11.01%	12026.80c
15	Al-17		26.9815386	100.00%	13027.80c
16	Si-nat	Silicon	28.0855		
17	Si-28			92.22%	14028.80c
18	Si-29			4.69%	14028.80c
19	Si-30			3.09%	14028.80c
20	S-nat	Sulfur	32.065		
21	S-32			94.99%	16032.80c
22	S-33			0.75%	16033.80c
23	S-34			4.25%	16034.80c
24	S-36			0.01%	16036.80c
25	Cl-nat	Chlorine	35.453		
26	Cl-35			75.76%	17035.80c
27	Cl-37			24.24%	17037.80c
28	K-nat	Potassium	39.0983		
29	K-39			93.26%	19039.80c
30	K-40			0.01%	19040.80c
31	K-41			6.73%	19041.80c
32	Ca-nat	Calcium	40.078		
33	Ca-40			96.94%	20040.80c
34	Ca-42			0.65%	20042.80c
35	Ca-43			0.14%	20043.80c
36	Ca-44			2.09%	20044.80c
37	Ca-46			0.00%	20046.80c
38	Ca-48			0.19%	20048.80c
39	Ti-nat	Titanium	47.867		
40	Ti-46			8.25%	22046.80c
41	Ti-47			7.44%	22047.80c
42	Ti-48			73.72%	22048.80c
43	Ti-49			5.41%	22049.80c
44	Ti-50			5.18%	22050.80c
45	Fe-nat	Iron	55.845		
46	Fe-54			5.85%	26054.80c
47	Fe-56			91.75%	26056.80c
48	Fe-57			2.12%	26057.80c
49	Fe-58			0.28%	26058.80c

a) Atomic weight and abundance values taken from Ref. [BA09]. Note – no radionuclides are present in WIPP rock salt.

b) Nuclear cross section ZAID identifiers taken directly from the ENDF (Evaluated Nuclear Data Files) which are distributed with MCNP[TM] (see Ref. [PE13] for details). For this list of nuclide, there exists nuclear cross sections for only 38 out of the 49 item entries. Note – these ".80c" nuclear cross section identifiers actually correspond to ENDF/B-VII.1 libraries (see Refs. [CO13] and [CO14] for details. **Special Note – Do Not use ENDF/B-VII.0 nuclear cross sections (*e.g.,* *.70c cross sections)**, there are data corruption problems with those cross sections libraries.

c) Note – nuclear cross sections are missing for Oxygen-18. A commonly used fix was applied, in which the O-16 cross sections are used as a replacement since these nuclides are expected to have similar cross sections and, also, because the atomic abundance for O-18 is small.

		Stochiometric Constants (by element)							Stochiometric Constants (by nuclide)						
		1	2	3	4	5	6	7	1	2	3	4	5	6	7
Item	Symbol	Halite	Anhydrite	Gypsum	Magnesite	Polyhalite	Corrensite	Water	Halite	Anhydrite	Gypsum	Magnesite	Polyhalite	Corrensite	Water
1	H (nat)			4		4	28	2							
2	H-1										3.99954		3.99954	27.99678	1.99977
3	H-2										0.00046		0.00046	0.00322	0.00023
4	C (nat)				1							1.00000			
5	O (nat)		4	6	3	18	31	1							
6	O-16									3.99028	5.98542	2.99271	17.95626	30.92467	0.99757
7	O-17									0.00152	0.00228	0.00114	0.00684	0.01178	0.00038
8	O-18									0.00820	0.01230	0.00615	0.03690	0.06355	0.00205
9	F-19														
10	Na-23	1					0.2		1.00000					0.2	
11	Mg (nat)				1	1	5								
12	Mg-24											0.78990	0.78990	3.9495	
13	Mg-25											0.10000	0.10000	0.5	
14	Mg-26											0.11010	0.11010	0.5505	
15	Al-17						3							3	
16	Si-nat						6								
17	Si-28													5.53338	
18	Si-29													0.2811	
19	Si-30													0.18552	
20	S-nat		1	1		4									
21	S-32									0.94990	0.94990		3.79960		
22	S-33									0.00750	0.00750		0.03000		
23	S-34									0.04250	0.04250		0.17000		
24	S-36									0.00010	0.00010		0.00040		
25	Cl-nat	1													
26	Cl-35								0.75760						
27	Cl-37								0.24240						
28	K-nat					2	0.2								
29	K-39												1.86516	0.1865162	
30	K-40												0.00023	0.0000234	
31	K-41												0.13460	0.0134604	
32	Ca-nat		1	1		2	0.6								
33	Ca-40									0.96941	0.96941		1.93882	0.581646	
34	Ca-42									0.00647	0.00647		0.01294	0.003882	
35	Ca-43									0.00135	0.00135		0.00270	0.00081	
36	Ca-44									0.02086	0.02086		0.04172	0.012516	
37	Ca-46									0.00004	0.00004		0.00008	0.000024	
38	Ca-48									0.00187	0.00187		0.00374	0.001122	
39	Ti-nat														
40	Ti-46														
41	Ti-47														
42	Ti-48														
43	Ti-49														
44	Ti-50														
45	Fe-nat						3								
46	Fe-54													0.17535	
47	Fe-56													2.75262	
48	Fe-57													0.06357	
49	Fe-58													0.00846	
	Mineral Sum =	2	6	12	5	31	77	3	2	6	12	5	31	77	3

Table C-5. Atomic Weights and Atom Percent Abundance of Nuclides within Rock Salt Minerals

Item	Symbol	Stochiometric Constant x Atomic Weight {by mineral type} (AMU)							Atom Fraction Abundance (a) {for bulk mixture} (--) [values used for quality check]						
		1 Halite	2 Anhydrite	3 Gypsum	4 Magnesite	5 Polyhalite	6 Corrensite	7 Water	1 Halite	2 Anhydrite	3 Gypsum	4 Magnesite	5 Polyhalite	6 Corrensite	7 Water
1	H (nat)														
2	H-1			4.031296348		4.031296348	28.21907443	2.015648174			9.7000E-03		2.7698E-03	4.4414E-03	1.7885E-02
3	H-2			0.000463652		0.000463652	0.003245567	0.000231826			1.1156E-06		3.1856E-07	5.1083E-07	2.0570E-06
4	C (nat)				12.0107							4.9525E-03			
5	O (nat)														
6	O-16		63.82053832	95.73080748	47.86540374	287.1924224	494.609172	15.95513458		1.2238E-02	1.4516E-02	1.4821E-02	1.2435E-02	4.9059E-03	8.9217E-03
7	O-17		0.02431088	0.03646632	0.01823316	0.10939896	0.18840932	0.00607772		4.6619E-06	5.5297E-06	5.6459E-06	4.7369E-06	1.8688E-06	3.3985E-06
8	O-18		0.1311508	0.1967262	0.0983631	0.5901786	1.0164187	0.0327877		2.5150E-05	2.9831E-05	3.0458E-05	2.5554E-05	1.0082E-05	1.8334E-05
9	F-19														
10	Na-23	22.98976928					4.597953856		4.3458E-01						
11	Mg (nat)														
12	Mg-24				19.1985195	19.1985195	95.9925975					3.9120E-03	5.4703E-04	6.2655E-04	
13	Mg-25				2.4305	2.4305	12.1525					4.9525E-04	6.9253E-05	7.9321E-05	
14	Mg-26				2.6759805	2.6759805	13.3799025					5.4527E-04	7.6248E-05	8.7332E-05	
15	Al-17						80.9446158								
16	Si-nat														
17	Si-28						155.407744								
18	Si-29						7.89483405								
19	Si-30						5.21042196								
20	S-nat														
21	S-32		30.4585435	30.4585435			121.834174			2.9134E-03	2.3038E-03			2.6313E-03	
22	S-33		0.2404875	0.2404875			0.96195			2.3003E-05	1.8190E-05			2.0776E-05	
23	S-34		1.3627625	1.3627625			5.45105			1.3035E-04	1.0307E-04			1.1773E-04	
24	S-36		0.0032065	0.0032065			0.012826			3.0671E-07	2.4253E-07			2.7701E-07	
25	Cl-nat														
26	Cl-35	26.8591928							3.2924E-01						
27	Cl-37	8.5938072							1.0534E-01						
28	K-nat														
29	K-39					72.92466342	7.292466342						1.2917E-03	2.9589E-05	
30	K-40					0.009149002	0.0009149						1.6205E-07	3.7122E-09	
31	K-41					5.262787573	0.526278757						9.3217E-05	2.1354E-06	
32	Ca-nat														
33	Ca-40		88.85201398	88.85201398		77.70402796	23.31120839			2.9732E-03	2.3511E-03		1.3427E-03	9.2273E-05	
34	Ca-42		0.25930466	0.25930466		0.51860932	0.155582796			1.9844E-05	1.5692E-05		8.9613E-06	6.1585E-07	
35	Ca-43		0.0541053	0.0541053		0.1082106	0.03246318			4.1405E-06	3.2741E-06		1.8698E-06	1.2850E-07	
36	Ca-44		0.83602708	0.83602708		1.67205416	0.501616248			6.3979E-05	5.0591E-05		2.8892E-05	1.9856E-06	
37	Ca-46		0.00160312	0.00160312		0.00320624	0.000961872			1.2268E-07	9.7011E-08		5.5402E-08	3.8074E-09	
38	Ca-48		0.07494586	0.07494586		0.14989172	0.044967516			5.7354E-06	4.5353E-06		2.5901E-06	1.7800E-07	
39	Ti-nat														
40	Ti-46														
41	Ti-47														
42	Ti-48														
43	Ti-49														
44	Ti-50														
45	Fe-nat														
46	Fe-54						9.79242075								
47	Fe-56						153.7200639								
48	Fe-57						3.55006665								
49	Fe-58						0.4724487								
	Mineral Sum =	58.44276928	136.119	172.13876	84.2977	602.84136	1099.01835	18.00988	8.6915E-01	1.8402E-02	2.9103E-02	2.4763E-02	2.1468E-02	1.0280E-02	2.6830E-02

a) Note – atom fraction abundance values given by;   AFA (i) = vol fraction (i) * theoretical atom density / total atom density   (*Eq.* C-3)

Table C-6. Atom Number Densities of Salado Rock Salt Minerals by Nuclide
(the atom densities to be used in radiation transport code are shown in blue font)

Item	Symbol	Theoretical Atom Density (a) {each mineral} (#/b-cm)							Bulk Mixture Atom Density (b) {includes all minerals} (#/b-cm)							Total
		1 Halite	2 Anhydrite	3 Gypsum	4 Magnesite	5 Polyhalite	6 Corrensite	7 Water	1 Halite	2 Anhydrite	3 Gypsum	4 Magnesite	5 Polyhalite	6 Corrensite	7 Water	Roll-Up Values
1	H (nat)															
2	H-1			3.2462E-02		1.1087E-02	4.2955E-02	6.6868E-02			4.6422E-04		1.3256E-04	2.1256E-04	8.5591E-04	5.9677E-04
3	H-2			3.7335E-06		1.2752E-06	4.9404E-06	7.6907E-06			5.3391E-08		1.5246E-08	2.4447E-08	9.8441E-08	6.8637E-08
4	C (nat)				2.1496E-02							2.3701E-04				2.3701E-04
5	O (nat)															
6	O-16		4.6076E-02	4.8580E-02	6.4331E-02	4.9777E-02	4.7447E-02	3.3357E-02		5.8570E-04	6.9471E-04	7.0931E-04	5.9512E-04	2.3478E-04	4.2697E-04	2.5848E-03
7	O-17		1.7552E-05	1.8505E-05	2.4505E-05	1.8961E-05	1.8074E-05	1.2706E-05		2.2311E-07	2.6463E-07	2.7020E-07	2.2670E-07	8.9435E-08	1.6264E-07	9.8463E-07
8	O-18		9.4686E-05	9.9831E-05	1.3220E-04	1.0229E-04	9.7503E-05	6.8548E-05		1.2036E-06	1.4276E-06	1.4576E-06	1.2230E-06	4.8248E-07	8.7741E-07	5.3118E-06
9	F-19															
10	Na-23	2.2309E-02					3.0686E-04		2.0798E-02							2.0798E-02
11	Mg (nat)															
12	Mg-24				1.6980E-02	2.1897E-03	6.0596E-03					1.8722E-04	2.6179E-05	2.9985E-05		2.1340E-04
13	Mg-25				2.1496E-03	2.7721E-04	7.6714E-04					2.3701E-05	3.3143E-06	3.7961E-06		2.7016E-05
14	Mg-26				2.3667E-03	3.0521E-04	8.4462E-04					2.6095E-05	3.6490E-06	4.1795E-06		2.9744E-05
15	Al-17						4.6028E-03									
16	Si-nat															
17	Si-28						8.4897E-03									
18	Si-29						4.3129E-04									
19	Si-30						2.8464E-04									
20	S-nat															
21	S-32		1.0969E-02	7.7097E-03		1.0533E-02				1.3943E-04	1.1025E-04		1.2593E-04			3.7561E-04
22	S-33		8.6603E-05	6.0873E-05		8.3163E-05				1.1009E-06	8.7051E-07		9.9428E-07			2.9656E-06
23	S-34		4.9075E-04	3.4494E-04		4.7126E-04				6.2382E-06	4.9329E-06		5.6342E-06			1.6805E-05
24	S-36		1.1547E-06	8.1163E-07		1.1088E-06				1.4678E-08	1.1607E-08		1.3257E-08			3.9542E-08
25	Cl-nat															
26	Cl-35	1.6901E-02							1.5756E-02							1.5756E-02
27	Cl-37	5.4077E-03							5.0413E-03							5.0413E-03
28	K-nat															
29	K-39					5.1704E-03	2.8617E-04						6.1816E-05	1.4161E-06		6.1816E-05
30	K-40					6.4867E-07	3.5902E-08						7.7554E-09	1.7766E-10		7.7554E-09
31	K-41					3.7314E-04	2.0652E-05						4.4611E-06	1.0219E-07		4.4611E-06
32	Ca-nat															
33	Ca-40		1.1194E-02	7.8681E-03		5.3746E-03	8.9241E-04			1.4229E-04	1.1252E-04		6.4258E-05	4.4159E-06		3.1907E-04
34	Ca-42		7.4710E-05	5.2513E-05		3.5871E-05	5.9561E-06			9.4968E-07	7.5096E-07		4.2887E-07	2.9473E-08		2.1295E-06
35	Ca-43		1.5589E-05	1.0957E-05		7.4847E-06	1.2428E-06			1.9815E-07	1.5669E-07		8.9485E-08	6.1496E-09		4.4433E-07
36	Ca-44		2.4087E-04	1.6931E-04		1.1565E-04	1.9203E-05			3.0619E-06	2.4212E-06		1.3827E-06	9.5023E-08		6.8657E-06
37	Ca-46		4.6188E-07	3.2465E-07		2.2177E-07	3.6823E-08			5.8713E-09	4.6427E-09		2.6514E-09	1.8221E-10		1.3165E-08
38	Ca-48		2.1593E-05	1.5178E-05		1.0368E-05	1.7215E-06			2.7448E-07	2.1705E-07		1.2395E-07	8.5184E-09		6.1548E-07
39	Ti-nat															
40	Ti-46															
41	Ti-47															
42	Ti-48															
43	Ti-49															
44	Ti-50															
45	Fe-nat															
46	Fe-54						2.6904E-04									
47	Fe-56						4.2233E-03									
48	Fe-57						9.7534E-05									
49	Fe-58						1.2980E-05									
	Sum =	4.4618E-02	6.9283E-02	9.7396E-02	1.0748E-01	8.5936E-02	1.1814E-01	1.0031E-01	4.1595E-02	8.8069E-04	1.3928E-03	1.1851E-03	1.0274E-03	4.9197E-04	1.2840E-03	4.6081E-02

a) Theoretical densities are given by; Atom density (i) = $\dfrac{Mass\ Density(i) * Avogadro\ Constant}{ATWT(i)}$ (Eq. C-4)

b) Bulk (mixture) densities given by; Bulk atom density (i) = volume fraction (i) * theoretical atom density (Eq. C-5)

15 November 2019

REFERENCES

[BR90] Brush, L.H., "Test Plan for Laboratory and Modeling Studies of Repository and Radionuclide Chemistry for the Waste Isolation Pilot Plant", SAND90-0266, Sandia National Laboratories, Albuquerque, New Mexico, September 1990 (see pp. 21 and 81). {web address: http://infoserve.sandia.gov/sand_doc/1990/900266.pdf, access date: 2019.08.05} [Note: on page 81, the following weight percentages were identified for rock salt; 93.2 ^{wt}% halite, 1.7 ^{wt}% anhydrite, 1.7 ^{wt}% gypsum, 1.7 ^{wt}% magnesite, and 1.7 ^{wt}% polyhalite. The mass density for the WIPP rock salt was not reported, this requires the conversion of weight fractions into volumes fractions and then determination of the rock salt mass density.]

[CRC91] CRC Handbook of Chemistry and Physics, 72nd Ed., D.R. Lide (Editor); CRC Press, Inc., Boca Raton, Florida, 1991.

[PE13] (OUO/ECI) – "MCNP6™ User's Manual", Version 1.0, Manual Rev. 0, D.B. Pelowitz, *et al*, May 2013 – (OUO).

[RE19] Personal communications with R.P. Rechard (Org 08842), Subject: "WIPP RH-TRU Horizontal Emplacement", July 2019.

[ST85] Stein, C. L. (1985). Mineralogy in the Waste Isolation Pilot Plant (WIPP) Facility Stratigraphic Horizon. SAND85-0321, Sandia National Laboratories, Albuquerque, NM. {Web address: : https://prod-ng.sandia.gov/techlib-noauth/access-control.cgi/1985/850321.pdf , access date: 2019.09.19}

Appendix D -- Salado Rock Salt – Data Analysis of Composition

Salado Rock Salt

TRU waste is disposed within the Salado rock salt formation of the Waste Isolation Pilot Plant (WIPP). Ref. [BR90, *pp*. 21 & 81] indicated that experimental measurements of the mineral composition of this host rock is documented in Ref. [ST85]. This appendix contains the data analysis of the three key tables from that reference, these are presented in the following figures and tables:

Tables & Figures	Description
Fig. D-1	LINEAR-SCALE Weight percentages of water-insoluble residues in WIPP Salado rock salt
Fig. D-2	SEMI-LOG-SCALE Weight percentages of water-insoluble residues in WIPP Salado rock salt
Fig. D-3	LINEAR-SCALE Weight (per water-insoluble residue) percentages of EDTA-insoluble residues in WIPP Salado rock salt
Fig. D-4	SEMI-LOG Weight (per water-insoluble residue) percentages of EDTA-insoluble residues in WIPP Salado rock salt
Fig. D-5	LINEAR-SCALE Weight (per whole rock) percentages of EDTA-insoluble residues in WIPP Salado rock salt
Fig. D-6	SEMI-LOG Weight (per whole rock) percentages of EDTA-insoluble residues in WIPP Salado rock salt
Tab. D-1	WIPP Salado Rock Salt – Weight Percentages of Water-Insoluble Residues
Tab. D-2	WIPP Salado Rock Salt – Weight Percentages of EDTA-Insoluble Residues

Findings

The key statistical results are:

1) Average (mean) weight percent (per whole rock) of water-insoluble residues in Salado rock salt = 6.77 wt%
2) Average (mean) weight percent (per water-insoluble residue) of EDTA-insoluble residues in Salado rock salt = 33.73 wt%
3) Average (mean) weight percent (per whole rock) of EDTA-insoluble residues in Salado rock salt = 0.64 wt%

These values indicate the following values for the constituents of the Salado rock salt:

Bulk Density of WIPP Rock Salt		
Name	**Theoretical Density**	**Wt Fraction (dry)**
	(gm/cm³)	**(--)**
Halite	2.165	0.932300 (a)
Anhydrite	2.61	0.015325 (c)
Gypsum	2.32	0.015325 (c)
Magnesite	3.009	0.015325 (c)
Polyhalite	2.775	0.015325 (c)
Corrensite	2.8	0.006400 (b)
Porosity/Void	0	0
Porosity/water	1.0000	
(*porosity* = 0.0128 (d))	*sum* =	1.000000

(a) The 93.23 wt% for Halite is a detailed calculation based on the Stein-1985 report (using 4 significant decimal digits).

(b) The 0.64 wt% is the remainder (non EDTA soluble) of the materials within Salado rock salt, this is assumed to be clay (corrensite).

(c) The reminder of the wt% is assumed to equal proportions of these four (4) minerals.

(d) Porosity from Ref. [RE19].

Notes on Lognormal Distribution:

Many probability and geologic data are best fit using the log-normal distribution. This is represented by Equation C-1 below. Extra care is needed for using this distribution, this is identified by the following:

1) The lognormal distribution uses parameters μ and σ which are location and scale parameters for a normally distributed logarithm $ln(X)$ (see Equations C-6 and C-7) {see Ref. [WI19] for details}.
   (They are not parameters for a lognormally distributed random variable X !!)
2) The parameters μ and σ are determined from Equations C-2 and C-3.
3) Most importantly – plots of the data and fitted distributions are needed for visual inspection.

$$\text{Lognormal Distribution} \quad PDF(x) = \frac{1}{x\sigma\sqrt{2\pi}} exp\left(-\frac{(\ln x - \mu)^2}{2\sigma^2}\right) \qquad (Eq.\ D\text{-}1)$$

$$Mean\ = exp\left(\mu + \frac{\sigma^2}{2}\right) \qquad (Eq.\ D\text{-}2)$$

$$Median\ = exp(\mu) \qquad (Eq.\ D\text{-}3)$$

$$Mode\ = exp(\mu - \sigma) \qquad (Eq.\ D\text{-}4)$$

$$Variance\ = [exp(\sigma^2) - 1]\, exp(2\mu + \sigma^2) \qquad (Eq.\ D\text{-}5)$$

where, "μ" and "σ" are lognormal distributions parameters given by the following expressions;

$$\mu = ln\left(\frac{m}{\sqrt{1+\frac{v}{m^2}}}\right) \qquad (Eq.\ D\text{-}6)$$

$$\sigma^2 = ln\left(1 + \frac{v}{m^2}\right) \qquad (Eq.\ D\text{-}7)$$

CAUTION

In this case,
"m" is the normally distributed mean value, and
"v" is the normally distributed variance value.

REFERENCES

[BR90]   Brush, L.H., "Test Plan for Laboratory and Modeling Studies of Repository and Radionuclide Chemistry for the Waste Isolation Pilot Plant", SAND90-0266, Sandia National Laboratories, Albuquerque, New Mexico, September 1990 (see pp. 21 and 81). {web address: http://infoserve.sandia.gov/sand_doc/1990/900266.pdf, access date: 2019.08.05} [Note: on page 81, the following weight percentages were identified for rock salt; 93.2 wt% halite, 1.7 wt% anhydrite, 1.7 wt% gypsum, 1.7 wt% magnesite, and 1.7 wt% polyhalite. The mass density for the WIPP rock salt was not reported, this requires the conversion of weight fractions into volumes fractions and then determination of the rock salt mass density.]

[RE19]   Personal communications with R.P. Rechard (Org 08842), Subject: "WIPP RH-TRU Horizontal Emplacement", July 2019.

[ST85]   Stein, C. L. (1985). Mineralogy in the Waste Isolation Pilot Plant (WIPP) Facility Stratigraphic Horizon. SAND85-0321, Sandia National Laboratories, Albuquerque, NM. {Web address: : https://prod-ng.sandia.gov/techlib-noauth/access-control.cgi/1985/850321.pdf , access date: 2019.09.19}

[WI19]   "Log-normal distribution", Wikipedia fact sheet, {web address: https://en.wikipedia.org/wiki/Log-normal_distribution , access date: 2019.09.21}.
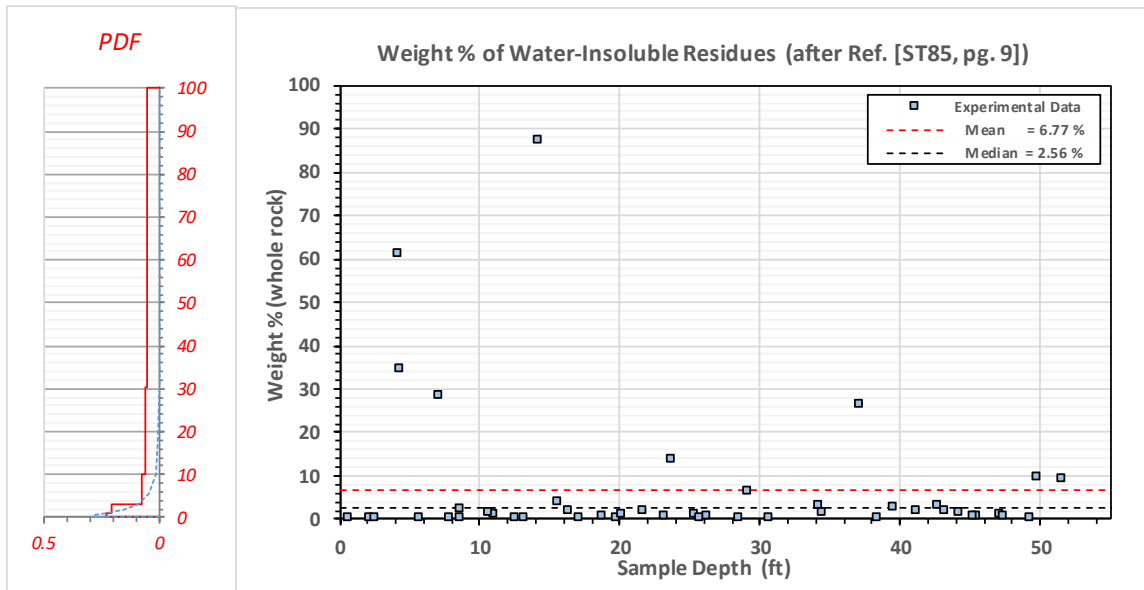
15 November 2019

Figure D-1 LINEAR-SCALE. Weight percentages of water-insoluble residues in WIPP Salado rock salt (see Table D-1 for values, original data taken from Ref. [ST85, pg. 9]). Several high percentage values exist, which required a lognormal distribution. The distribution used the following lognormal parameters; μ=0.9402, σ=1.3945, m=6.7702, and v=274.62.
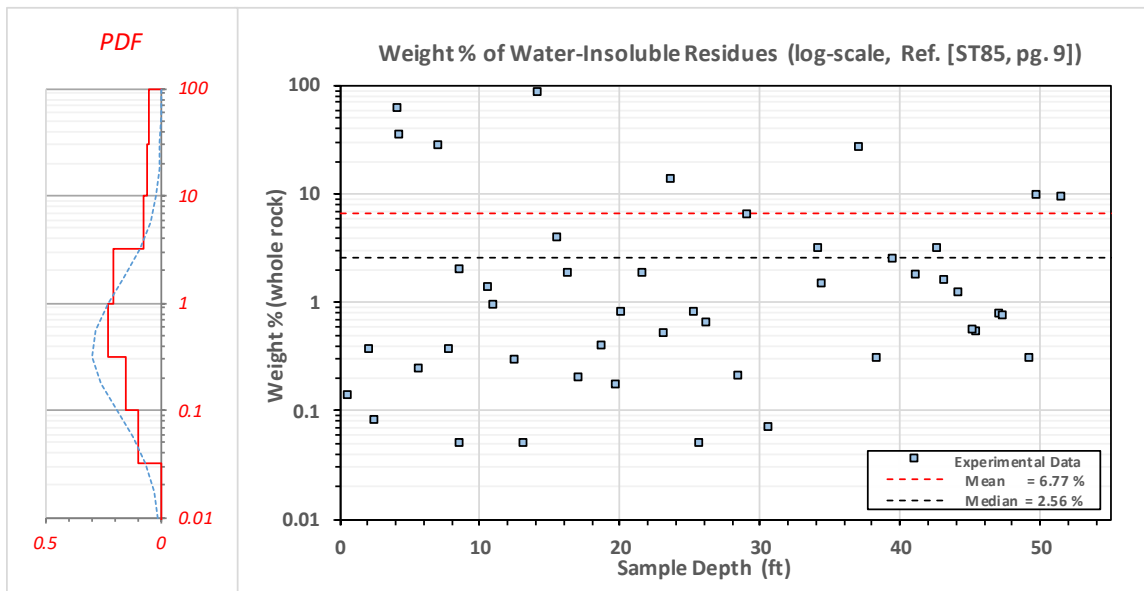

Figure D-2 SEMI-LOG-SCALE. Weight percentages of water-insoluble residues in WIPP Salado rock salt (see Table D-1 for values, original data taken from Ref. [ST85, pg. 9]). The distribution used the following lognormal parameters; μ=0.9402, σ=1.3945, m=6.7702, and v=274.62 .

Sample No.	Sample Depth		Sample Weight	Weight of Water-Insoluble Residue	Weight % (whole rock)
	From	To			
	(ft)		(g)	(g)	(wt%)
FH-201	2	2.5	757	2.76	0.36
FH-202	4	4.7	482	165.58	34.35
FH-203	8.3	9	649	13.09	2.02
FH-204	10.8	11.3	734	6.83	0.93
FH-205	13	13.55	715	0.38	0.05
FH-206	15.55	15.85	696	27.05	3.89
FH-207	16.9	17.45	700	1.41	0.2
FH-208	18.4	19.1	670.2	2.69	0.4
FH-209	19.65	20.05	641.3	1.1	0.17
FH-210	21.5	22	742.55	13.86	1.87
FH-211	23	23.5	700	3.6	0.51
FH-212	25.1	25.7	700	5.7	0.81
FH-213	26	26.5	700	4.57	0.65
FH-214	28.25	28.85	751	1.54	0.205
FH-215	30.5	31.05	700	0.47	0.07
FH-216	31	38*	674	9.93	1.47
FH-217	39.25	39.85	535	13.42	2.51
FH-218	41	41.5	617.5	10.95	1.77
FH-219	42.5	43	676.5	21.13	3.12
FH-220	44	44.5	700	8.72	1.245
FH-221	45.3	45.85	743.85	4.04	0.54
FH-222	47	47.5	747.5	5.94	0.79
FH-223	49.05	49.55	739.5	2.2	0.3
FH-224	4	4.5**	385.6	235.74	61.14
*core loss zone					
**From RM-4					
FH-228	0.4	0.9	1,000	1.425	0.14
FH-229	2.3	2.8	1,000	0.77	0.08
FH-230	4.75	6.75	1,000	2.38	0.24
FH-231	7.1	7.3	600	169.89	28.32
FH-232	7.75	8.15	900	3.27	0.36
FH-233	8.15	9.1	1,000	0.45	0.05
FH-234	10.5	10.9	1,000	13.46	1.35
FH-235	12.5	12.6	1,000	2.87	0.29
FH-236	14	14.45	200	174.15	87.08
FH-237	16.1	16.6	700	12.99	1.86
FH-238	29	29.5	550	34.68	6.31
FH-239	34.05	34.5	600	18.58	3.1
FH-240	36.9	37.6	700	184.11	26.3
FH-241	38.2	38.7	1,000	3.04	0.3
FH-242	43.05	43.55	600	9.7	1.62
FH-243	47.2	47.7	850	6.41	0.75
FH-244	49.65	50	300	29.03	9.68
FH-245	51.3	52.1	400	37.19	9.3
FH-246*	20.05	20.45	1,000	8	0.8
FH-247*	23.45	23.95	600	81.2	13.53
FH-248*	25.5	26	1,000	0.47	0.05
FH-249*	45	45.65	900	4.96	0.55
*From RM-7					
				Average =	6.770
				(sample) Std dev =	16.572
				Median =	0.805
				(sample) Variance =	274.620

Table D-1. WIPP Salado Rock Salt – Weight Percentages of Water-Insoluble Residues   (Taken from Ref. [ST85, pg. 9, Table 1])
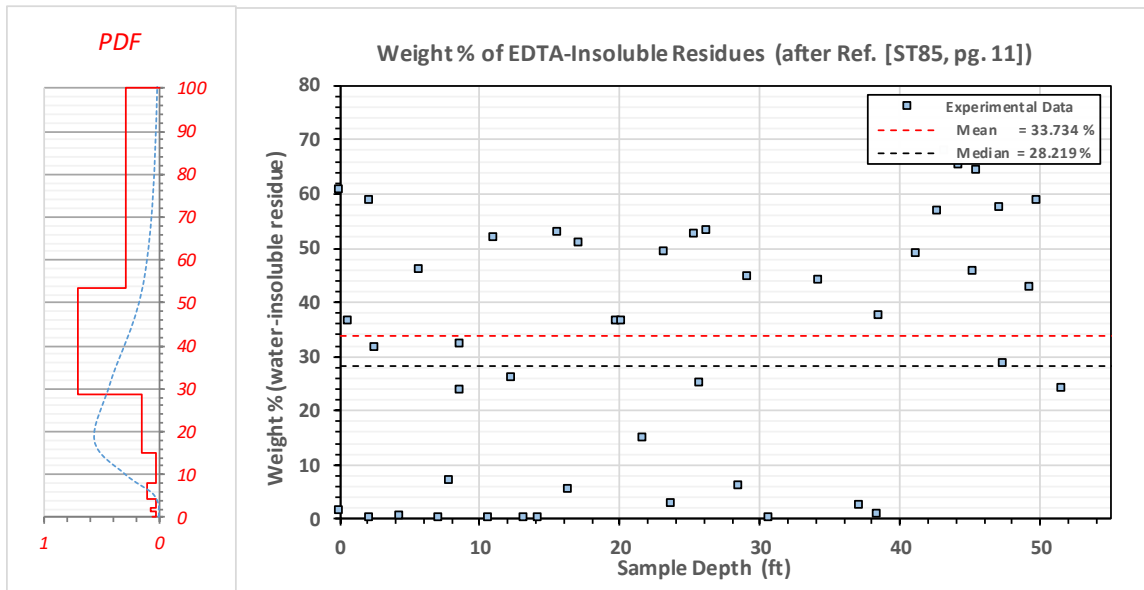
Figure D-3 LINEAR-SCALE. Weight (per water-insoluble residue) percentages of EDTA-insoluble residues in WIPP Salado rock salt (see Table D-2 for values, original data taken from Ref. [ST85, pg. 11]). Several very low percentage values exist which required a lognormal distribution. The distribution used the following lognormal parameters; μ=3.3400, σ=0.5975, m=33.734, and v=488.28.
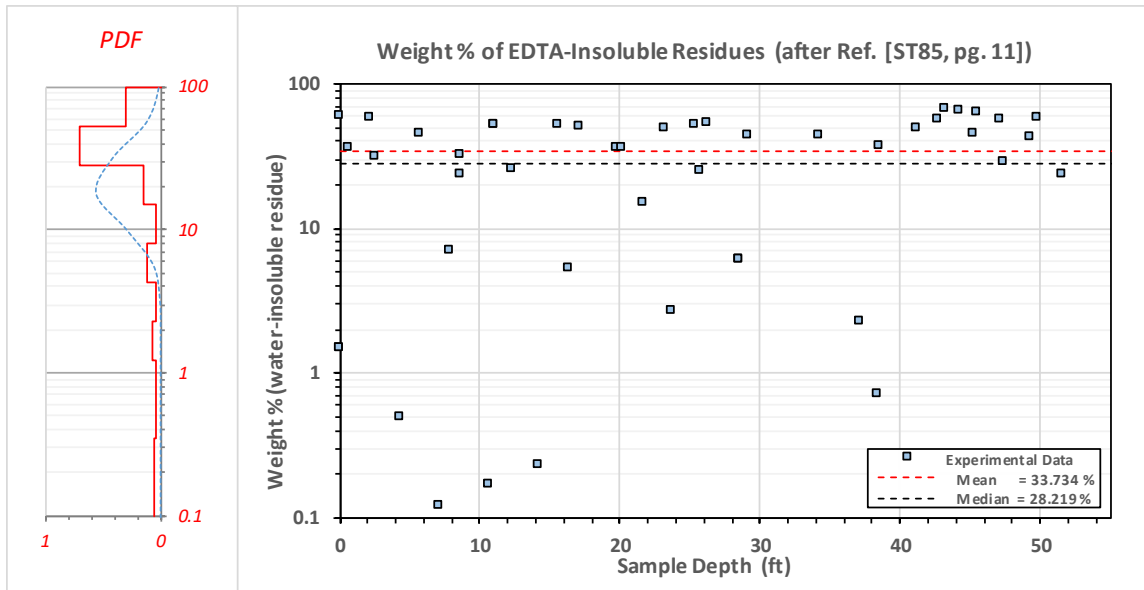

Figure C-4 SEMI-LOG-SCALE. Weight (per water-insoluble residue) percentages of EDTA-insoluble residues in WIPP Salado rock salt (see Table C-2 for values, original data taken from Ref. [ST85, pg. 11]). The distribution used the following lognormal parameters; μ=3.3400, σ=0.5975, m=33.734, and v=488.28 .
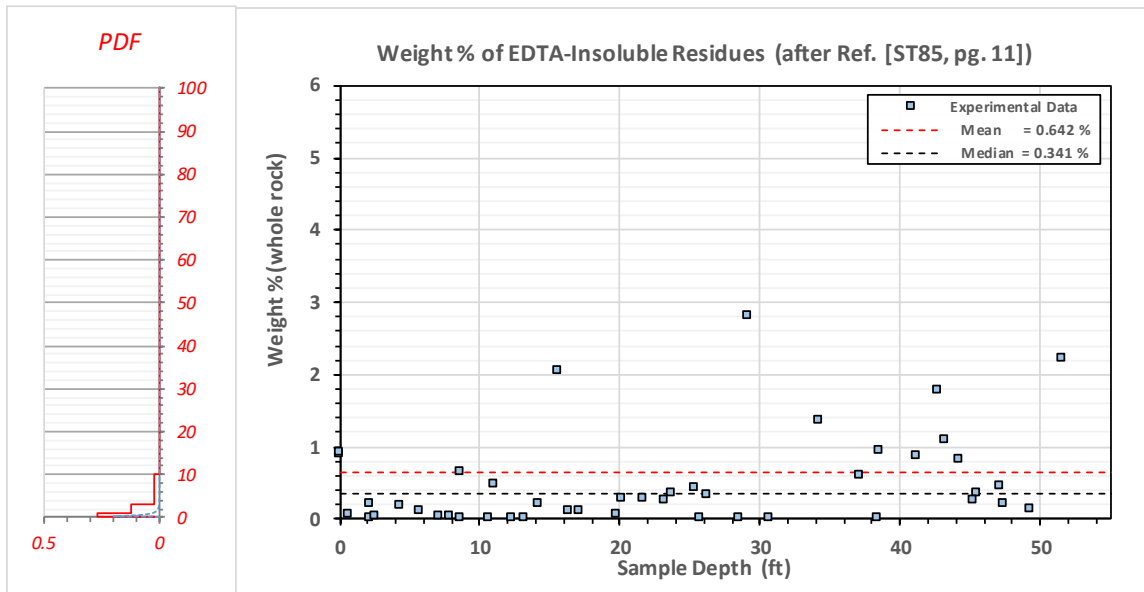
Figure D-5 LINEAR-SCALE. Weight (per whole rock) percentages of EDTA-insoluble residues in WIPP Salado rock salt (see Table D-2 for values, original data taken from Ref. [ST85, pg. 11]). Several high percentage values exist, which required a lognormal distribution. The distribution used the following lognormal parameters; μ=-1.0755, σ=1.1244, m=0.64186, and v=1.0464.
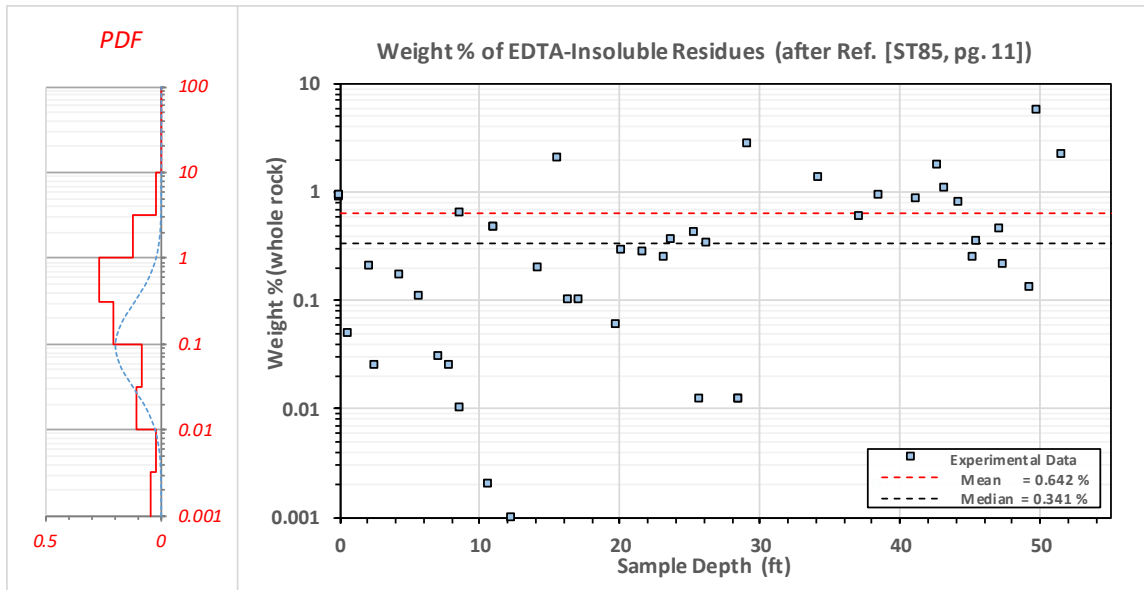

Figure D-6 SEMI-LOG-SCALE. Weight (per whole rock) percentages of EDTA-insoluble residues in WIPP Salado rock salt (see Table D-2 for values, original data taken from Ref. [ST85, pg. 11]). The distribution used the following lognormal parameters; μ=-1.0755, σ=1.1244, m=0.64186, and v=1.0464 .

Sample No.	Sample Depth		Sample Weight	Weight of EDTA-Insoluble Residue	Weight % (water-insoluble residue)	Weight % (whole rock)
	From	To				
	(ft)		(g)	(g)	(ʷᵗ%)	(ʷᵗ%)
201	2	2.5	1.025	0.6	58.54	0.21
202	4	4.7	4	0.02	0.5	0.17
203	8.3	9	3	0.97	32.33	0.65
204	10.8	11.3	3	1.55	51.67	0.48
205	13	13.55	Insufficient material			
206	15.55	15.85	4	2.11	52.75	2.05
207	16.9	17.45	0.53	0.27	50.94	0.1
209	19.65	20.05	0.52	0.19	36.54	0.06
210	21.5	22	4	0.6	15	0.28
211	23	23.5	2.1	1.03	49.05	0.25
212	25.1	25.7	4	2.1	52.5	0.425
213	26	26.5	3.65	1.935	53.01	0.34
214	28.25	28.85	0.9	0.055	6.11	0.0125
215	30.5	31.05	Insufficient material			
216	31	38 *	4	2.43	60.75	0.89
217	39.25	39.85	4	1.5	37.5	0.94
218	41	41.5	4	1.95	48.75	0.86
219	42.5	43	4	2.27	56.75	1.77
220	44	44.5	4	2.61	65.25	0.81
221	45.3	45.85	2.3	1.48	64.35	0.35
222	47	47.5	4	2.3	57.5	0.45
223	49.05	49.55	1.075	0.46	42.79	0.13
224	4	4.5**	4	0.06	1.5	0.92
*core loss zone						
**From RM-4						
228	0.4	0.9	0.7	0.255	36.4	0.05
229	2.3	2.8	0.475	0.15	31.6	0.025
230	4.75	6.75	2.075	0.955	46	0.11
231	7.1	7.3	4.1	0.005	0.12	0.03
232	7.75	8.15	3	0.21	7	0.025
233	8.15	9.1	0.38	0.09	23.7	0.01
234	10.5	10.9	3	0.005	0.17	0.002
235	12.15	12.6	2.5	0.65	26	0.001
236	14	14.45	3	0.007	0.23	0.2
237	16.1	16.6	3	0.16	5.3	0.1
238	29	29.5	2.9	1.29	44.5	2.81
239	34.05	34.5	3	1.315	43.8	1.36
240	36.9	37.6	3	0.07	2.3	0.6
241	38.2	38.7	2.8	0.02	0.71	0.002
242	43.05	43.55	3	2.03	67.7	1.1
243	47.2	47.7	3	0.86	28.7	0.215
244	49.65	50	3	1.76	58.7	5.68
245	51.3	52.1	2.7	0.645	23.9	2.22
246*	20.05	20.45	3	1.09	36.3	0.29
247*	23.45	23.95	3	0.08	2.67	0.36
248*	25.5	26	0.36	0.09	25	0.0125
249*	45	45.65	3	1.37	45.7	0.25
*From RM-7						
				Average =	33.734	0.642
				(sample) Std dev =	22.097	1.023
				Median =	36.540	0.280
				(sample) Variance =	488.282	1.046

Table C-2. WIPP Salado Rock Salt – Weight Percentages of EDTA-Insoluble Residues (Taken from Ref. [ST85, pg. 11, Table 3])